

DETERMINING TRANSMISSION LINE PARAMETERS FROM TIME-STAMPED DATA

by

Martin Grobler

Submitted in partial fulfillment of the requirements for the degree

Master of Engineering (Electrical-Engineering)

in the

Faculty of Engineering, the Built Environment and Information Technology

UNIVERSITY OF PRETORIA

July 2007

SUMMARY

Determining Transmission Line Parameters from Time-Stamped Data by

Martin Grobler

Supervisor: R. M. Naidoo

Department of Electrical, Electronic and Computer Engineering

Masters in Engineering (Electrical)

The main aim of this project was to find a practical and accurate method to determine the parameters of a transmission line by using current and voltage measurements. The term line parameters refer to the inherent series resistance and inductance that is found on transmission lines.

The line parameters were determined by using the voltage and current measurements from either side of the transmission line. An accurate reference signal is needed to precisely compare the measured signals. The timing signals from GPS units were used to reference the measurements. In a field implementation data transfer of the measured signals would be a necessity which can be accomplished by GPRS modems.

Three methods are proposed for determining line parameters. These methods were thoroughly tested in the following ways:

- A model was built in SIMULINK with known elements and values. The three methods were then applied to the model and simulations were run. The results from the simulations are compared to the known values.
- A system was built in the laboratory with known parameters. The results gathered from testing the system on all three methods are compared to known values.
- Finally, the methods were applied to field data from recorders of a utility. This was done to see how well the methods would perform on a real system. Accuracy was determined from what the utility accepts as the correct values.

Another focus of the project was to determine the surge impedance loading (SIL) curve from measured data. This curve can be used to determine the loadability limit of the transmission line as well as to visually show at what point the line is operating at any given time. The curve is also useful as it provides insight into the additional reactive power needed for a certain active power transfer.

The concept of drawing a SIL curve from actual measurements was first tested by means of simulation. The drawing of the proposed curve is also tested on actual measurements from a transmission line.

This investigation posed many challenges. These challenges are discussed in detail in the dissertation. Some of these challenges have easily implementable solutions while others still leave room for further research. The results and findings are published in this document.

Keywords: Transmission line, line parameters, line models, measurement, GPS, time-stamping, GPRS, SIL curve, simulation, serial communication

OPSOMMING

Determinering van Transmissie Lyn Parameters vanaf Tyd Bestempelde Data deur
Martin Grobler
Toesighouer: R. M. Naidoo
Departement van Elektriese, Elektroniese en Rekenaar Ingenieurswese
Magister in Ingenieurswese (Elektries)

Die hoof doel van die genoemde projek, was om 'n praktiese en akurate metode te vind om die parameters van 'n transmissie lyn te bepaal deur die gebruik van gemete spannings en strome. Die term 'lyn parameters' verwys na die inherente weerstand en induktansie wat in serie met mekaar voorkom op 'n transmissie lyn.

Die lyn parameters is bepaal deur die gemete spanning en stroom waardes van beide kante van die transmissie lyn te gebruik. 'n Akurate verwysing word benodig om die verskillende gemete seine presies met mekaar te vergelyk. GPS modules is gebruik om 'n akurate verwysing te lewer in die vorm van 'n tyd puls. Wanneer die sisteem prakties geïmplementeer word kan GPRS modems gebruik word om die gemete seine na 'n sentrale punt te stuur.

Drie metodes word voorgestel vir die bepaling van die lyn parameters. Hierdie metodes is deeglik getoets op die volgende wyse:

- 'n Model met bekende elemente en waardes is gebou in SIMULINK. Die metodes is toegepas op die model en gesimuleer. Resultate is met bekende waardes vergelyk.
- 'n Stelsel is gebou in die laboratorium met bekende parameters. Die resultate verkry deur al die metodes op die stelsel toe te pas, is vergelyk met die bekende parameters.
- Laastens was al drie metodes toegepas op veld data wat verkry was vanaf fout opnames wat behoort aan 'n utiliteit. Dit was gedoen om te bepaal hoe goed die metodes sal vaar in 'n werklike stelsel. Akuraatheid was bepaal deur die uitgewerkte waardes te vergelyk met wat die utiliteit beskou as korrek.

Die tweede gedeelte van die projek het gefokus op die bepaling van die dring impedansie belading (DIB) kurwe, deur die gebruik van gemete data. Hierdie kurwe kan gebruik word om die beladings limiet van 'n transmissie lyn te bepaal sowel as om 'n grafiese aanduiding van die operationele punt van 'n lyn te gee. Verder is die kurwe van belang omdat dit 'n benadering gee vir die reaktiewe krag benodig om 'n spesifieke aktiewe las te ondersteun.

Die konsep om 'n DIB kurwe te trek vanaf gemete waardes is eerste getoets deur simulasies te doen. Nadat die simulasies suksesvol was, is die konsep ook getoets op 'n werklike transmissie lyn se gemete waardes.

Daar was 'n groot verskeidenheid probleme wat blootgele was gedurende die loop van die navorsing. Hierdie probleme word in diepte bespreek in hierdie dokument. Sommige van die probleme het eenvoudige oplossings terwyl ander die deur ooplos vir toekomstige navorsing. Hierdie dokument bevat die resultate en bevindinge.

Sleutel woorde: Transmissie lyn, lyn parameters, lyn modelle, meting, GPS, tyd bestempel, GPRS, DIB kurwe, simulاسie, serie kommunikasie

TABLE OF CONTENTS

1	Introduction	1
1.1	Overview of Transmission lines	1
1.1.1	Transmission line models	1
1.2	Determining line parameters	4
1.2.1	Modelling	4
1.2.2	Simulation	5
1.3	Surge impedance loading	6
1.4	Overview of GPS modules	7
1.5	Overview of GPRS modules	8
2	Literature study	9
2.1	Sources for timing	9
2.1.1	GPS module	9
2.1.2	Ethernet	9
2.2	Applications of GPS time-stamping	9
3	Contribution	12
3.1	Transmission line parameters	12
3.2	SIL curve	13
4	Challenges	14
4.1	Clock frequency	14
4.2	Measurements	17
4.3	GPS modules	21
4.4	Communication	21
4.5	Substation VT and CT errors	21
5	Method and Experimental setup	23
5.1	Method	23
5.1.1	GPS modem communication	23
5.1.2	GPRS modules	24
5.1.3	Transmission line parameter determination	25
5.1.4	Determining the SIL curve	28
5.2	Experimental setup	29
5.2.1	Simulation	29

5.2.2	Lab implementation	31
5.2.3	Field implementation	34
6	Simulation results	36
6.1	Line parameter determination	36
6.1.1	Method 1	36
6.1.2	Method 2	39
6.1.3	Method 3	42
6.2	Determining the SIL curve	45
6.3	Discussion of results	47
6.3.1	Line parameters	47
6.3.2	SIL curves	50
7	Laboratory results	51
7.1	Method 1	51
7.1.1	Short line	51
7.1.2	Medium line	53
7.1.3	Long line	55
7.2	Method 2	57
7.2.1	Short line	57
7.2.2	Medium line	59
7.3	Method 3	59
7.3.1	Short line	59
7.3.2	Medium line	61
7.3.3	Long line	63
7.4	Discussion of results	65
7.4.1	Method 1	65
7.4.2	Method 2	66
7.4.3	Method 3	67
7.5	Alternatives considered	68
7.5.1	Method	68
7.5.2	Timing considerations	68
8	Field results	69
8.1	Acquiring line data	69
8.1.1	Line recorders	69

8.1.2	Acquiring usable data	69
8.2	Results from field data	70
8.2.1	Impedance calculations	70
8.2.2	SIL curve	82
8.3	Discussion of results	83
8.3.1	Parameter calculations	83
8.3.2	SIL curve	87
8.4	Alternatives considered	88
9	Summary of findings	90
10	Conclusion	92
10.1	Work Presented	92
10.2	Future research	93
	References	95

1 INTRODUCTION

1.1 OVERVIEW OF TRANSMISSION LINES

Electricity is the driving force behind industry and subsequently the economy. This very important commodity is transported from power generation to the end user by means of overhead power lines. Within South Africa coal fired power stations are the main source of generation. The highveld is predominantly known for its large quantities of raw coal that can be used for this purpose. Electricity thus has to be transported to the outlying areas since it is cheaper to transport electricity than coal. As a result, there is an abundance of power lines within South Africa.

Transmission lines play an important part in the economy of not only South Africa but also the rest of the world. Therefore the integrity of these lines is of the utmost importance. Transmission lines are largely fabricated out of aluminium which is a good conductor of electricity. Like all other conductors it has a resistive value. Depending on the configuration of the three phases of the transmission line, there is also a line inductance and capacitance. All of the above influence the efficiency of the power network as a whole.

In order to determine the system fault level¹, the parameters of generation, transmission and distribution has to be known. Thus, the impedance of transmission lines has to be determined in order to have a trustworthy system model. Here, line impedance refers to the equivalent shunt capacitance and the series resistance and inductance of a transmission line. The fault level in turn is used for the grading of protection systems and the sizing of circuit breakers.

1.1.1 *Transmission line models*

There are three ways in common practice to model power-lines. The three models are the short line, medium line and the long line models. Short lines are commonly accepted to be shorter than 80km. A line is considered to be medium up to the length of approximately 240km. Anything longer is classified as a long transmission line [1]. Figure 1.1 shows the common circuit model for the short transmission line.

¹Fault level or short circuit impedance refers to the equivalent impedance seen from the actual generator delivering the power to that specific point in the network.

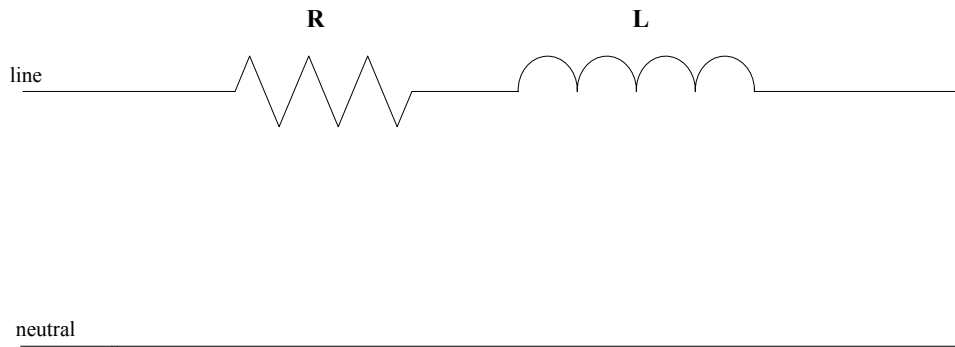


Figure 1.1: Short transmission line model.

A short transmission line is modelled as having only a resistance and inductance in series with each other [2], [3]. This model is commonly applied to distribution networks since the distance between connecting lines are relatively short. The longer the transmission line, the larger the capacitive effect. The capacitive effect represents the charge that is stored between the lines and the neutral.

It was found that when a line's length increases beyond 80km, the effect of capacitance on the line can no longer be neglected (as is the case with the short line). Figure 1.2 shows the medium line model. There is a lumped capacitance present in the model at the start and the end of the line. The total capacitive value between line and neutral is divided by two and lumped for the capacitances shown in Figure 1.2.

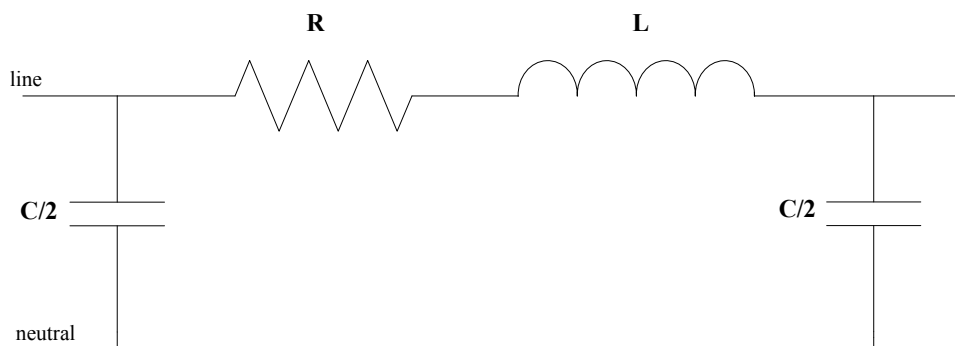


Figure 1.2: Medium transmission line model.

When the transmission line's length increases above 240km the medium line model does not provide an adequately accurate system. The reason for this is that the capacitance and inductance of a line increases over every section of the line as a whole. The medium line model in Figure 1.2 is an approximation of the real system that is used to make computation easier. For the long line the effect of uniformly distributed inductance, ca-

capacitance and resistance cannot be ignored. For this reason the more complex model of a long transmission line, Figure 1.3, has been developed [1].

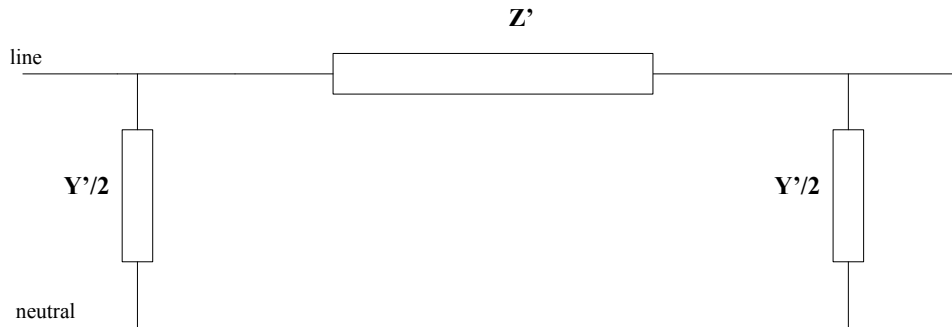


Figure 1.3: Long transmission line model.

The model of the long transmission line is similar to that of the medium line model, but the impedances are defined differently. To derive the model shown in Figure 1.3 the line is considered on a differential per section basis. By solving the system, Z' can be defined by (1.1).

$$Z' = Z \frac{\sinh(\gamma l)}{\gamma l} \quad (1.1)$$

Z is the total series impedance of the line, the same value as that of the medium transmission line model and is expressed in Ohm. Using the terms from Figure 1.2, Z is determined using (1.2).

$$Z = j2\pi fL + R \quad (1.2)$$

The term γl is determined from (1.3).

$$\gamma l = \sqrt{yz} \cdot l \quad (1.3)$$

The term l in the equation above is the total length in meters of the transmission line in question, while y and z are the shunt admittance per unit length [Siemens/m], phase to neutral, and the series impedance per unit length respectively.

The term $Y'/2$ in Figure 1.3 can be defined by (1.4),

$$\frac{Y'}{2} = \frac{Y \tanh(\gamma l/2)}{\gamma l/2} \quad (1.4)$$

The new term Y [Siemens] represents the total shunt admittance of the line, phase to neutral. The admittance of the line can be easily determined from the capacitance as

represented in Figure 1.2 by applying the following equation.

$$Y = 2\pi fC \quad (1.5)$$

Common methods to determine the line impedance are modelling and simulation.

1.2 DETERMINING LINE PARAMETERS

1.2.1 Modelling

At present the most common way of determining the transmission line parameters is by the use of modelling. There are standard classes of transmission lines used in industry (Hare, Bull, Ostrich etc.). Each of these individual lines are made up of a specific amount of strands and consists of a unique support structure. The manufacturer of these lines give typical values for DC resistance per unit length for a certain temperature and the diameter of the conductor.

Another factor that influences line parameters, over and above the type of material it is constructed out of, is the operating frequency, temperature and the length of the actual transmission line. Geometry also influences it *i.e.* are the three phases equilaterally spaced or is it a flat arrangement or another spacing that is employed. The distance between the phases and the distance between the lines and ground also play a part in the values.

The resistance that is presented on the line model is the AC resistance. To get from the DC resistance (R_{DC}) that is provided by the manufacturer, at a reference temperature t_1 [$^{\circ}\text{C}$], to the AC resistance of the model at an operating temperature t_2 [$^{\circ}\text{C}$], (1.6) is used [1].

$$R_{AC} = (1 + \delta) \cdot \left(\frac{T + t_2}{T + t_1} \right) \cdot R_{DC} \cdot l \quad (1.6)$$

In (1.6) the symbol δ represents the skin effect coefficient of the conductor. This is a phenomena that is observed in alternating current conductors where the alternating flux is non-uniform across the surface of the conductor. This gives rise to higher current densities near the outside of the conductor. The skin effect is a measure of the average reduction in conductor surface area due to the unevenly distributed current. T is the slope of the graph of temperature versus resistance for the specific type of material and is given in degrees Celsius. The last factor that has to be brought into the calculation to determine

the AC resistance is the length of the line l .

The inductance and capacitance associated with a power line is caused by flux linkage [4], [5], [6]. The formula for inductance is given in (1.7), where the inductance value is the line-to-neutral inductance given in H/m, and the capacitance equation is given in (1.8) with the result in F/m.

$$L = 2 \times 10^{-7} \cdot \ln \left(\frac{GMD}{GMRL} \right) \quad (1.7)$$

GMD or geometric mean distance is a measure of the mean distance between the three phases. This value is influenced by the actual spacing and also whether there are two or more circuits in parallel. The geometric mean radius (GMR) is a measure of the mean radius of conductor per phase. This value varies greatly when there is more than one conductor per phase (bundling). There is a differentiation between the way the GMR value is worked out for the calculation of the inductance (GMRL) and the calculation of the capacitance (GMRC). The capacitance is determined as in (1.8),

$$C = \frac{2\pi k}{\ln \left(\frac{GMD}{GMRC} \right) - \ln(DG)}. \quad (1.8)$$

In (1.8) the constant k refers to the permittivity of free space [$k = 8.85 \times 10^{-12}$ F/m]. The value for GMD is the same for the calculation of both the inductance and the capacitance. DG represents the average distance between the three phases and the physical ground.

1.2.2 Simulation

A less labor intensive method is to calculate the impedance and hence fault level for sections of the network by simulation. A simulation package that is largely in use today is EDSA. A whole section of the network is built in a simulation window from standard components. These components are then defined according to the manufacturer's data sheets with typical values for resistance and component configuration. The configuration of the implemented system is also included in the simulation, for example the length of transmission lines.

When the simulation is run, the software follows an iterative approach using the voltage sources and loads to provide results. From the output one can get the line impedance, short circuit level, expected values for voltage and current, active and reactive power as well as

the power factor. By changing the configuration in the simulation software *i.e.* opening and/or closing circuit breakers, different scenarios can be tested.

1.3 SURGE IMPEDANCE LOADING

The surge impedance loading (SIL) is defined as the the amount of active power that is transferred to a load at unity power factor. This makes the line appear purely resistive [1], [7]. It means that the line capacitance provides all reactive power that is absorbed by the inductance of the line. This implies that depending on the system load, the line can be either absorbing or providing reactive power. The SIL value can be determined by using the capacitance and the inductance of the total line in (1.9) [8].

$$SIL = \frac{|V_L|^2}{\sqrt{L/C}} \quad (1.9)$$

The voltage, V_L is the line to line voltage of the three phase transmission line. The SIL value in the equation above is given in Watts. When a line is loaded below the SIL value the line is providing reactive power which means that the system operates more efficiently [9]. The inverse also applies that when the line is loaded above the surge impedance value it absorbs reactive power. When a transmission line absorbs reactive power, additional sources of reactive power has to be supplied to the line. This is done by means of capacitor banks that support power transfer over lines under heavy loading conditions.

The SIL curve is closely related to the surge impedance loading value. Traditionally this graph is drawn for a transmission line providing power to a load with a unity power factor. The reactive power that is absorbed or provided by the line is plotted against the active power delivered to the load. By changing the amount of power that is supplied to the load, and recording the resultant change in reactive power, a SIL curve can be constructed. The SIL value for a transmission line can also be read off the SIL curve. The SIL value will be the active power on the graph that results in a zero net reactive power on the line.

Each transmission line has its own SIL curve. A SIL curve is useful as it can be applied to determine the following.

- The size of reactive power support needed to sustain a certain load on the line can be closely approximated.

- The stability limit of the transmission line can be determined.
- The current loading on the line can be used to determine whether it would be possible to increase the power transfer across the line.

1.4 OVERVIEW OF GPS MODULES

As the title of the project indicates, there has to be a reliable source for time. One such accurate timing device is a GPS module [10], [11]. Using the time of a GPS module, that is accurate to the nanosecond range, data on two sides of a transmission line can be accurately compared to determine the line impedance as well as the SIL curve.

The GPS module has two outputs that are of use for this project. The first is a pulse that is defined as 1PPS or one pulse per second [12]. The 1PPS is configurable with certain modules so that the frequency and pulse duration can be changed by the user. This pulse comes directly from the GPS satellite system, on the second, at a very high accuracy that is typically in the nanosecond range. This means that if the frequency is set to a higher value the output is dependant on the internal oscillator of the GPS module.

The second output of interest is delivered by the module through RS232 serial communication. This communication updates the time, date, geographic position and elevation above sea level once every second². The message from the serial communication provides the actual time according to GMT (Greenwich Mediterranean Time). South Africa uses the GMT+2 time zone, which means that any time that is received from the GPS module should be added by two hours in order to determine the local time. The time update from the serial communication is not accurate enough for exact timing applications since there is an amount of drift in the update from one second to the next. Another reason is that the baud rate of the RS232 communication can be changed by the user.

The GPS module is used in this project to time-stamp measured data. Time-stamping is the name given to the process of adding the exact time and date to data that is sampled. When the data is measured the 1PPS is used to find the exact increment of the second. Once the actual time and date is received through serial communication a few cycles later

²This interval can also be adjusted same as the 1PPS output

the time is added to the point in data where the pulse occurred.

1.5 OVERVIEW OF GPRS MODULES

GPRS is a wireless service provided by mobile companies that allows the user to connect to the internet or send data messages. There are commercially available GPRS modules that can be purchased for this purpose. The module connects to a personal computer via serial communication. By using this technology it is possible to send data from the remote measuring stations to a central location where the data can be processed and stored. For data transfer this is a very attractive option as the customer only pays for the actual data transferred. This means that the connection does not have to be broken to be re-established at a later stage.

This dissertation will take the reader through the various steps involved with determining the parameters of a transmission line. All the required support equipment is quantified and the system integration described. The scope will cover simulation to laboratory experiments and then finally an implementation on physical overhead power lines is done.

2 LITERATURE STUDY

2.1 SOURCES FOR TIMING

2.1.1 *GPS module*

GPS time-stamping makes use of the NAVSTAR global positioning system, which is a network of 24 satellites orbiting the earth. The timing of the satellites is held by atomic clocks that are synchronized to accuracy better than 100nanoseconds. Using equipment such as the HP 59551A GPS measurements synchronization module, that derives it's timing from the GPS satellite system, the time-stamping of values can be done to an accuracy of up to 110nanoseconds [13], [14]. There are various other GPS modules on the market that can be employed and the above mentioned is only cited for background information.

2.1.2 *Ethernet*

Another method that provides accurate time to the microsecond is mentioned in [15]. In this paper it is discussed how simple network time protocol (SNTP) can be used over Switched Fast Ethernet to gain an accuracy of up to $25\mu s$ using standard switches. By using a special Ethernet switch from OnTime Networks and specific filtering techniques a timing accuracy of $1\mu s$ can be attained. A timeserver is used to provide the master time for all the other devices that are connected to the network. To ensure that the timeserver has the correct time it is synchronized with a GPS receiver.

2.2 APPLICATIONS OF GPS TIME-STAMPING

GPS time-stamping is featuring with increasing recurrence in Power Systems. The data received from two different points can be time stamped so that the two waveforms can be compared to each other in both phase and magnitude.

In [13] and [16] travelling waves are used for fault location. When a fault is induced on a power line it will produce a transient waveform that propagates close to the speed of light [17], [18]. The principle is based on the assumption that lightning strikes a power line that is situated between two substations that each have a GPS timing device. The GPS module in each of the substations measure the occurrence of the transient and sends this information to a central control system. By using the following equation the distance

from the substation to the fault can be calculated with an accuracy of within 300 meters.

$$x = \frac{l - c(\tau_a - \tau_b)}{2} \quad (2.1)$$

In (2.1), $(\tau_a - \tau_b)$ represents the difference in arrival times of the travelling waves between the two substations. The constant c is the propagation speed of the wave which is equal to $299.79 \mu\text{m}/\mu\text{sec}$. The length of the transmission line is given by l and x is the distance to the fault from substation a . The method has also been applied successfully to non-lightning related faults on both distribution and transmission systems [19], [20], [21].

Another application has been to correlate the time of the lightning strike with anomalies observed in the power system [22]. For this implementation lightning location data, fault monitor disturbance data and distribution feeder location data is compared to determine within a few hundred meters the fault location on a distribution system. This limits the time that the customer is left without power since locating of the fault is not the major time consumer. The distribution disturbance data is the voltages and currents at a specific substation when there is a fault on the network. By using a GPS module for time-stamping the disturbance data, it can be compared with the location of lightning strikes at that specific time. If exact correlation is found between lightning and disturbance data the fault can be located to the area of the lightning strike.

In [23] the measurement of circuit breaker status with time and other signals is used for two different applications. It is used for fault analysis, where the sequence of events are accurately recorded in time using GPS timing. The operation helps to determine whether the relay settings are correct for clearing the fault and also where improvements can be made. The values and phasors of current and voltage on the sending and receiving side of the transmission lines are measured. From short-circuit studies that have been done the recorded data is then compared to the simulated signals. The best fit between these two measurements will give a good indication as to where the fault is located on the network. The second application is state estimation of the topology of the network in real time. It is well known that circuit breaker status readings provide for regular errors in the system model when there are inaccurate readings. If these readings are done in conjunction with GPS timing modules, it would be possible to determine the switching state of the entire network very accurately at any given point in time. The objective is to

interface with a SCADA system to make the operation of the current system more reliable.

In [24] digital differential current is used for the protection of transmission lines. This is done by sampling the current at the two terminals and then time-stamping the measured data with a GPS module. The two sets of time-stamped data is then sent to a central processing system. At the central system the GPS time-stamped data of the currents are compared with the help of an algorithm. Since the algorithm is based on the superposition theorem the timing has to be very accurate. Based on the comparison between the operating current and the restraint current over 5 consecutive data points a decision is made as to whether the protection of the transmission line must operate.

3 CONTRIBUTION

3.1 TRANSMISSION LINE PARAMETERS

As stated in Chapter 1, transmission line parameters are largely determined by means of simulation and modelling. The drawback of this is as follows:

- Temperature variations are not considered.
- The ageing of conductors over long periods of time is not accounted for.
- Changes in conductors used due to repairs made on lines are not updated on the system model.

In (1.6), it is shown that the resistance of a transmission line is dependant on the temperature of that line. As the ambient temperature varies between night and day as well as summer and winter the actual resistance of the line changes. To obtain an accurate value for the resistance is of importance since the loading on a power line is limited by the maximum allowable sag. The sag of a line is the minimum distance that the line is allowed to hang above ground level. A line will expand if it becomes warm and retract when it is cooled. The losses on the line are from the resistance which in turn determine the temperature of the line. In short, this means that a line can handle a greater load in cold weather than in warm weather.

This project is aimed in part at determining the parameters, *i.e.* resistance, inductance and capacitance of a line in real time. This means that as the temperature drops the change in parameter value will be reflected practically through measurement.

The ageing of conductors occurs over several years if the ratings of the line are adhered to. This means that as time progresses the line parameters will slowly change. Since the values are measured in real time these changes will be incorporated in the calculated values. In effect the calculated parameters will gradually change with time.

The aim in outcome for this project is to have a system that can be interfaced to a central data acquisition system used by utilities. This implies that the parametric values that are calculated can be used to update the system model that the utility has for a specific section of line. When a repair is made on a section of line and a different conductor is

used from the original one, the changes will be reflected in the calculated values. Thus the system model will be updated.

The research aims to present a more accurate system model that will be used. As stated in Chapter 1 this will aid in determining a more accurate fault level.

3.2 SIL CURVE

The SIL curve is drawn by plotting the reactive power absorbed or supplied by the line against the various levels of active power provided to a load with a unity power factor. For this project the definition is changed to include loads that do not have a power factor of unity as this is very seldom in practice achievable.

The SIL curve will be determined by means of measurement of the active and reactive power transmitted across the transmission line in question. In time, the database will have practical SIL curves for various power factor loads. The benefits to this SIL curve above that of the traditional curve is that the reactive power that has to be provided to the load is included in the graph, since the load has a non-unity power factor. Decisions that have to be made to determine the extra reactive support for power transmission will be easier [25].

In general, the SIL curve will be more accurate as compared to the theoretical one since the actual operating conditions of the line provides the data for the curve and not an estimate of what the parametric values are. A more accurate SIL curve will ensure that the stability limits and the loading level will be much more accurate on the line.

4 CHALLENGES

4.1 CLOCK FREQUENCY

The current and voltage measurements had to be done with two units on either side of the transmission line. One of the major problems experienced was that the clock frequencies of the DSP units were not exactly matched. The DSP units were used for the measurement of analogue signals and to control the system by communicating with a computer. Due to the difference in clock frequency an error in the measured values were experienced that became larger with increased time.

To graphically represent this error, measurements were taken from the same current flowing in a resistive circuit with two separate CT's. The current was measured on two different DSP units at the same time and on the same piece of conductor. After the measurement was completed over a period of six seconds, the data was retrieved from the individual units. By subtracting the currents from each other discreetly the error introduced by the clock frequency mismatch was calculated. These error values were plotted against time in Figure 4.1.

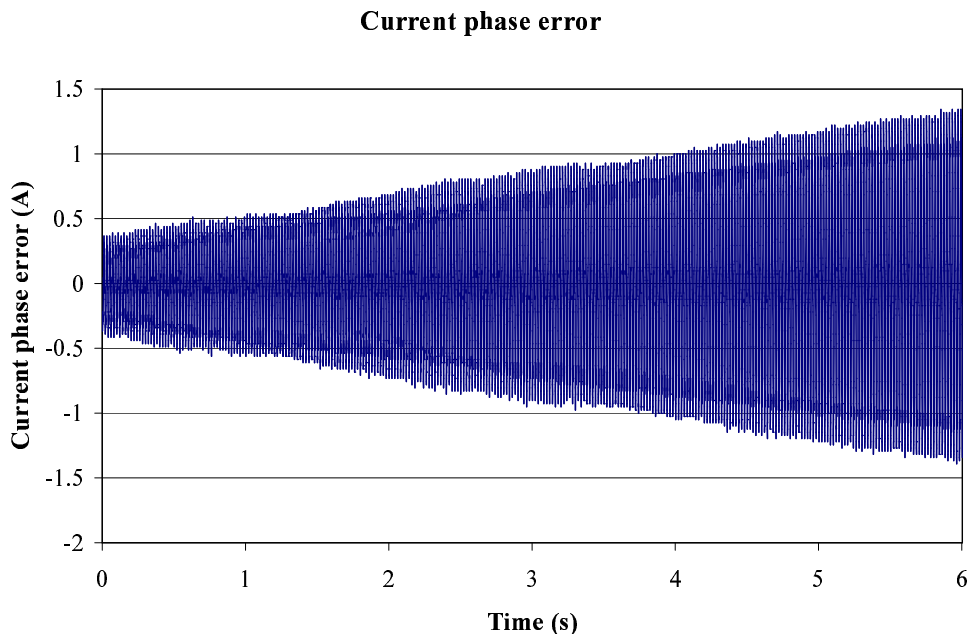


Figure 4.1: Error introduced between current measurements due to clock mismatch.

The error shown in Figure 4.1 does not influence the rms value of the measured current or voltage. The error becomes a problem when discreet values have to be compared to each other or even subtracted from each other. This problem has been considered in other

literature. In [24] where discrete current points has to be compared, the problem is solved by using a separate oscillator. A very accurate and highly stable oscillator was used in conjunction with the time signal from a GPS unit to provide a highly accurate timing signal. This timing signal was then used as an external clock for the DSP units used to measure the current values.

The article proves that this method works to eliminate the clock frequency error experienced. The reason this method was not employed in this dissertation was that highly accurate oscillators are very expensive. Alternatives were considered as a solution to keep the error introduced small.

The time pulses from two GPS units were used to initialize the measurements on both DSP units whose results were used in Figure 4.1. One solution that was considered was to not only limit the GPS Time-pulse to the initialization of the recording of the data, but to realign the measurements with every time pulse if needed. This meant that as soon as the difference between the time pulses of the two GPS units were measured to be one data point corrective action would be taken. Figure 4.2 included shows visual results for the same data used to construct Figure 4.1. Here the GPS time pulses and measured data is realigned.

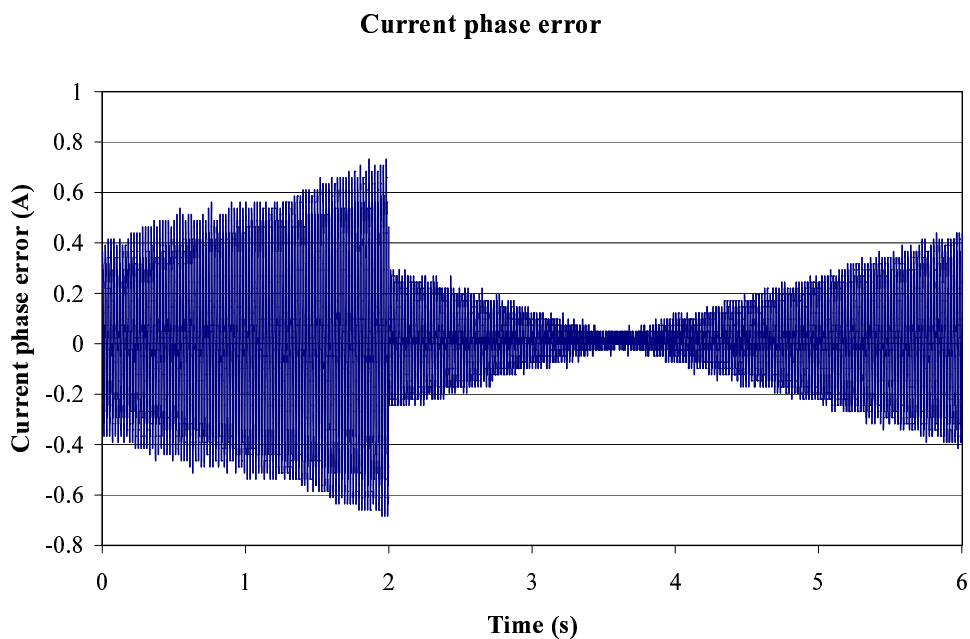


Figure 4.2: Figure showing the influence on phase error with a realignment in measured values.

The correction can only be done once the measured values of the two DSP units are compared. This is only done once the data is retrieved. The correction is done by moving the measured units that is lagging forward by one data point. By doing this the GPS time pulses are measured at the same interval. As can be seen in Figure 4.2 the realignment occurred at two seconds. The maximum magnitude of the error is in this way reduced from 1.3A to 0.7A. This method reduced the error by 50% for a period of six seconds.

After numerous simulations it is clear that the error starts off small at initialization and then becomes larger with time. This in itself provides an alternative to limit the error by using a shorter period of measurements to calculate the line impedance values. Ten cycles is enough to ensure that the network is not in a transient condition and to work out the needed parameters. Figure 4.3 shows how the calculated impedance varies over a period of six seconds.

Line impedance

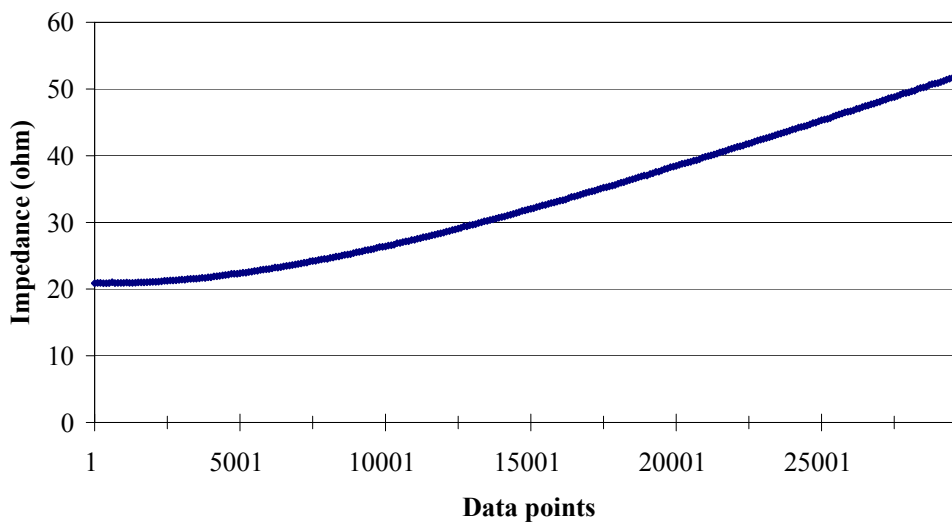


Figure 4.3: Impedance measurement over six seconds.

Figure 4.3 shows that the impedance calculated remained relatively constant for the first 5000 data points or the first second. The actual impedance value in the circuit was 20.8Ω . This impedance value was calculated by subtracting the instantaneous voltage values on the sending and receiving sides. The error thus introduced was due to the voltage error introduced by the clock frequency inequality between the two DSP units. The error remains small during the first 5000 data points (refer to Figure 4.4). Thus the voltage error remains small over a longer period if considered in conjunction with Figure 4.1.

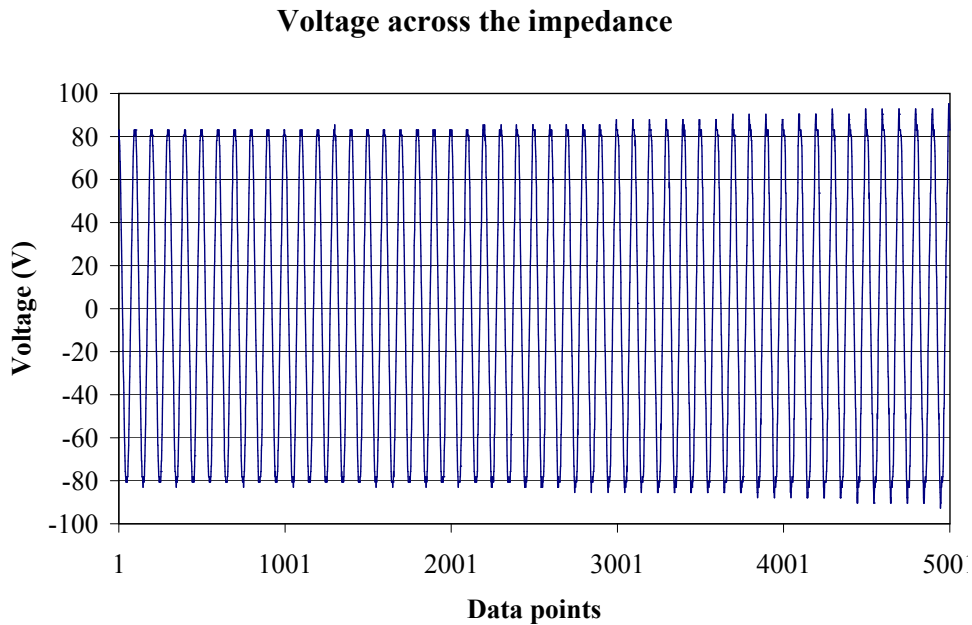


Figure 4.4: The instantaneous voltage across the impedance representing a transmission line.

The reason for smaller apparent error in Figure 4.4 when compared to Figure 4.1, is that Figure 4.1 was drawn from two different measurements of the same current. The voltages that are subtracted in Figure 4.4 represents the resultant voltage drop across the transmission line which is large when compared with the initial error value. As the error becomes larger this changes, and a more pronounced influence is seen on the calculated impedance value.

Errors introduced in the measurement of the individual currents and voltages was another challenge that had to be dealt with. This is discussed more in depth in the following section.

4.2 MEASUREMENTS

A factor that also influences the overall accuracy of the project is the accuracy of the measuring equipment used for sampling the analogue voltages and currents. A small discrepancy between the magnitude and/or phase of the current probes on either side of the transmission line, could have a drastic effect on the impedance. Figure 4.5 and Figure 4.6 are included to graphically illustrate the problem experienced.

Resistance measurement

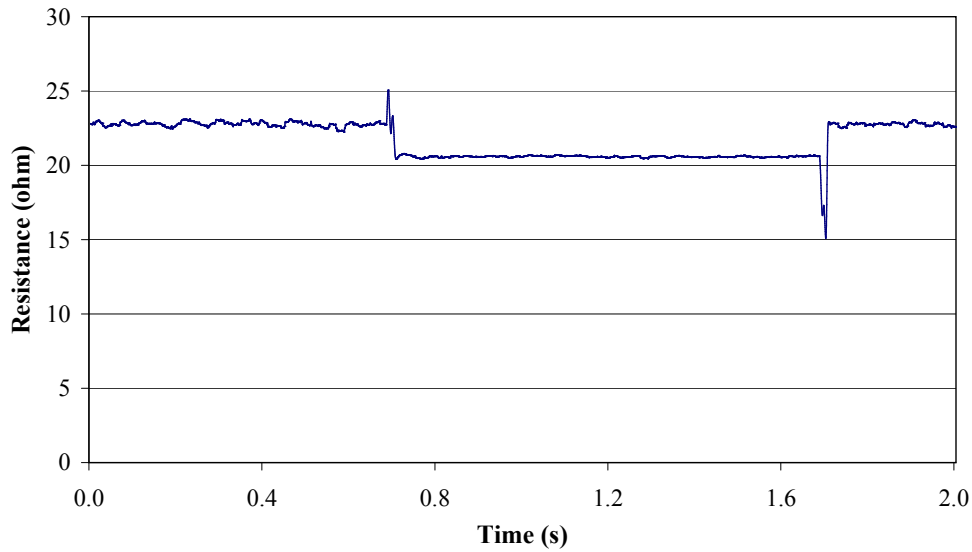


Figure 4.5: Error in resistance measurement in combination with step change in load.

The resistance that was used was 20.8Ω . The load was step changed at around 0.7 seconds and then stepped back to the original value at 1.7 seconds. A major difference in the measured impedance with the introduction of a step change in load is noted. The error in the measured current reading becomes smaller as the current increases. This can be seen from the time period of between 0.7 and 1.7 seconds. The problem is that the error reaches a maximum of 13% under light loading conditions. This error is too large to make the system practically implementable.

In a similar manner the inductance used for the experiment was 42mH. Figure 4.6 shows that the value of the measured inductance also has a step change with the load although it is not as large.

The total error introduced in the measurement of the system is dependant on many factors.

- The voltage and current probes may introduce a small error.
- This might be compounded with an error in the measurement of the DSP unit.
- There is also the error due to the inequality of the clock frequencies of the separate DSP units.

Even if the error introduced by one of these factors is less than 5%, the compounded error

Inductance measurement

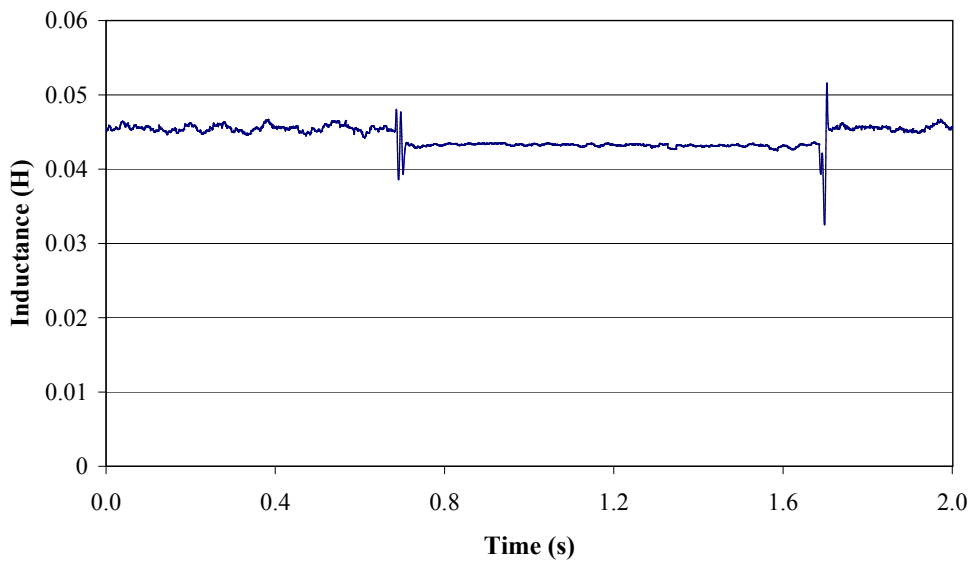


Figure 4.6: Error of the measured inductance in combination with step change in load.

may not be.

The only way to reduce the error introduced by the probes to a small enough value is to increase the quality of the probe. For this reason the current transformers (CT's) that were originally proposed for the current measurements had to be replaced by more expensive but accurate Hall effect current sensors. Even with this, errors were still introduced between the two opposite measurements. Figure 4.7 and Figure 4.8 was possible only after finding two current probes that matched each other exactly in phase and magnitude.

As can be seen from Figure 4.7 the impedance measurement is more stable and constant, even when a major step change in load is introduced.

The problem shown above is not only limited to the current measurements. The voltage had to also be measured on both sides of the transmission line. In order to accurately match the voltage measurement, differential voltage probes were used.

It should be noted that the matching of the current and voltage probes are not the only factor of importance. The active and reactive power at a the measurement point also needs to be recorded. This is directly dependant on the phase angle measured between the voltage and the current signal. The probes had to be very accurate in their relaying of

Resistance measurement

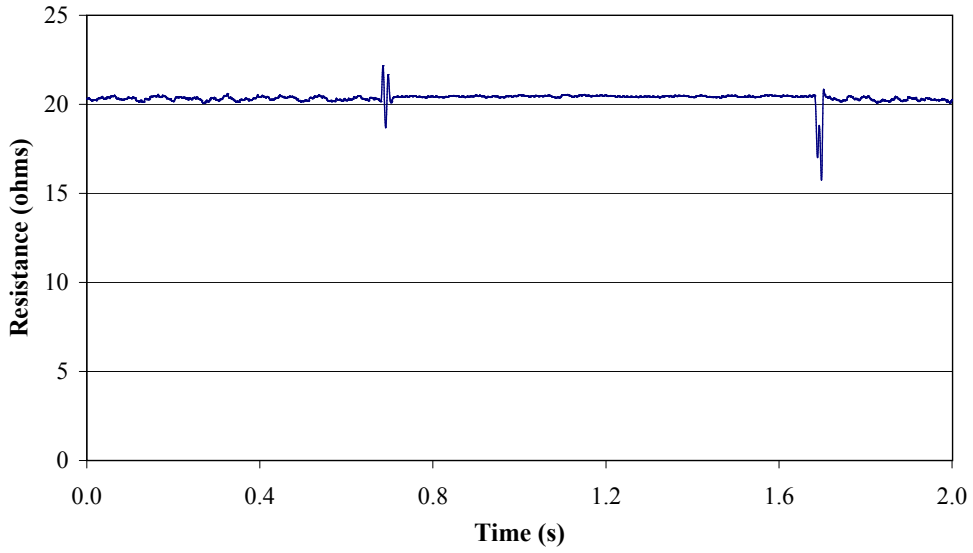


Figure 4.7: Error in resistance measurement in combination with step change in load.

Inductance measurement

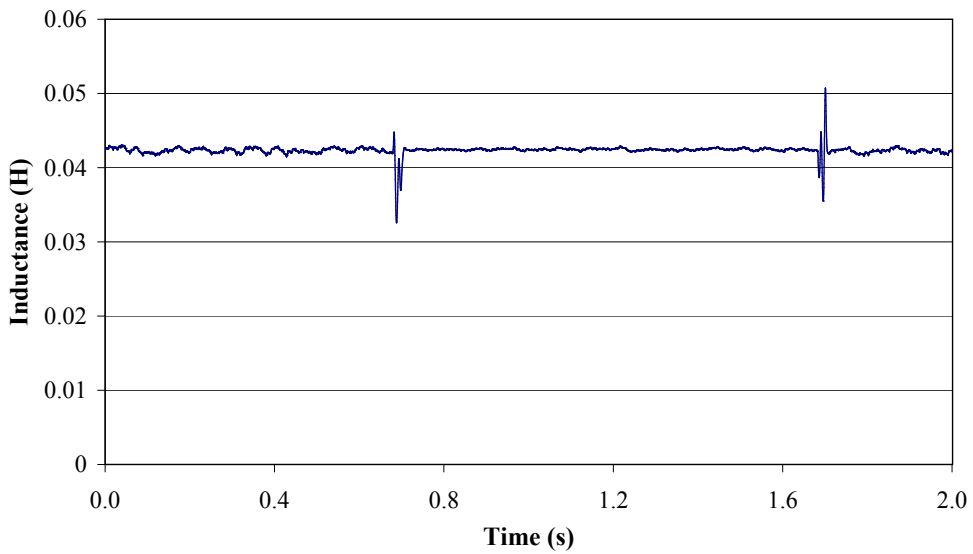


Figure 4.8: Error of the measured inductance in combination with step change in load.

the original signal in the circuit. This is used for the justification of the high-end measuring equipment used.

4.3 GPS MODULES

The baud rate of the serial communication from the GPS modem and the simulation time of the SIMULINK model were dependent on each other. By reducing the model's frequency, the amount of data points sampled per cycle was dramatically reduced. This made it possible for larger errors to be incorporated.

The time pulse duration had to be altered such that it does not get triggered more than once a second. Increasing the 1PPS period to more than one second was not feasible, as it took about one second for the phase error between the measurements to reach one data point.

4.4 COMMUNICATION

GPRS network connection covers a large section of the country. A GPRS modem makes use of dynamic IP addresses. Finding a specific computer and communicating to it can be very difficult as a result. There are providers that provides fixed IP addresses that can be used in conjunction with the modem.

4.5 SUBSTATION VT AND CT ERRORS

The magnitudes of voltage and current is measured in substations by the instrumentation on the network. By the use of voltage transformers (VT's) and current transformers (CT's) the transmission or distribution waveforms are measured. The voltage level is reduced to 110V and the current is stepped down to 5A. The problem is that CT's and VT's introduce phase and magnitude errors, since they are not highly accurate.

From the measurement section it is seen that phase and/or magnitude errors will introduce a major error in the calculation of the line parameters. The errors can be reduced by compensating in the measurements for the phase and magnitude. In the MATLAB model this can be accomplished by adding a phase shift and a gain to each of the measured values.

The problem is that there is no way to determine the actual errors introduced except through measurement of each individual device. Since the utility generally have no records of these values, it is a huge task to measure the errors and create a database.

5 METHOD AND EXPERIMENTAL SETUP

5.1 METHOD

The methods used to determine the SIL curve and the transmission line parameters are exactly the same for both simulation and practical implementation. The only difference is that time-stamping does not have to be done in the simulations since all the data is on one personal computer. However in practice when measurements are done on two opposite sides of a transmission line the measured values have to be time-stamped. The reason for this is that the measurements are done by two separate units that could be kilometers apart. When the measured data is later combined, the time-stamp is used to compare data from the exact same times.

5.1.1 *GPS modem communication*

The GPS modem provides two usable outputs in the form of a pulse per second and serial data communication. Since the system is controlled by means of a SIMULINK model, for the lab implementation, the serial communication had to be done with a MATLAB function as well.

The first step in reading data from the RS232 port was to configure the baud rate of the GPS modem. Due to the dependency between the simulation frequency and the baud rate of the serial communication, the fastest possible baud rate for the GPS modem was limited. This baud rate was 115200 with a resultant simulation frequency of 0.2 milliseconds. This translated to a sampling frequency of 5kHz which meant that 100 discrete data points would represent a fundamental cycle (50Hz).

The second issue was the decoding of the actual serial data received from the GPS modem. Every section of data that is transmitted through the RS232 port is preceded by a unique code. For the time and data that code is "GPZDA:". This is specific to the GPS modem used. The function in MATLAB was written so that the incoming data was decoded one bit at a time. The ASCII code for characters was used to first find the 'G' then the 'P' and so forth until the whole string is recognized in the correct order. There is a single space after the string and then the time follows directly.

By reading each of the bit values that follow the space into a variable, the time can be determined. In the same way, the date is determined by reading the numbers that follow the time. The process is described in Figure 5.1.

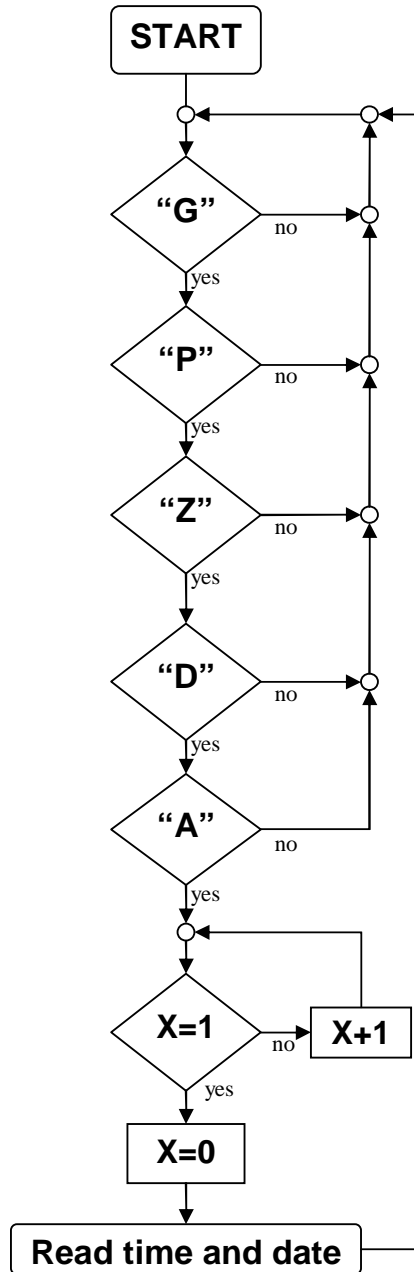


Figure 5.1: Flow diagram describing the process of reading the time and date from a GPS modem.

5.1.2 GPRS modules

The GPRS modules that were purchased for use in the project was the Siemens MC35i terminals. Since the GPRS functionality is used of a mobile service provider, SIM cards had to be purchased. The standard SIM cards that are bought are not data enabled by

default. Therefore, this had to be enabled by the service provider before continuing.

The SIM cards are placed in the GPRS modules. The module can receive and send short messages, make phone calls and be a fax modem besides acting as a modem for connecting to the internet. The GPRS modem connects to a PC through the RS232 port. It was decided against using the GPRS modem for field implementation since the utility has field recorders in place with remote data sending capability.

5.1.3 Transmission line parameter determination

From the onset of the project three methods were considered for determining the parameters of the line from measured data.

Method 1

Equation (5.1) shows a method of approximating the line impedance value (Z_L). The line impedance value represents the series resistance and inductive reactance of the transmission line.

$$Z_L = \frac{(V_S - V_R)_{RMS}}{I_{RMS}} \quad (5.1)$$

The sending end voltage (V_S) is measured at the beginning of the power line in question, while the receiving end voltage (V_R) is measured at the termination of the line. V_S and V_R are subtracted discretely from each other. The rms value of the resultant waveform or the equivalent voltage drop across the transmission line is recorded. The rms current can be either sending or receiving end values.

For a short transmission line the sending and receiving end current is approximately the same (Figure 1.1). It does not matter which current value is used in (5.1). When medium and long transmission lines are being considered, the influence of the line capacitance begins to have an influence on the model (Figure 1.2 and Figure 1.3) and thus the sending and receiving end current will differ in both magnitude and phase.

Since the line models shown in the introduction is for phase to neutral values, the model only accounts for balanced system operation. In view of this, the practical implementation of the project needs to measure only one current and one voltage (phase to neutral) value. To test the method thoroughly all the phases will be considered.

The line reactance can have a leading or lagging component that it adds to the load current. This will depend on the loading on the line [26]. This means that the absolute value of current measured on the one side of the line can be either smaller or larger than that of the other side. It was found that the larger of the two currents gives the best estimate of the total current through the series resistance and inductance [27].

The drawback of this method is that only the impedance magnitude of the line is determined by (5.1), and excludes the phase angle. If the phase angle is not known the exact portion of the line impedance that represents resistance and reactance can not be determined. The X/R ratio of the transmission line can be used to approximate the resistance and the reactance from the impedance value. The X/R ratio of a transmission line is the approximate ratio between the inductive reactance and the resistance of a transmission line. This is provided by the manufacturer. It should be kept in mind that this is only an approximation, because the inductance and resistance of a line vary depending on a number of factors.

Method 2

A different method that was considered involved determining the total impedance as seen from the sending end (Z_T , *i.e.* the line and load impedance). At the same time the impedance at the receiving side must be calculated (Z_{load}). This constitutes the load impedance. Equation (5.2) was used for the calculation of both Z_T and Z_{load} .

$$Z = \frac{(V)_{RMS}}{(I)_{RMS}} \quad (5.2)$$

In (5.2) the rms voltage and current is the sending end values when Z_T is calculated and the receiving end values when Z_{load} is calculated.

By working out the active (P) and reactive power (Q) on both the sending and receiving sides the value of the angle between the voltage and current is determined [28], [29].

$$\theta = \tan^{-1} \left(\frac{Q}{P} \right) \quad (5.3)$$

This angle is used to separate the impedance values into the resistive and reactive compo-

nents. This is easily subtracted from each other to determine the line parameter values.

$$Z_L = (Z_T \cdot \cos \theta_T - Z_{load} \cdot \cos \theta_{load}) + j (Z_T \cdot \sin \theta_T - Z_{load} \cdot \sin \theta_{load}) \quad (5.4)$$

The benefit of using this method is that the series line impedance is given in terms of the resistance and inductive reactance, *i.e.* $R = (Z_T \cdot \cos \theta_T - Z_{load} \cdot \cos \theta_{load})$ and $X = (Z_T \cdot \sin \theta_T - Z_{load} \cdot \sin \theta_{load})$.

Method 3

Method 3 was first proposed in [30]. This method uses the two-port ABCD parameters that is defined in [1]. The ABCD parameters give the relationship between the voltages and currents at two points. For a transmission line this means that the ABCD parameters represent the influence that the capacitance, inductance and resistance of the line has on the voltage and current values measured at the sending and receiving sides. The relationship is given by the following equations.

$$V_s = AV_r + B I_r \quad (5.5)$$

$$I_s = CV_r + B I_r \quad (5.6)$$

A and B is defined with the following equations.

$$A = \cosh \gamma l \quad (5.7)$$

$$B = Z_c \sinh \gamma l \quad (5.8)$$

The variable γ was defined in (1.3) and Z_c by (5.9).

$$Z_c = \sqrt{\frac{z}{y}} \quad (5.9)$$

From the preceding equations it is seen that once A and B is known, z and y can be calculated. In (1.3) z and y have been defined as the series impedance and shunt admittance per unit length. In order to solve A and B two operating points that are linearly independent have to be considered. A matrix can be constructed for the measurements of the two cases.

$$\begin{bmatrix} V_{s1} \\ V_{s2} \end{bmatrix} = \begin{bmatrix} V_{r1} & I_{r1} \\ V_{r2} & I_{r2} \end{bmatrix} \begin{bmatrix} A \\ B \end{bmatrix} \quad (5.10)$$

Using Cramer's Rule, A and B can be calculated.

$$A = \frac{\det \begin{bmatrix} V_{s1} & I_{r1} \\ V_{s2} & I_{r2} \end{bmatrix}}{\det \begin{bmatrix} V_{r1} & I_{r1} \\ V_{r2} & I_{r2} \end{bmatrix}} \quad (5.11)$$

$$B = \frac{\det \begin{bmatrix} V_{r1} & V_{s1} \\ V_{r2} & V_{s2} \end{bmatrix}}{\det \begin{bmatrix} V_{r1} & I_{r1} \\ V_{r2} & I_{r2} \end{bmatrix}} \quad (5.12)$$

To calculate y and z , the results from (5.11) and (5.12) are substituted into (5.7) and (5.8), while Z_C and γl is substituted with (5.9) and (1.3). This will provide two equations with two unknowns to solve.

This method is very useful since the impedance is given as a value with an angle. This means that the resistance and inductance is given as separate values. This is also the only method that gives the shunt admittance (y), from where the capacitance can be calculated.

5.1.4 Determining the SIL curve

In Chapter 1, it was mentioned that the surge impedance load (SIL) curve is a graph of the reactive power used by the line verses the active power that is supplied to the load. By taking measurements over time, with changing loads, a database of measured points is built up that can be used to draw the SIL curves. The only measurements that need to be taken is that used for determining the transmission line parameters.

Figure 5.2 shows a practical example of what a SIL curve looks like. The first step is to determine the power factor of the load. The cosine of θ_{load} , determined with (5.3), is used to calculate this. Every power factor (within a range of 0.1) will have its own SIL curve. The active power transferred to the load is calculated from the voltage and current measurements taken at the receiving end of the line. Using time-stamped values and

subtracting the sending and receiving end reactive power, the net reactive power provided or absorbed by the transmission line is determined.

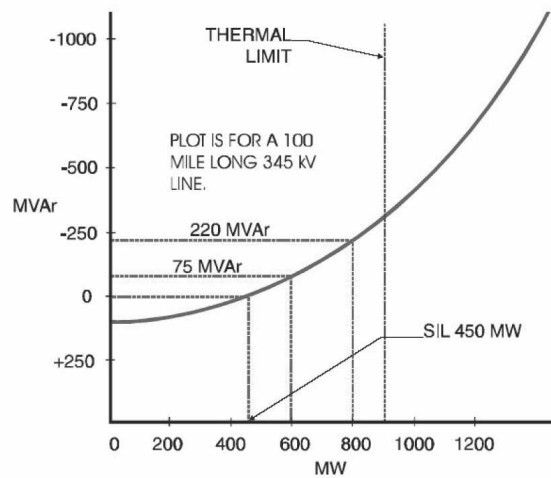


Figure 5.2: A SIL curve.

5.2 EXPERIMENTAL SETUP

5.2.1 Simulation

MATLAB SIMULINK was used to test the various methods described above. The first test was to determine whether it was possible to calculate the transmission line parameters accurately by means of voltage and current measurements taken on either side of the line. As noted in the previous subsection three different methods were considered for the calculation of the line parameters. Each of these methods were simulated for the same setup described below.

Line parameters

The Simulink model that was used is shown in Figure 5.3. The length of the transmission line (T1) was varied to simulate the short, medium and long line. The transmission line model made use of distributed line parameters for the resistance, inductance and the capacitance. This more closely mimics a real transmission line. The three-phase generator (G1) shown in Figure 5.3 is quantified as having a terminal voltage of 132kV with a system frequency of 50Hz.

The parameters as well as line lengths used for the simulation of each case is given in Table 5.2. In order for a sizable current to flow in the lines, loads were connected to the line

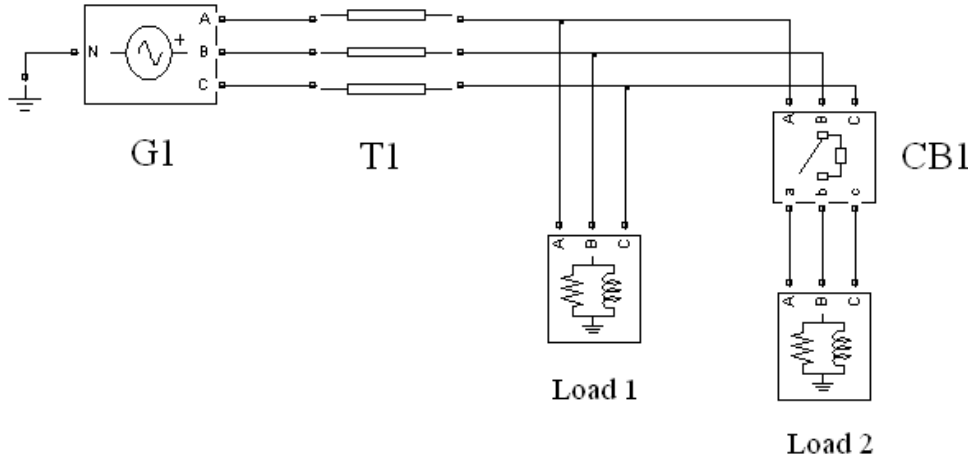


Figure 5.3: Simulation circuit used for line parameter determination.

in Figure 5.3. Only Load 1 is connected during light loading conditions. During heavy loading conditions Load 2 is switched in with the circuit breaker (CB1).

Method 3 relies on a change in load to determine the parameters. For this reason two loads were placed on the transmission line. For the first second of the simulation a light load was placed on the transmission line. Thereafter a circuit breaker switched in the second load. Under heavy loading the circuit was simulated for another second. This means that Method 1 and Method 2 is simulated for a total of two seconds. Method 3 uses both sets of loading results to calculate the parameters for one second. Table 5.1 quantifies the two loads used in the simulations.

	Short line	Medium line	Long line
Light loading (VA)	600+j330	600+j330	600+j330
Heavy loading (VA)	1200+j660	1200+j660	1200+j660

Table 5.1: Sizes of loads.

The impedance values is calculated with measured currents and voltages. These are compared to the impedance values calculated from the parameters in Table 5.2. By doing this the accuracy and feasibility of the method can be determined.

SIL curve

The next test was to determine whether it would be possible to draw a SIL curve from the measured data across a transmission line. The model that was used to determine the

Parameters	Transmission-line		
	Short line	Medium line	Long line
R (Ω)	6.50	19.50	58.50
L (mH)	46.69	140.06	420.17
C (μ F)	1.64	4.91	14.73
Length (km)	50	150	450
Z _{calculated} (Ω)	16.04	48.13	144.38

Table 5.2: Parameters for the transmission lines shown in Figure 5.3.

feasibility of the SIL curve is shown in Figure 5.4.

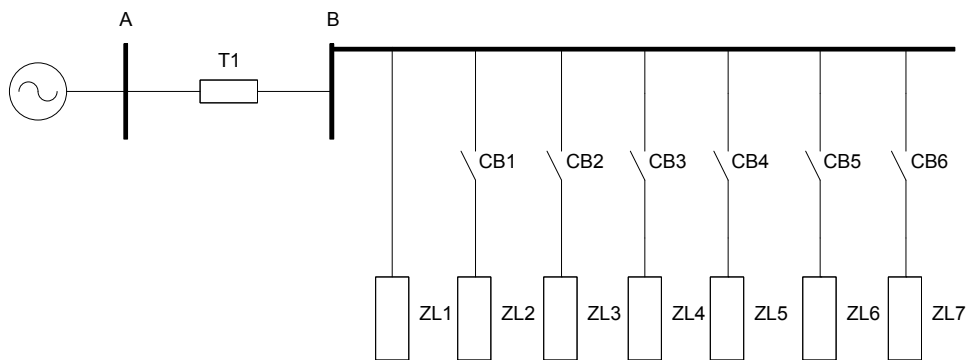


Figure 5.4: Simulation circuit used for drawing the SIL curve.

The figure shows seven loads with six circuit breakers. The circuit breakers are used to switch the selected load across the power line. Every 0.7 seconds a circuit breaker is closed so that the total load would increase. The simulation was done over a total time of 4.9 seconds. The power factor of the load must be kept the same for all seven of the loads. The reason for this is that the transmission line reacts differently to different amounts of reactive power transferred.

For this part of the simulation three SIL curves were constructed under three distinct operating conditions. For the first and second conditions the loads had a power factor of 0.5 and 0.9 respectively. The last simulation was done for loads with varied power factors. In Table 5.3 the values of the loads that were used are shown.

5.2.2 Lab implementation

A DSPACE interface is used to take the measurements for the laboratory results. The serial communication from the GPS modem was connected to the DSPACE interface. The

Time (s)	Load (MVA)		
	PF = 0.5	PF = 0.9	Mixed PF
0-0.7	20	11.110	11.11
0.7-1.4	30	16.665	21.11
1.4-2.1	50	27.775	41.11
2.1-2.8	60	33.330	46.66
2.8-3.5	80	44.440	66.66
3.5-4.2	90	49.995	76.66
4.2-4.9	110	61.105	87.77

Table 5.3: Size of impedance load in conjunction with time over the power line in Figure 5.4.

reason DSPACE was used is that it connects directly to a SIMULINK model that is created in MATLAB and allows real time simulations. The connection diagram for the whole system is shown in Figure 5.5.

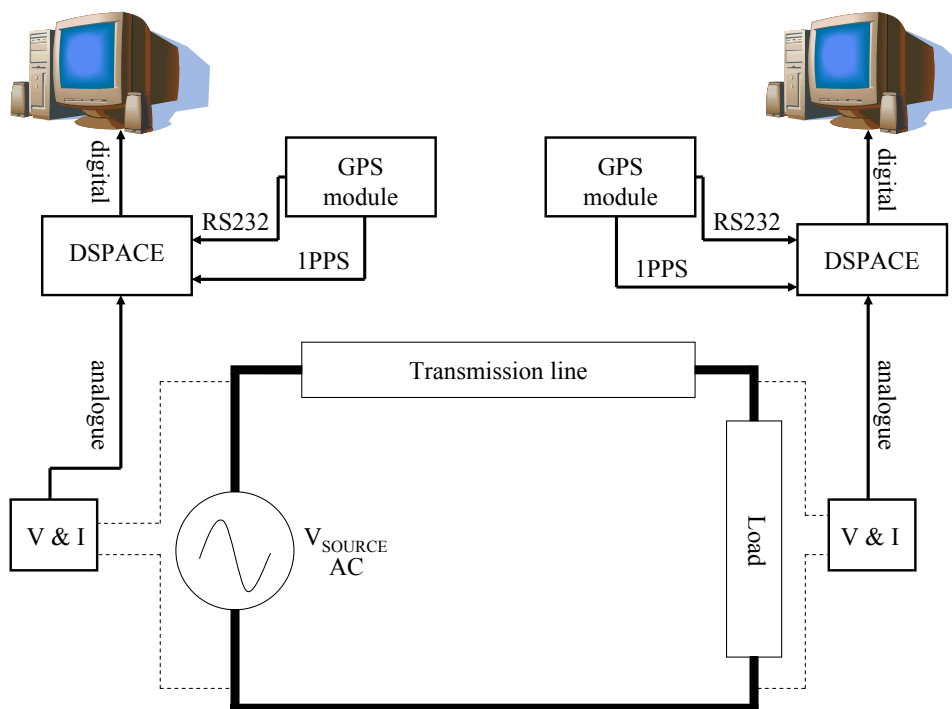


Figure 5.5: The connection diagram for the setup in the laboratory.

It is difficult to simulate in a lab the capacitance of a transmission line that builds up over the entire length of the line. Thus to prove the concept lumped capacitor, resistor and inductor values were used. Referring back to Figure 1.1-Figure 1.3, the line parameters were defined between line and neutral for a three phase system. Taking this into consideration the setup shown in Figure 5.6-Figure 5.8 was used to measure the line impedance for the different lines.

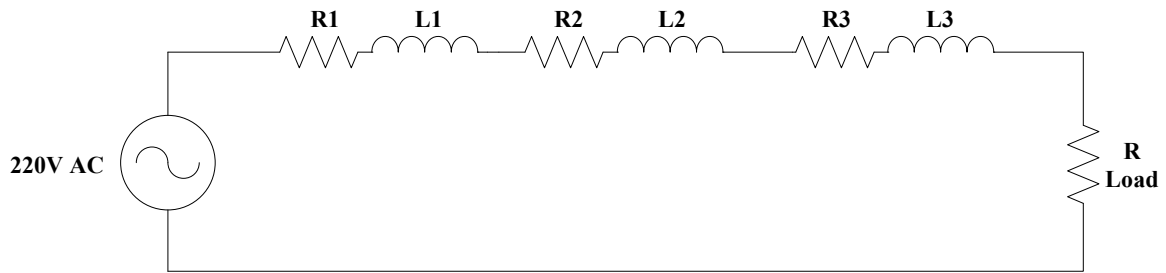


Figure 5.6: The experimental setup in the laboratory representing a short line.

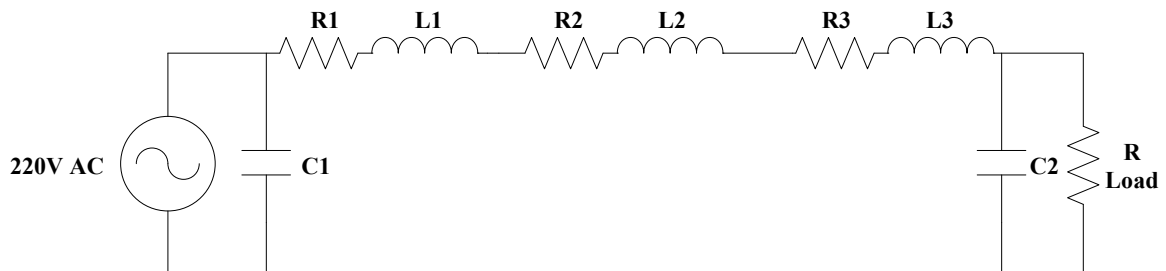


Figure 5.7: The experimental setup in the laboratory representing a medium line.

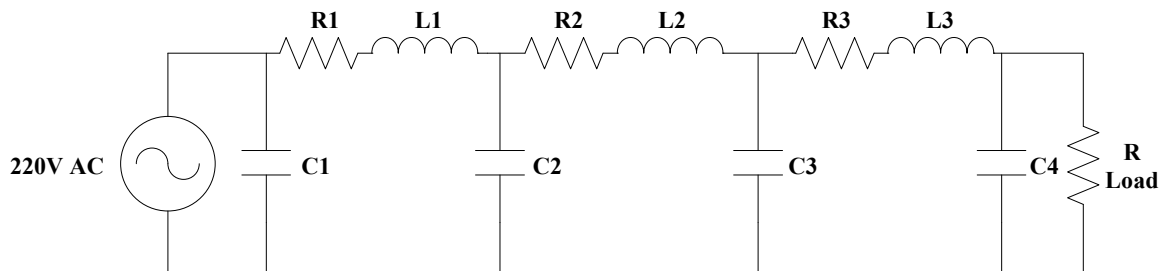


Figure 5.8: The experimental setup in the laboratory representing a long line.

The resistances defined as (R1-R3) and inductances (L1-L3) were used to represent the transmission line. Different resistive values were used to test the accuracy of the methods against the actual values. The power factor across a transmission line is close to unity thus only a resistor (R load) was used to represent the load. This ensures that the system closely resembles real loading conditions. The load was also varied.

Method 3 needs a change in load to determine the parameters of a line. Method 1 and Method 2 use instantaneous values to determine parameters. There are two results for Method 1 and Method 2 while Method 3 has one. The test values that were used for the laboratory setup is given in Table 5.4.

Line type	Case 1			Case 2		
	Short	Medium	Long	Short	Medium	Long
R1	9.13 Ω	9.13 Ω	9.13 Ω	4.3 Ω	4.3 Ω	4.3 Ω
R2	8.23 Ω	8.23 Ω	8.23 Ω	3.4 Ω	3.4 Ω	3.4 Ω
R3	7.23 Ω	7.23 Ω	7.23 Ω	1.9 Ω	1.9 Ω	1.9 Ω
L1	38.81mH	38.81mH	38.81mH	38.81mH	38.81mH	38.81mH
L2	41.43mH	41.43mH	41.43mH	41.43mH	41.43mH	41.43mH
L3	40.19mH	40.19mH	40.19mH	40.19mH	40.19mH	40.19mH
C1	-	19.98 μ F	19.98 μ F	-	19.98 μ F	19.98 μ F
C2	-	19.73 μ F	19.95 μ F	-	19.73 μ F	19.95 μ F
C3	-	-	19.96 μ F	-	-	19.96 μ F
C4	-	-	19.73 μ F	-	-	19.73 μ F
R Load (Light load)	107.6 Ω	107.6 Ω	107.6 Ω	107.6 Ω	107.6 Ω	107.6 Ω
R Load (Heavy load)	43.2 Ω	43.2 Ω	43.2 Ω	43.2 Ω	43.2 Ω	43.2 Ω

Table 5.4: The values for the line parameters used in Figure 5.6-Figure 5.8.

The measurements for the lab implementation was done with two separate DSPACE units. The units were connected to two personal computers with GPS modems. This was done to test whether the two measuring units would be able to operate independently. This is to ensure that the system can be implemented practically. The measurements recorded by the first computer was taken across the voltage source to encompass the whole system. The second computer measured the voltage and current of R Load.

The SIL curve is the product of the interaction of naturally occurring impedance of the line and power absorbed by the load. A line cannot be modelled this accurately in a laboratory. This means that a SIL curve cannot be accurately determined in a laboratory. The simulation results is the only indication that the SIL curve would work. Since the SIL curve is dependant on the accuracy of the measured active and reactive power, the simulation results proved satisfactory.

5.2.3 Field implementation

For the field implementation, fault data from utility recorders were used. Due to this fact, there were no complex systems to install. The data from the records were directly used to test Method 1, Method 2 and Method 3.

To test the methods on the field data, a reference is needed in the measured data. For permanent implementation this reference would be provided by GPS units on the sending

and receiving sides of a transmission line. Since the field data was fault recordings, the reference point is provided by the event itself.

The next chapter presents simulation results obtained using the three methods.

6 SIMULATION RESULTS

6.1 LINE PARAMETER DETERMINATION

The first part of the simulation results deals with determining the line parameters. In section 5.1.3 three ways of calculating line parameters were discussed, their results are presented here.

6.1.1 Method 1

Short line

The results for the transmission line of Figure 5.3 are shown below. The parameters and loading for the short transmission line is given in Table 5.2 and Table 5.1. For the sake of completeness the same two loading conditions used for Method 3 is used to simulate Method 1 and 2. This ensures that the results of all three methods can be compared with each other.

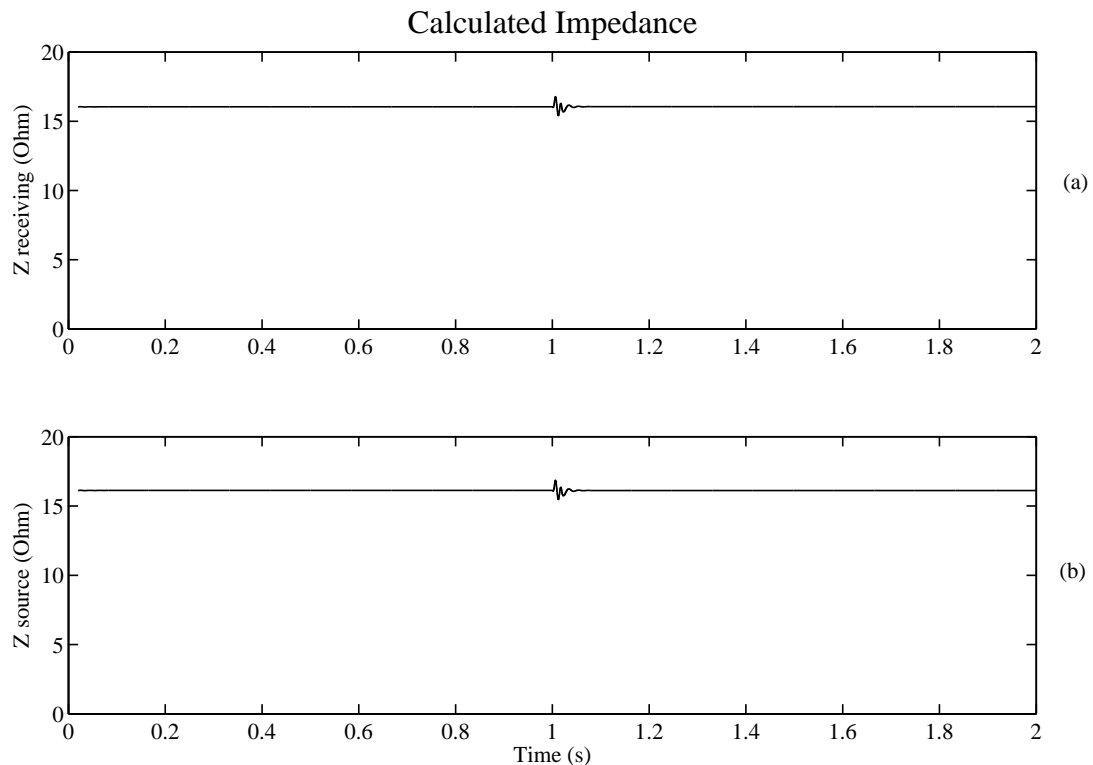


Figure 6.1: Line impedance of the 50km simulated line using Method 1.

Figure 6.1a gives the calculated impedance with the receiving end current substituted into (5.1). Figure 6.1b was calculated with the sending end current. Table 6.1 shows the results

from the simulation.

	Light loading	Heavy loading
Z receiving measured (Ω)	16.03	16.05
Z source measured (Ω)	16.12	16.12
Z actual (Ω)	16.04	16.04
Z receiving % error	0.06%	0.06%
Z source % error	0.50%	0.50%

Table 6.1: Errors introduced in the calculated parameters of a short transmission line by using Method 1

Medium line

The results for the medium transmission line is given in the same way it was for the short line. The results from the simulation of the medium transmission line is given in Figure 6.2 and Table 6.2.

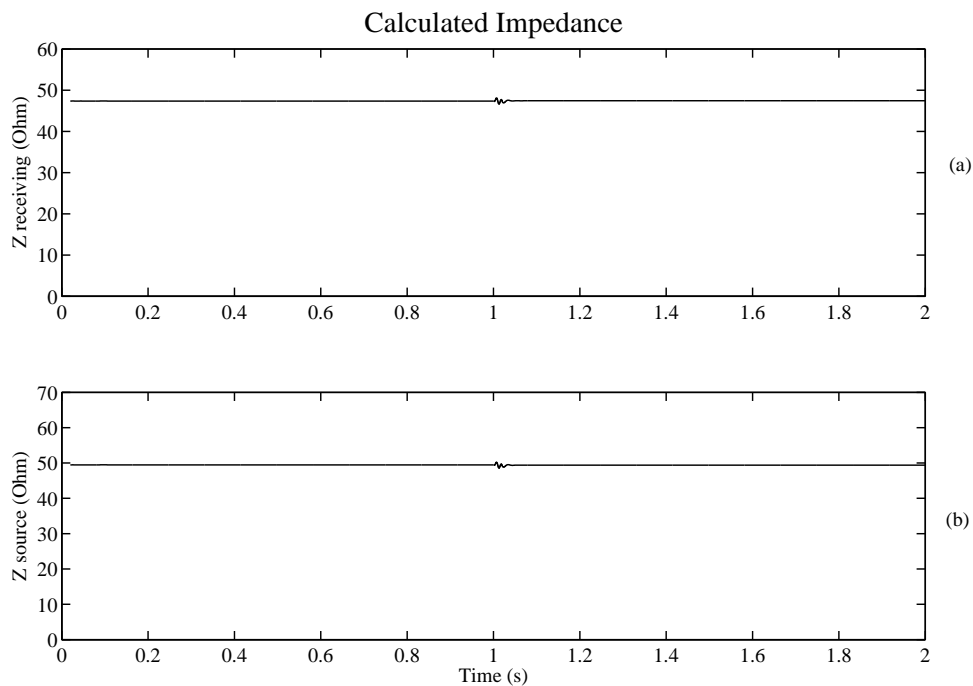


Figure 6.2: Line impedance of the 150km simulated line using Method 1.

	Light loading	Heavy loading
Z receive measured (Ω)	47.38	47.45
Z source measured (Ω)	49.46	49.38
Z actual (Ω)	48.13	48.13
Z receive % error	1.56%	1.41%
Z source % error	2.76%	2.60%

Table 6.2: Errors introduced in the calculated parameters of a medium transmission line by using Method 1.

Long line

Figure 6.3 and Table 6.3 shows the values and graphs for the long transmission line.

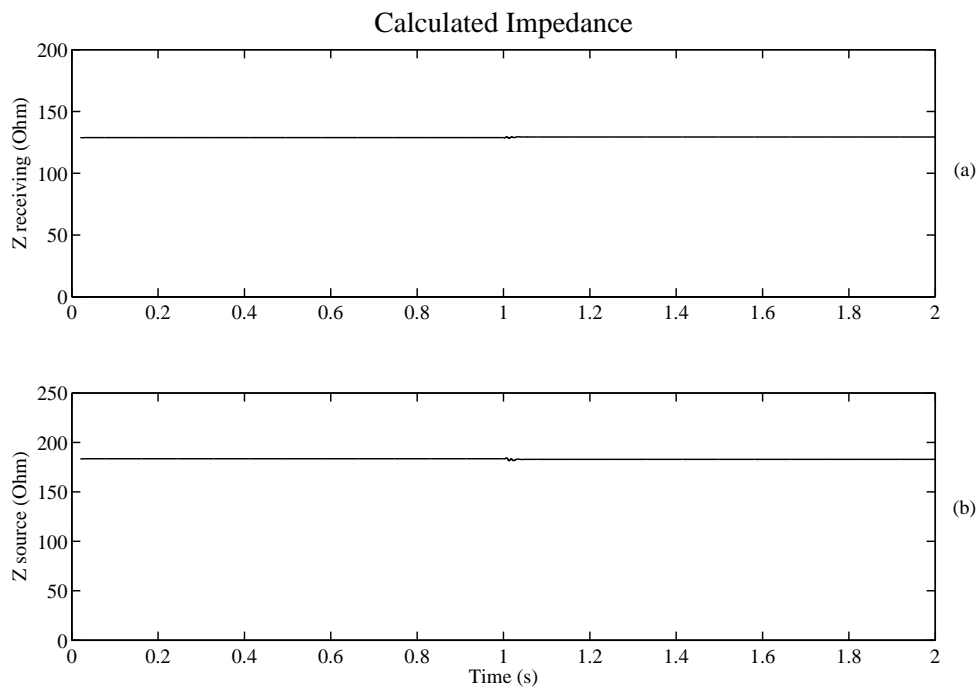


Figure 6.3: Line impedance of the 450km simulated line using Method 1.

	Light loading	Heavy loading
Z receive measured (Ω)	128.8	129.4
Z source measured (Ω)	183.4	182.8
Z actual (Ω)	144.4	144.4
Z receive % error	10.80%	10.39%
Z source % error	27.01%	26.59%

Table 6.3: Errors introduced in the calculated parameters of a long transmission line by using Method 1.

6.1.2 Method 2

Short line

The results for Method 2 is also based on the setup given in Figure 5.3. The results for the short transmission line are quantified in Table 6.4. Results are provided for the line resistance (Figure 6.4a), line inductance (Figure 6.4b) and the resultant series impedance (Figure 6.4c) of the line.

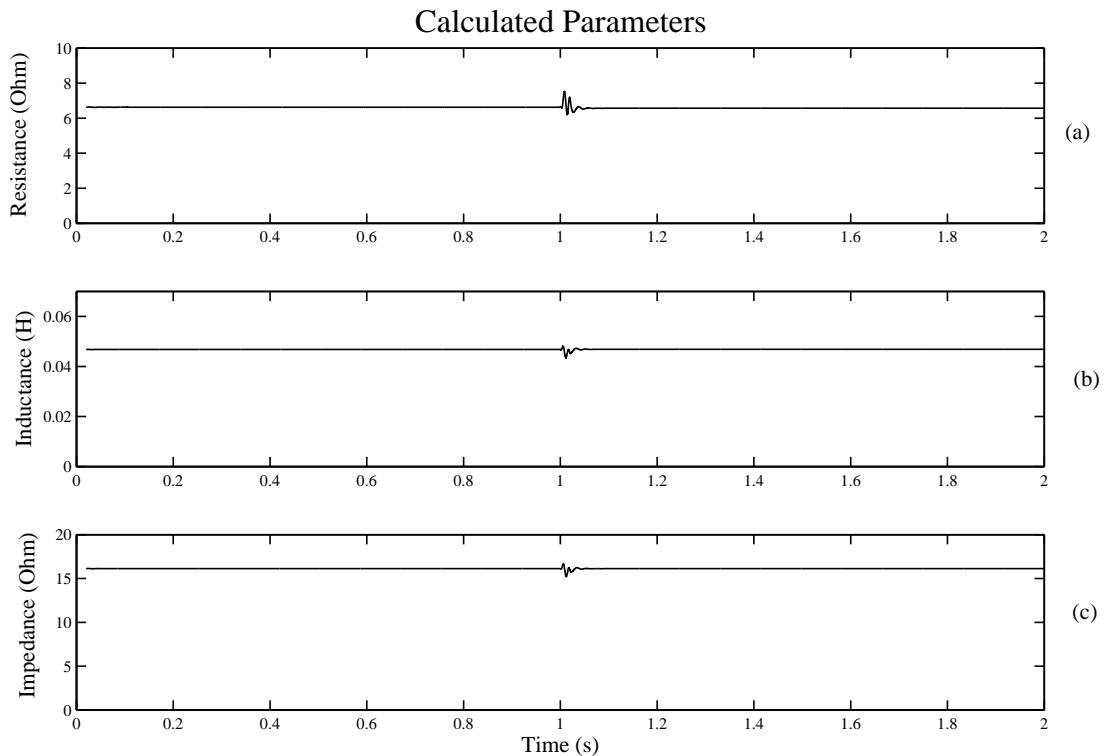


Figure 6.4: Line parameters of a 50km simulated line using Method 2.

The graphs shown in Figure 6.4 were simulated over a time period of 2 seconds. During this period step changes to the loading was made (Refer to Table 5.1).

	Light loading	Heavy loading
R measured (Ω)	6.63	6.57
L measured (mH)	46.79	46.85
Z measured (Ω)	16.13	16.12
R actual (Ω)	6.50	6.50
L actual (mH)	46.69	46.69
Z actual (Ω)	16.04	16.04
R % error	2.00%	1.08%
L % error	0.21%	0.34%
Z % error	0.56%	0.50%

Table 6.4: Errors introduced in the calculated parameters of a short transmission line by using Method 2.

Medium line

The method was applied to the rest of the transmission lines and the parameters were measured. These values are compared to the real parameters to determine the accuracy of the method employed. For the medium transmission line the results are given in Figure 6.5 and Table 6.5.

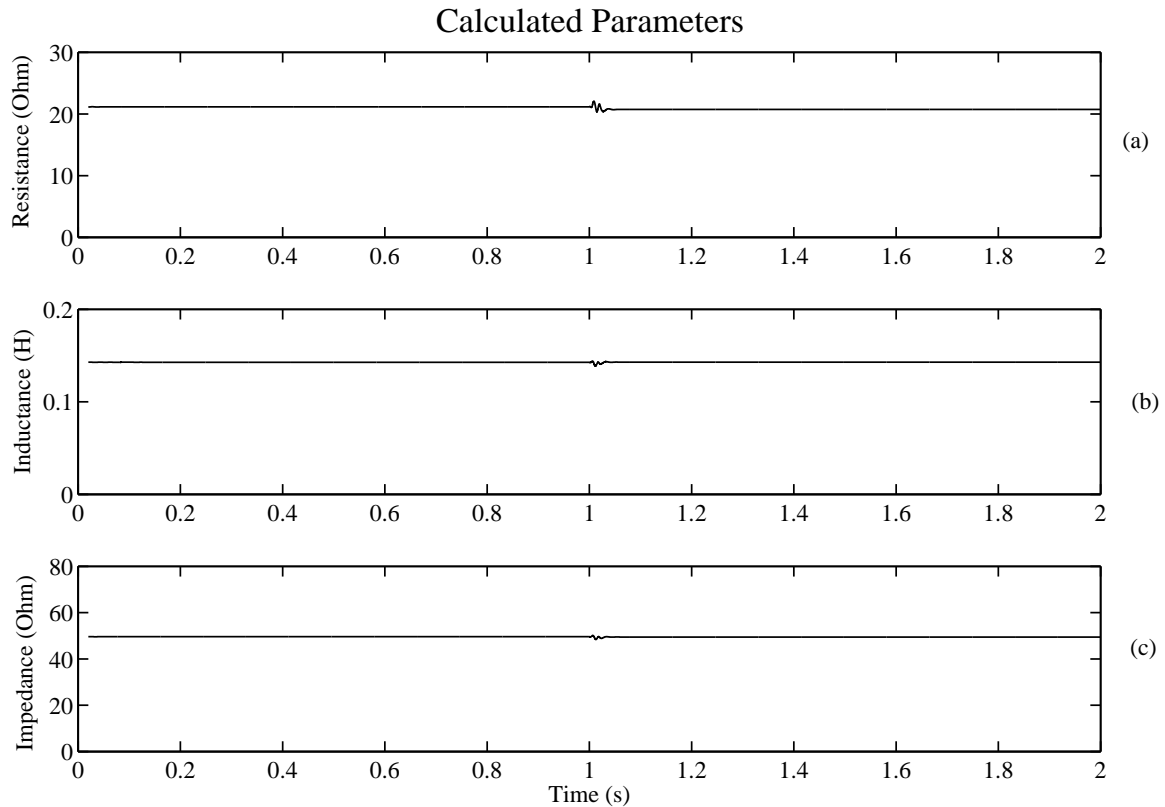


Figure 6.5: Line parameters of a 150km simulated line using Method 2.

	Light loading	Heavy loading
R measured (Ω)	21.14	20.73
L measured (mH)	142.8	142.9
Z measured (Ω)	49.60	49.45
R actual (Ω)	19.5	19.5
L actual (mH)	140.06	140.06
Z actual (Ω)	48.13	48.13
R % error	8.41%	6.31%
L % error	1.96%	2.03%
Z % error	3.05%	2.74%

Table 6.5: Errors introduced in the calculated parameters of a medium transmission line by using Method 2.

Long line

Figure 6.6 gives the graphic results for the long transmission line and Table 6.6 summarizes the recorded minimum and maximum values for each of the measured parameters.

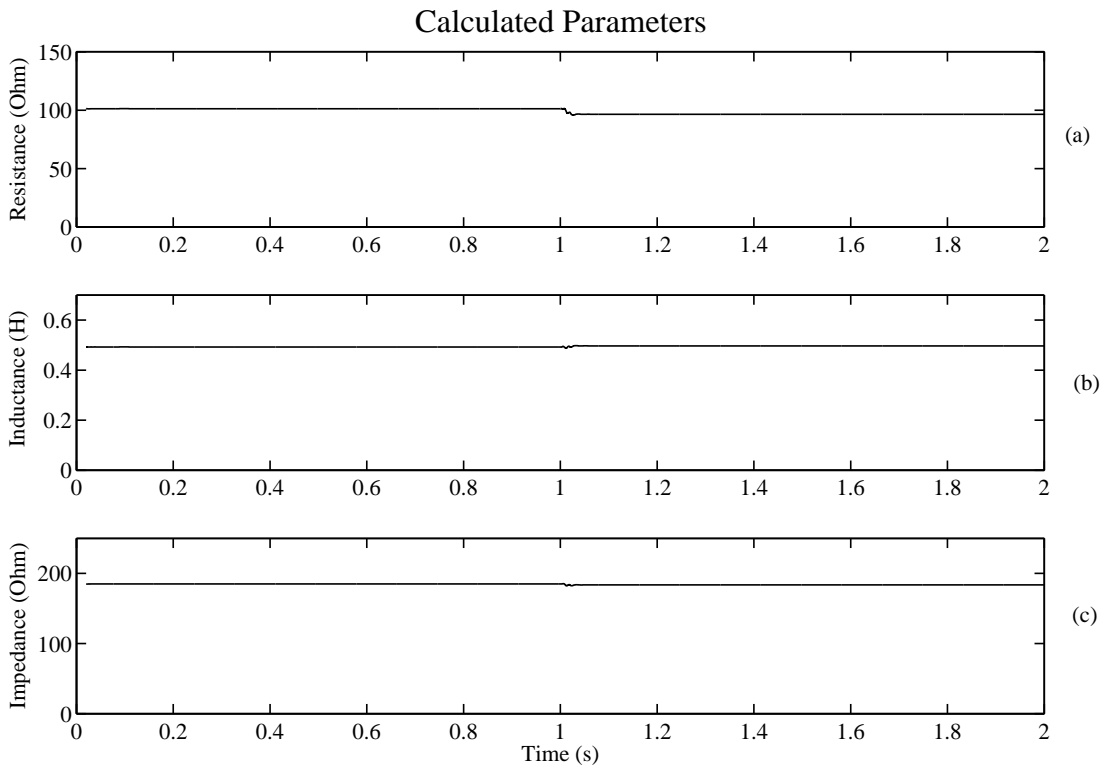


Figure 6.6: Line parameters of a 450km simulated line using Method 2.

	Light loading	Heavy loading
R measured (Ω)	101.2	96.51
L measured (mH)	492.6	497.0
Z measured (Ω)	185.0	183.6
R actual (Ω)	58.5	58.5
L actual (mH)	420.2	420.2
Z actual (Ω)	144.4	144.4
R % error	72.99%	64.97%
L % error	17.23%	18.28%
Z % error	28.12%	27.15%

Table 6.6: Errors introduced in the calculated parameters of a long transmission line by using Method 2.

6.1.3 Method 3

Short line

The setup for Method 3 is the same as for Method 1 and Method 2. The light and heavy loading described in Table 5.1 was used to determine all three line parameters. The results for resistance (Figure 6.7a), inductance (Figure 6.7b) and capacitance (Figure 6.7c) are given.

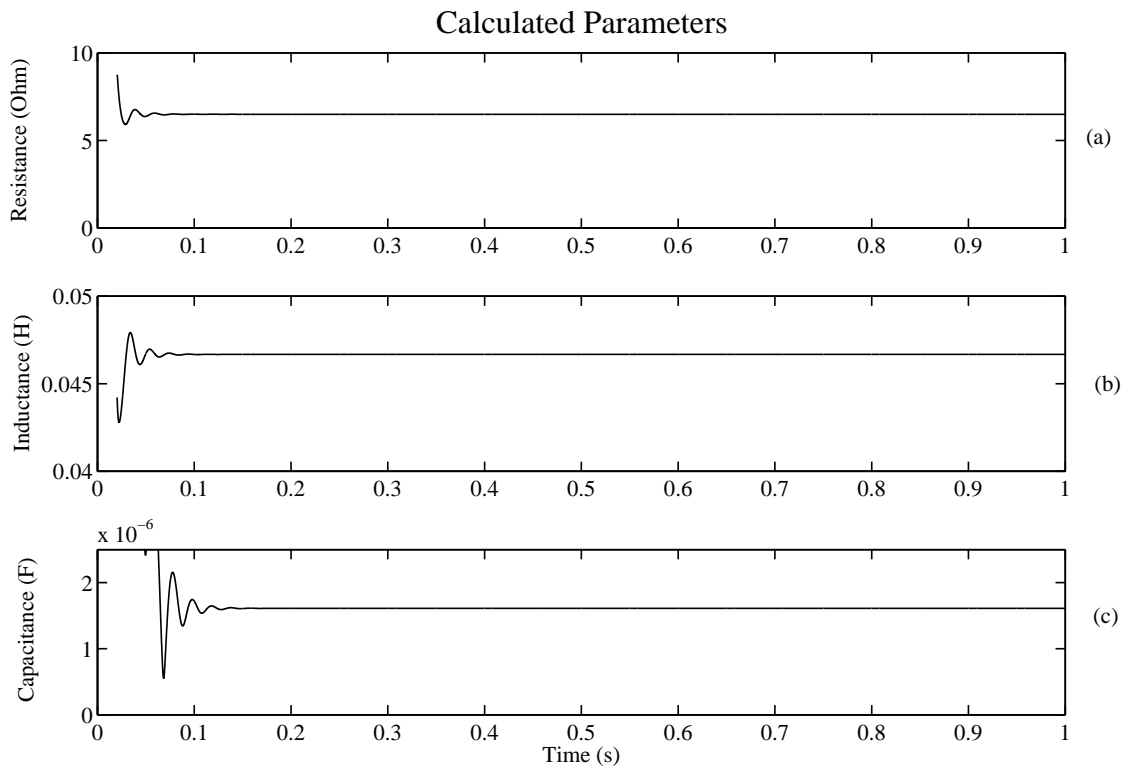


Figure 6.7: Line parameters of a 50km simulated line using Method 3.

The values measured in the simulation of Method 3 is free from external influences like errors in measuring equipment, noise in the system and errors introduced by the method. This means that the results shown in Figure 6.7 is stable even when the loading changes. Therefore only one result is given in Table 6.7 for each of the line parameters.

	R	L	C
Measured values	6.49 Ω	46.68mH	1.61 μ F
Actual values	6.50 Ω	46.69mH	1.64 μ F
% error	0.15%	0.02%	1.83%

Table 6.7: Errors introduced in the calculated parameters of a short transmission line by using Method 3.

Medium line

The results for the medium and long lines are given in the same way as the short line. First the graphs with the results is given, followed by a table that summarizes the results.

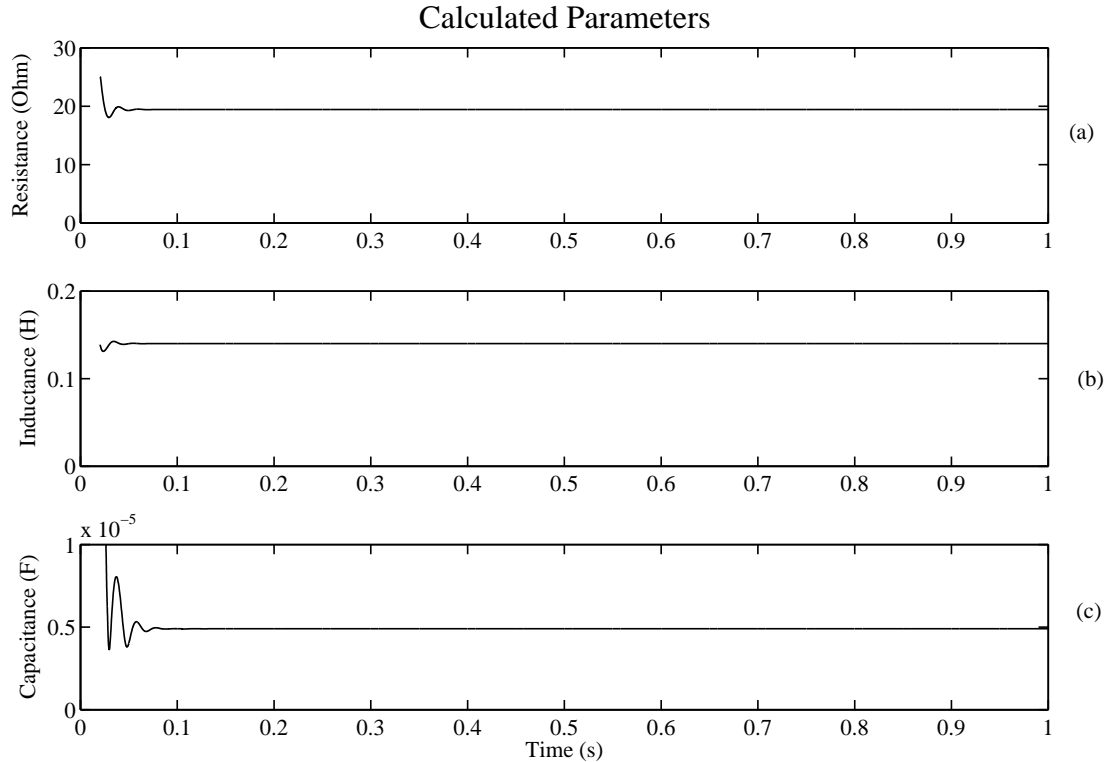


Figure 6.8: Line parameters of a 150km simulated line using Method 3.

	R	L	C
Measured values	19.43Ω	140.10mH	4.90μF
Actual values	19.50Ω	140.06mH	4.91μF
% error	0.36%	0.03%	0.20%

Table 6.8: Errors introduced in the calculated parameters of a medium transmission line by using Method 3.

Long line

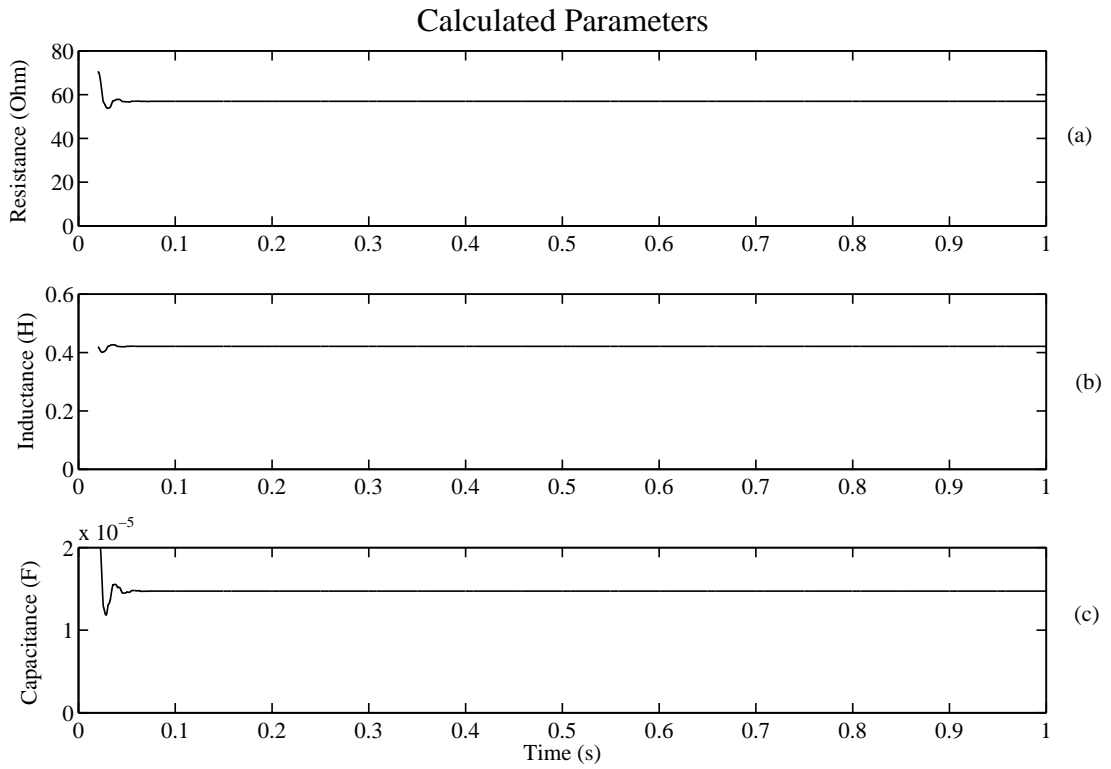


Figure 6.9: Line parameters of a 450km simulated line using Method 3.

	R	L	C
Measured values	56.94 Ω	421.10mH	14.72 μ F
Actual values	58.50 Ω	420.16mH	14.73 μ F
% error	2.67%	0.22%	0.07%

Table 6.9: Errors introduced in the calculated parameters of a long transmission line by using Method 3.

6.2 DETERMINING THE SIL CURVE

This section determines the feasibility of drawing practical SIL curves from measured data. It was mentioned in Chapter 5 that a SIL curve has to be drawn for different power factors. The first SIL curve that was drawn is shown in Figure 6.10. The power factor of the load is 0.5.

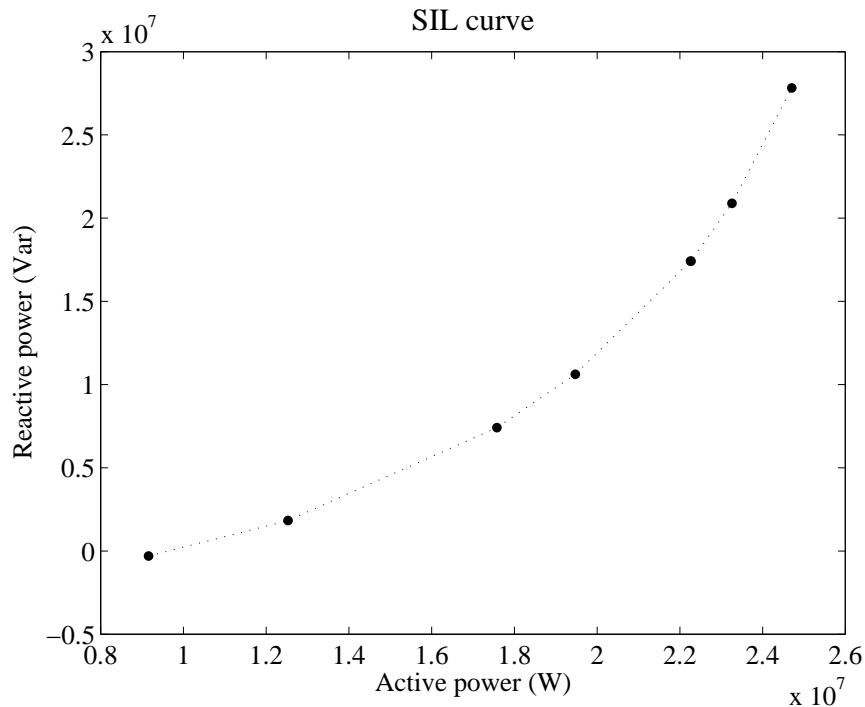


Figure 6.10: SIL curve from simulation of the circuit in Figure 5.4 with a power factor of 0.5.

A power factor of 0.5 is uneconomical. The typical values for the power factor across a transmission is in the range of 0.8 to 0.95. The reason that a power factor of 0.5 was used is to exaggerate the difference in curves between a power factor of 0.9 and 0.5. Both of these power factors are used in a later figure. Figure 6.11 shows the SIL curve that was constructed for a power factor of 0.9.

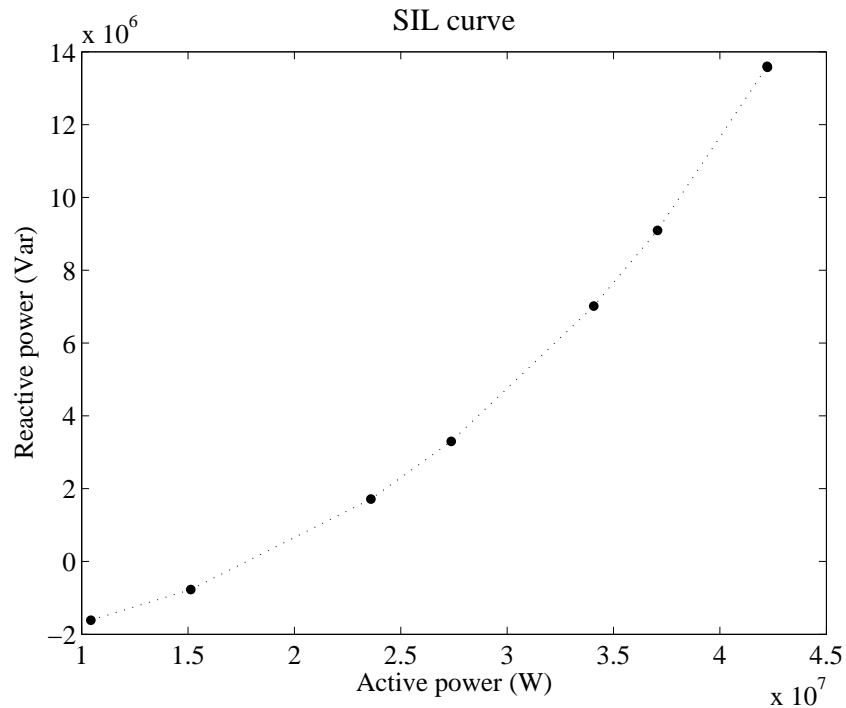


Figure 6.11: SIL curve from simulation of the circuit in Figure 5.4 with a power factor of 0.9.

An individual SIL curve does not have to be drawn for every possible power factor. Rather a SIL curve must be constructed for power factors within an operating step. It was decided to use a step size of 0.1. In this case there will be two SIL curves for the transmission line: one when the power factor ranges between 0.8 and 0.89 and another for the power factor equal to and larger than 0.9.

The decision for the size of the step change was based on the curve shown in Figure 6.12. For this SIL curve the power factor of the loads, that were switched in, varied between 0.5 and 0.9.

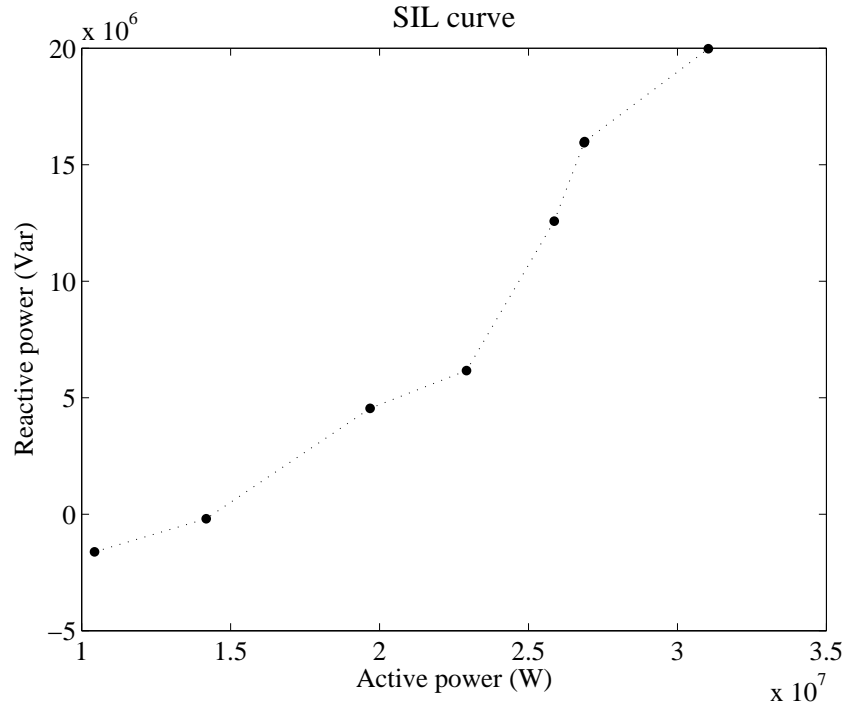


Figure 6.12: SIL curve from simulation of the circuit in Figure 5.4 with mixed power factor.

6.3 DISCUSSION OF RESULTS

6.3.1 Line parameters

In order to determine the accuracy of the measured values, the maximum percentage error introduced on each of the lines using all three methods must be determined. This was done by comparing the measured results from the previous sections with the actual line parameters as given in section 5.

Method 1

The short transmission line shows impedance values calculated by using both the sending end and receiving end current. It can be seen that the line capacitance does not have a large influence on the short line as the errors in Table 6.1 are all very small. This is because the sending and receiving end current and hence source and receiving impedance values are very close to each other. As a result the error is less than 1% for Method 1 on the short transmission line.

For the medium transmission line the absolute sending end current is smaller than the receiving end current. The receiving end impedance has a maximum error of 1.56% (Table

6.2). The sending end impedance (Z source) has a maximum error of 2.76%. What is seen from the results is that the receiving end current provided the closest approximation to the real impedance value. This is in line with what was stated in Chapter 5. For a medium line, Method 1 proves to be accurate as the capacitive influence is small.

Table 6.3 shows that the maximum error introduced by Method 1 on a long long transmission line is between 10.8% and 27.01%. This error can be acclaimed to the fact that no provision is made for the capacitance that is experienced on the transmission line. Thus the method becomes unusable for long transmission lines.

The difference between the results for heavy loading and light loading is small. Since the simulated measurements are very accurate. Even so the results under heavy loading proved more accurate than those for light loading. This will be seen more prominently when the system is practically implemented.

The biggest drawback of this method is that the result is given in terms of the impedance. Two solutions exist for overcoming this problem. First of all the X/R ratio will be able to give a good indication as to the relationship between the resistance and the reactance. But this would mean that the type of conductor should be known. Another way is to use the phase angle of the transmission line. For this the sending and receiving side reactive power has to be subtracted from each other. Once this has been done the active and reactive power supplied/absorbed by the line is known. By using (5.3) the phase angle can be determined. With the impedance and the phase angle known the line resistance and reactance can be determined.

The practical SIL curve needs the sending and receiving end active and reactive power. Since measurements have to be taken for the calculation of the line parameters already, no extra measurements are needed for the construction of the SIL curve.

Method 2

Table 6.10 gives a summary of the maximum errors introduced by Method 2 on the various lengths of lines.

	Maximum % error		
	Short line	Medium line	Long line
Resistance	2.00%	8.41%	72.99%
Inductance	0.34%	2.03%	18.28%
Impedance	0.56%	3.05%	28.12%

Table 6.10: Errors introduced by using Method 2 for parameter determination.

From the results shown in Table 6.10 it is clear that the method is practically viable for short to medium transmission lines.

For the short transmission line the resistance has an error of 2% and the inductance is less than 1%. For the medium transmission line the errors are bigger as the capacitance starts to have an influence. The resistance is smaller than the inductive reactance, and so the error seen will be bigger on the resistance. The resistance showed an maximum error of 8.41% and the inductance 2.03%. For a medium transmission line Method 2 gives acceptable results. When the impedance measurement is considered the percentage error is far less.

When the long transmission line is considered the errors become unacceptably high. The results do not give a good reflection of what the real values are. Method 2 can thus not be applied to long transmission lines.

Method 2 is of greater use than Method 1 since the timing does not have to be as accurate. Method 1 relies on a timing accuracy in the low micro second range whereas Method 2 works well as long as the load remains unchanged for the voltage and the current measurement. The reason for this is that the voltage waveforms are not subtracted from each other as is the case with Method 1. This makes Method 2 easier to implement and cheaper, as a less accurate timing source can be used in the place of the GPS unit.

Method 3

Method 3 differs from Method 1 and 2 in that it considers the capacitive influence on transmission lines. For the short transmission line the resistance and inductance produced errors smaller than 1% (Table 6.7). For a short transmission line the capacitance is ignored since it is small. The capacitance was accurate to 1.83% although it was small in

comparison to the other parameters.

When Method 3 was applied to a medium transmission line the results for resistance, inductance and capacitance measured had an error of less than 1% (Table 6.8). The long transmission line model measured a resistance with an error of 2.67% (Table 6.9). Both the inductance and capacitive values had errors of less than 1%.

From the simulation results it can be seen that Method 3 is very accurate. Transmission lines were simulated that ranged from 50 kilometers in length to 450 kilometers. For all these lines very good results were obtained. This shows that Method 3 is viable for parameter determination.

Method 3 is the most difficult of all the methods to implement. However this method is also practically most viable. It is the only method that calculates the line capacitance. It is therefore the only method that can be applied to a long transmission line.

6.3.2 *SIL curves*

The simulation results for the SIL curves proved that it is possible to construct a SIL curve from measured data. It is important to note that a different SIL curve has to be drawn for a range of power factors. From Figure 6.12 it is evident that a mixed power factor will not result in a smooth SIL curve. Even with the high difference in power factors, the SIL curve still retained its general shape. The deduction is thus made that a SIL curve will be smooth for a range of power factors.

In addition to the active and reactive power measurements needed for the construction of the SIL curve, the load side power factor has to be determined as well. This power factor is then used to determine the SIL curve to which the measured data can be added.

7 LABORATORY RESULTS

The laboratory results were obtained from the circuits of Figure 5.6-Figure 5.8. All three methods were applied to the lab results in order to determine the feasibility of each method.

7.1 METHOD 1

In Chapter 4, the problem with mismatch in clock frequencies is discussed. The simplest solution was to use only the first 10 cycles of recorded data to determine the impedance. As a result, the figures shown for Method 1 has only ten discrete data points. Since only ten cycles were available, the dynamics of the method were not tested with a step change in load. Individual tests however were conducted for different load and line values.

7.1.1 *Short line*

For the short transmission line model no capacitance was included in the system. This meant that the sending and the receiving end current are exactly equal in magnitude and phase. Based on this assumption, it does not matter whether the sending or receiving end current is used in the calculation of the impedance. For every line there is two results, one for light loading conditions and one for heavy loading conditions (except when Method 3 is applied).

The impedance values calculated from laboratory results under heavy and light loading for case one (described in section 5.2.2) is given in Figure 7.1a and Figure 7.1b. The results for case two is given in Figure 7.2a and Figure 7.2b.

The maximum and minimum values that is measured over the 10 cycles from the four figures is given in Table 7.1. The maximum errors introduced by the use of the Method 1 is also displayed. The maximum error given as a percentage is calculated with equation (7.1).

$$\text{max_}\% \text{_error} = \frac{|\text{Max_error}|}{Z_{\text{actual}}} \times 100 \quad (7.1)$$

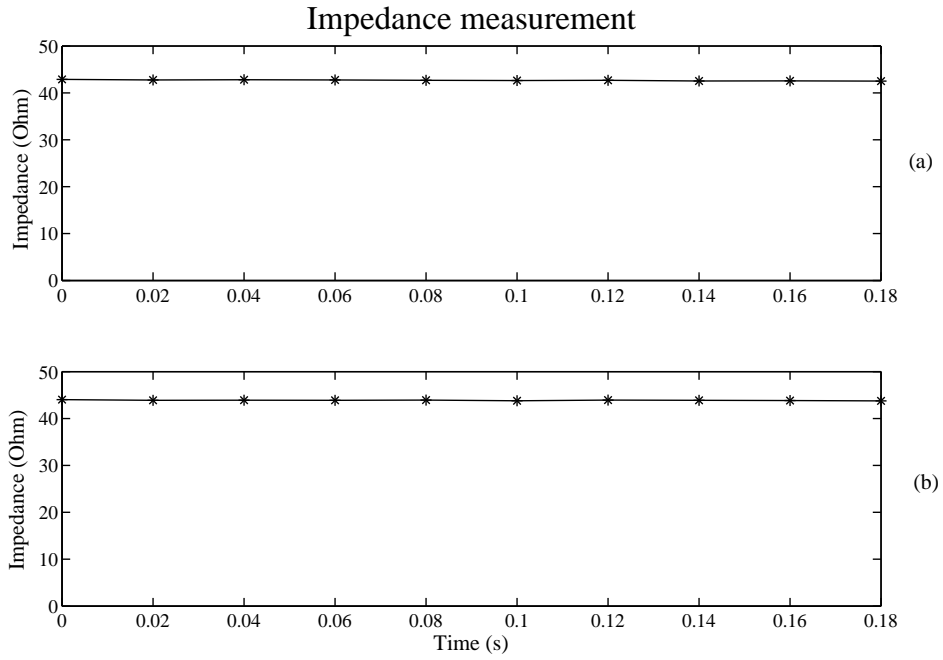


Figure 7.1: The line impedance calculated using Method 1 for case one.

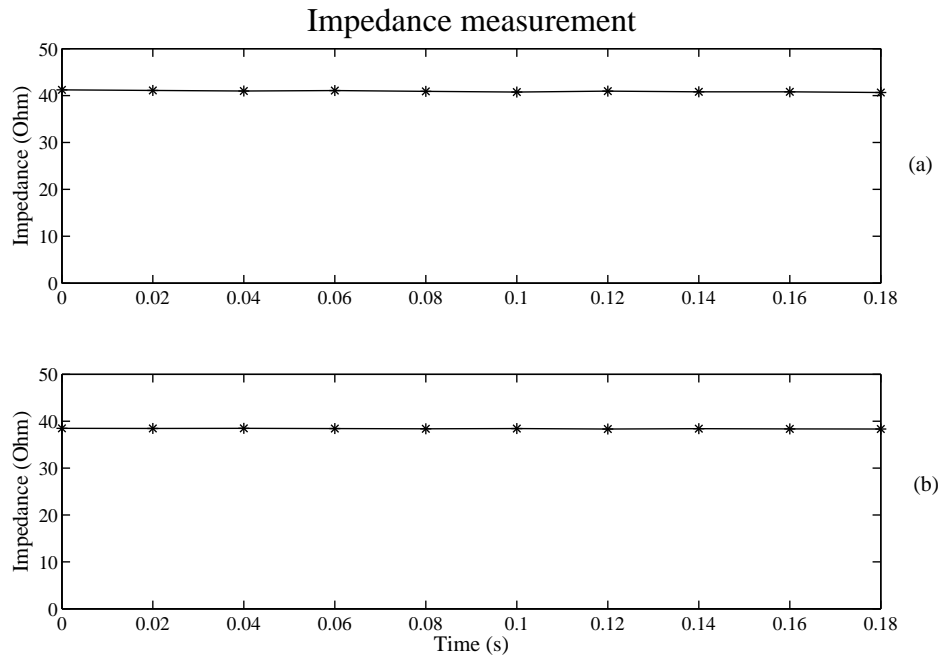


Figure 7.2: The line impedance calculated using Method 1 for case two.

	Case 1		Case 2	
	Light loading	Heavy loading	Light loading	Heavy loading
Z max (Ω)	42.88	44.02	41.22	38.47
Z min (Ω)	42.50	43.76	40.65	38.33
Actual Z (Ω)	45.13	45.13	39.03	39.03
Max error (Ω)	2.63	1.37	2.19	0.7
Max % error	5.83%	3.04%	5.61%	1.79%

Table 7.1: Errors introduced in the lab due to the use of Method 1 on the short line model.

7.1.2 Medium line

The medium and long line results are given in the same way as the short line's was. The first two graphs are the results for case 1 and the second two graphs are for case 2. Table 7.2 gives the maximum error introduced as a percentage calculated with (7.1).

Under light loading conditions the source current is larger than the receiving end current. Therefore the source current is used in the calculation of the impedances shown in Figure 7.3a and Figure 7.4a.

The receiving end current is larger than the sending end current under the heavy loading conditions of Figure 7.3b and Figure 7.4b. In these cases the load (receiving end) current is used in the calculation of the impedance.

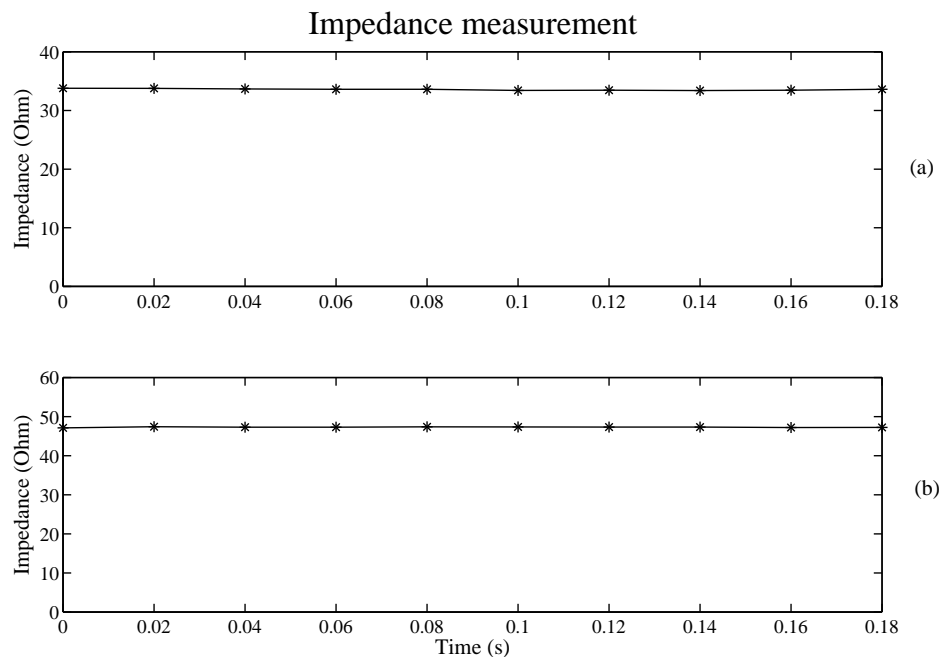


Figure 7.3: The line impedance calculated using Method 1 for case one.

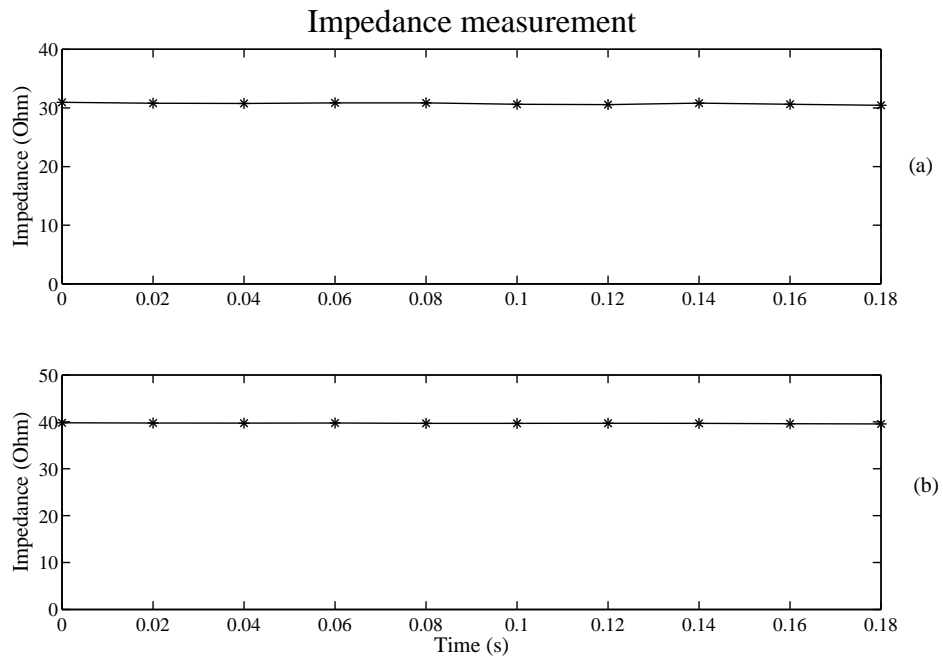


Figure 7.4: The line impedance calculated using Method 1 for case two.

	Case 1		Case 2	
	Light loading	Heavy loading	Light loading	Heavy loading
Z max (Ω)	33.80	47.41	30.95	39.79
Z min (Ω)	33.40	47.12	30.45	39.55
Actual Z (Ω)	45.13	45.13	39.03	39.03
Max error (Ω)	11.73	2.28	8.58	0.76
Max % error	25.99%	5.05%	21.98%	1.95%

Table 7.2: Errors introduced in the lab due to the use of Method 1 on the medium line model.

7.1.3 Long line

The capacitance for the long line model is much larger than the total capacitance of the medium line model. Due to this the sending end current will be bigger than the receiving end current for all loading conditions. The sending end current is thus used in the calculation of the impedance values shown in Figure 7.5 to Figure 7.6. Table 7.3 provides the errors that was introduced with the use of Method 3. The maximum percentage error is calculated with (7.1).

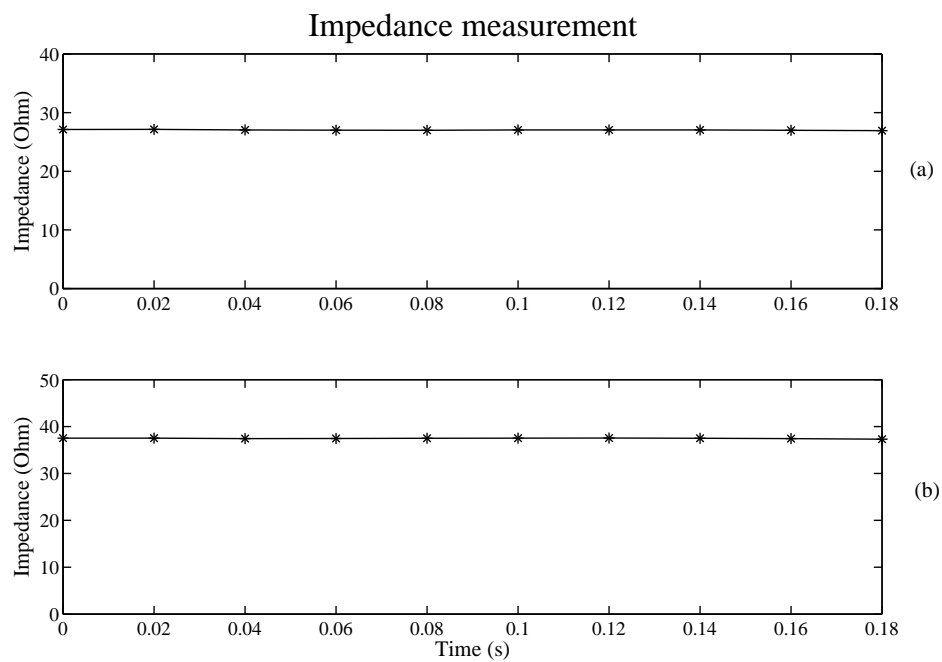


Figure 7.5: The line impedance calculated using Method 1 for case one.

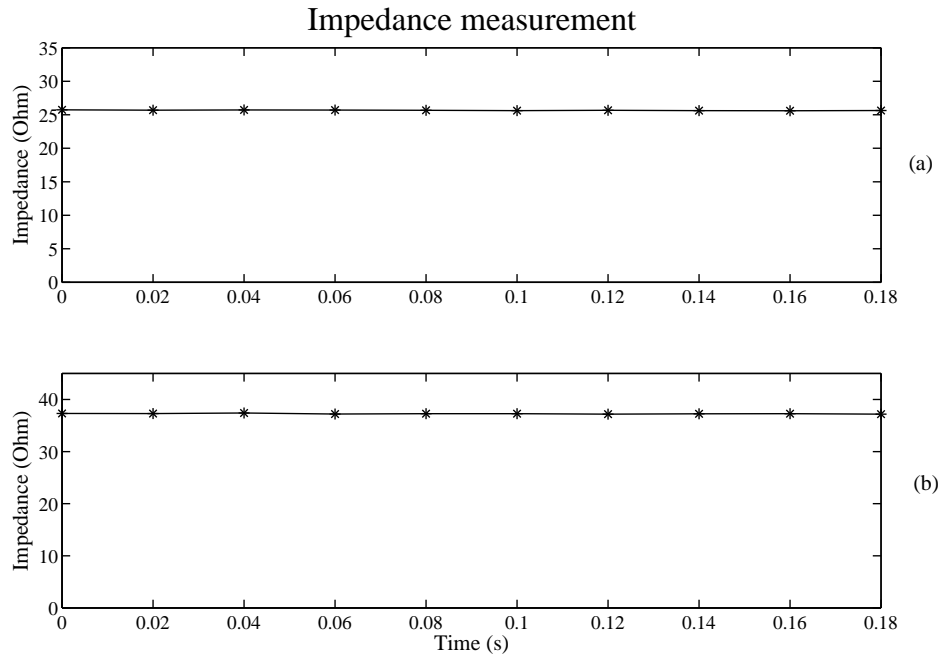


Figure 7.6: The line impedance calculated using Method 1 for case two.

	Case 1		Case 2	
	Light loading	Heavy loading	Light loading	Heavy loading
Z max (Ω)	27.14	37.54	25.73	37.41
Z min (Ω)	26.93	37.31	25.61	37.18
Actual Z (Ω)	45.13	45.13	39.03	39.03
Max error (Ω)	18.2	7.82	13.42	1.85
Max % error	40.33%	17.33%	34.38%	4.74%

Table 7.3: Errors introduced in the lab due to the use of Method 1 on the long line model.

7.2 METHOD 2

Method 2 was applied to the same model as Method 1 was. This section contains the results using the second method for the calculations of the resistance and inductance values.

7.2.1 Short line

Method 2 is not as dependant as Method 1 on the absolute matching of clock frequencies of the DSP's. Therefore the results are obtained every cycle for a total time of 2 seconds. The first second of the recorded data was taken from the system under light loading. Second two was recorded for the system under heavy loading. Figure 7.7a and Figure 7.8a gives the graphs for the resistance calculated for case one and two respectively. Figure 7.7b and Figure 7.8b gives the inductance values for the two cases. The results are summarized in Table 7.4.

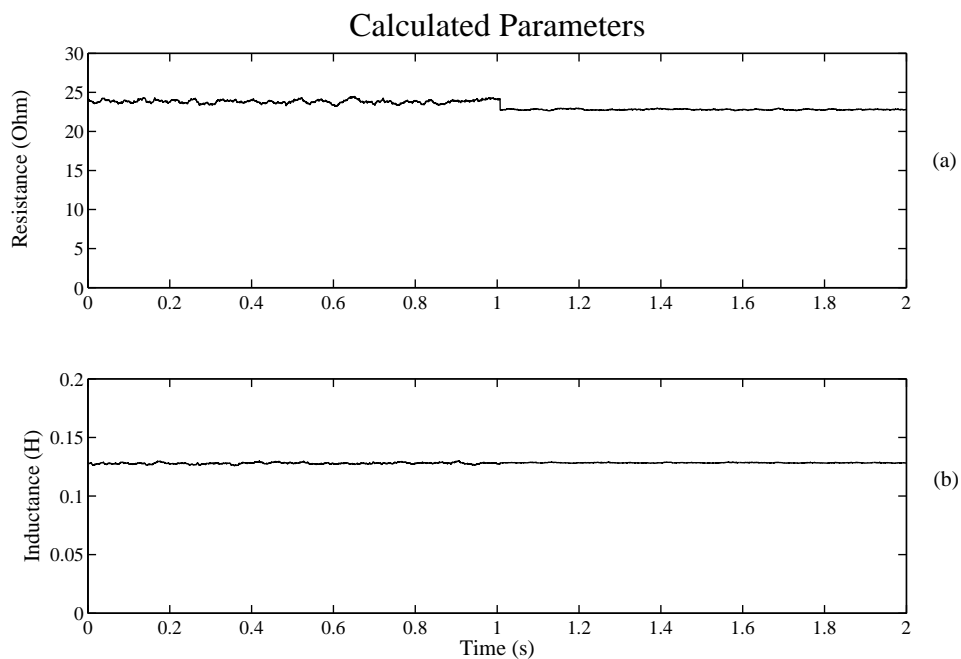


Figure 7.7: The line parameters calculated using Method 2 for case one.

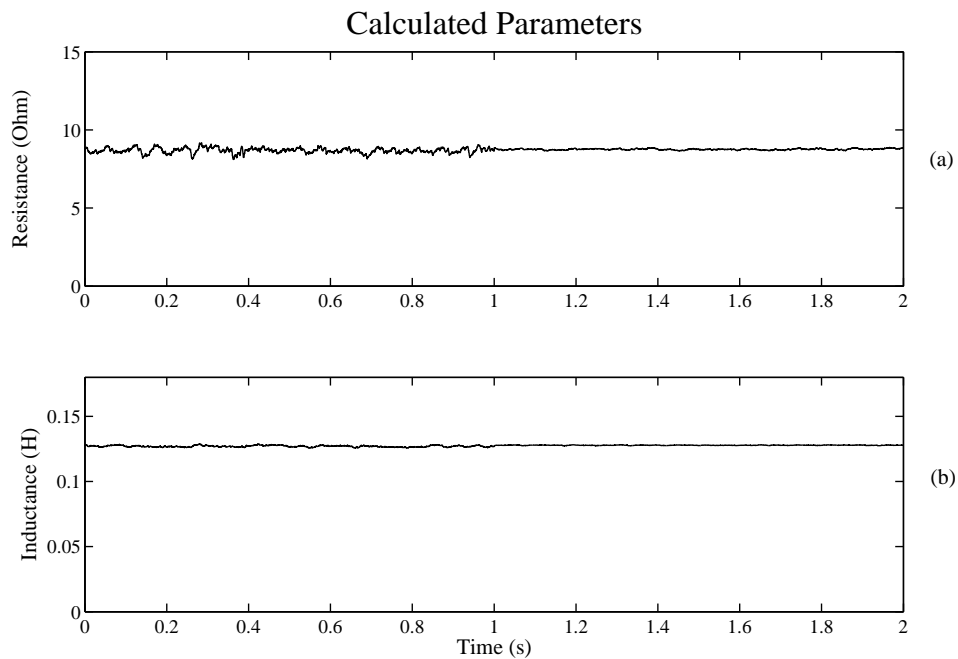


Figure 7.8: The line parameters calculated using Method 2 for case two.

	Case 1		Case 2	
	Light loading	Heavy loading	Light loading	Heavy loading
R max (Ω)	24.44	22.96	9.16	8.86
R min (Ω)	23.24	22.69	8.14	8.67
L max (mH)	130.24	128.88	128.79	128.23
L min (mH)	126	127.98	125.8	127.58
Actual R (Ω)	24.6	24.6	9.6	9.6
Actual L (mH)	120.43	120.43	120.43	120.43
R max error (Ω)	1.36	1.91	1.46	0.93
L max error (mH)	9.81	8.45	8.36	7.8
Max % R error	5.53%	7.76%	15.21%	9.69%
Max % L error	8.15%	7.02%	6.94%	6.48%

Table 7.4: Errors introduced in the lab due to the use of Method 2 on the short line model.

7.2.2 Medium line

The results given in this subsection is only for case one. From the graphs it can be seen that no usable data can be extracted. The same results were obtained for the long transmission line. Hence no results for Method 2 is recorded in this section for the medium and long line models.

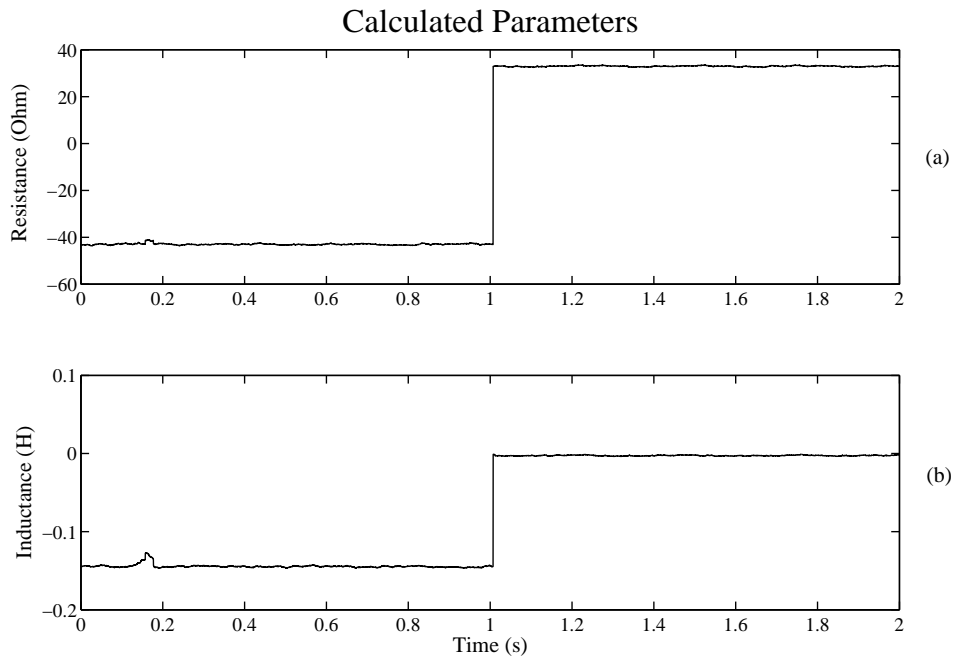


Figure 7.9: The line parameters calculated using Method 2 for case one.

7.3 METHOD 3

Using Method 3, it was possible to separate the inductive and capacitive components from each other. For this method both the magnitude and phase values of the measured components were needed. Due to the method's dependence on phase angle, errors are introduced in the calculations by the clock frequency of the DSP's. In order to keep this phase shift to a minimum, only the first 10 cycles of the heavy and lightly loaded system was compared with each other. This was the same solution that was proposed for Method 1.

7.3.1 Short line

With the short transmission the capacitance is negligible. For this reason no capacitive values were placed in the laboratory setup of a short transmission line. Results are shown

for the resistance and inductance values measured for the two cases described in section 5.2.2. The results for case one and two are given in Figure 7.10 and Figure 7.11 respectively.

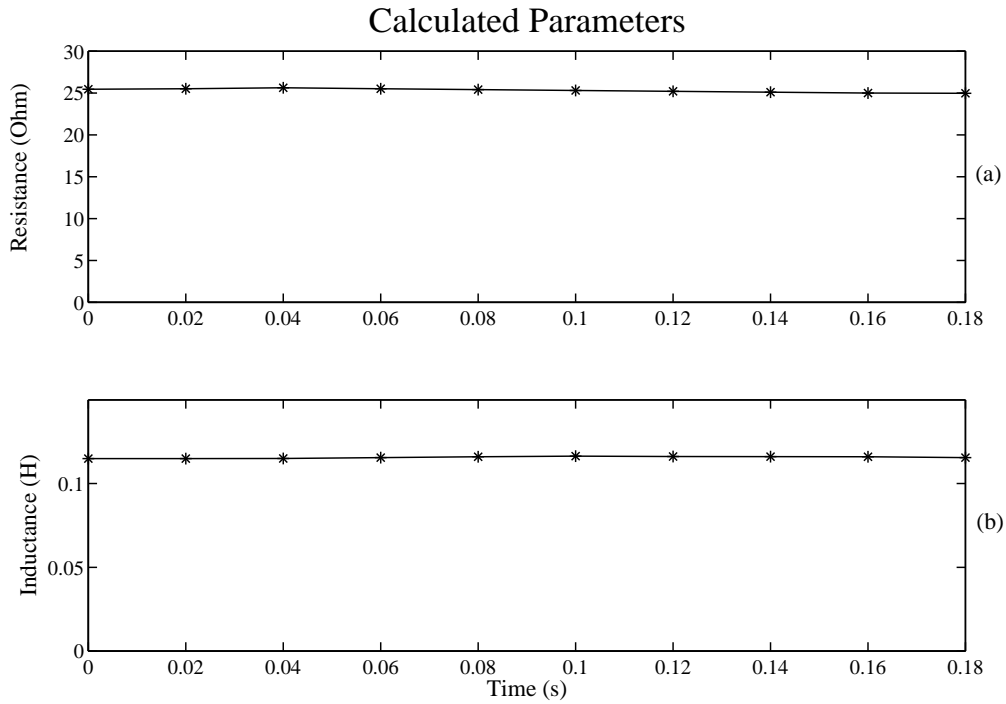


Figure 7.10: The line resistance and inductance calculated using Method 3 for case one.

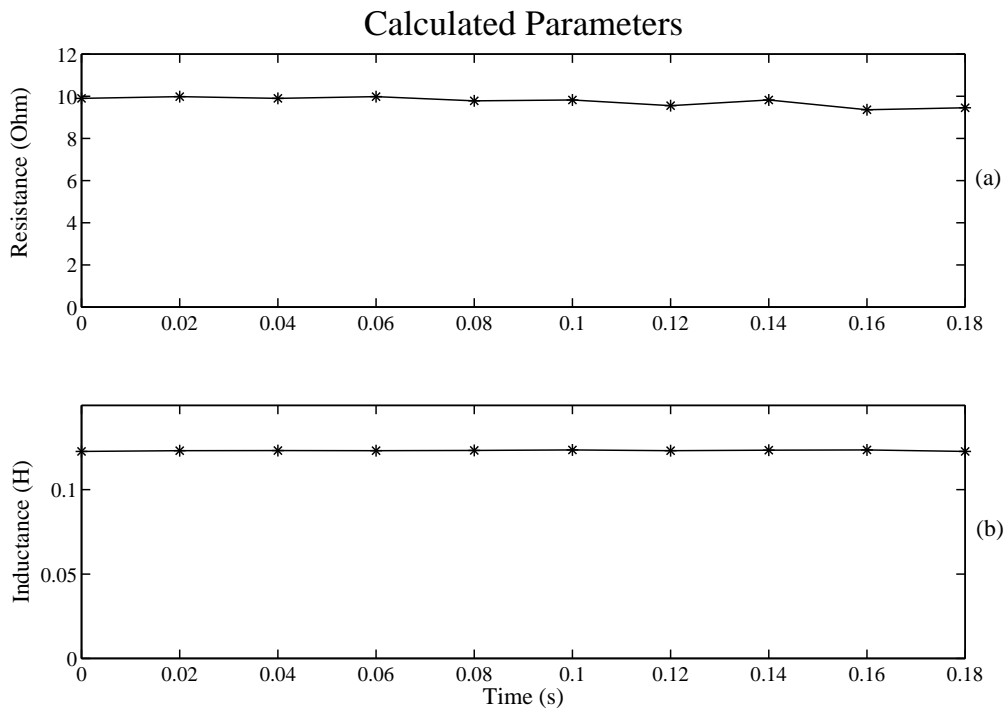


Figure 7.11: The line resistance and inductance calculated using Method 3 for case two.

The maximum and minimum values that were calculated for the resistance and inductance over the first ten cycles are given in Table 7.5. These values are also compared to the actual values in the circuit. In this way the maximum error introduced by Method 3 can be calculated.

	Case 1	Case 2
R max (Ω)	25.62	9.98
R min (Ω)	24.97	9.36
L max (mH)	116.4	123.6
L min (mH)	114.9	122.7
Actual R (Ω)	24.6	9.6
Actual L (mH)	120.43	120.43
R max error (Ω)	1.02	0.38
L max error (mH)	5.53	3.17
Max % R error	4.15%	3.96%
Max % L error	4.59%	2.63%

Table 7.5: Errors introduced in the lab due to the use of Method 3 on the short line model.

7.3.2 *Medium line*

In the medium line model substantial capacitance was included in the form of lumped values at the beginning and end of the line (Figure 5.7). For this section there will be a third graph that represents the capacitance (Figure 7.12c and Figure 7.13c) besides the two graphs for the resistance and the inductance. This capacitance represents the total capacitance that is present in the circuit.

As with the short line, the results are summarized in Table 7.6. This is the same way the results for the long transmission line model will be given.

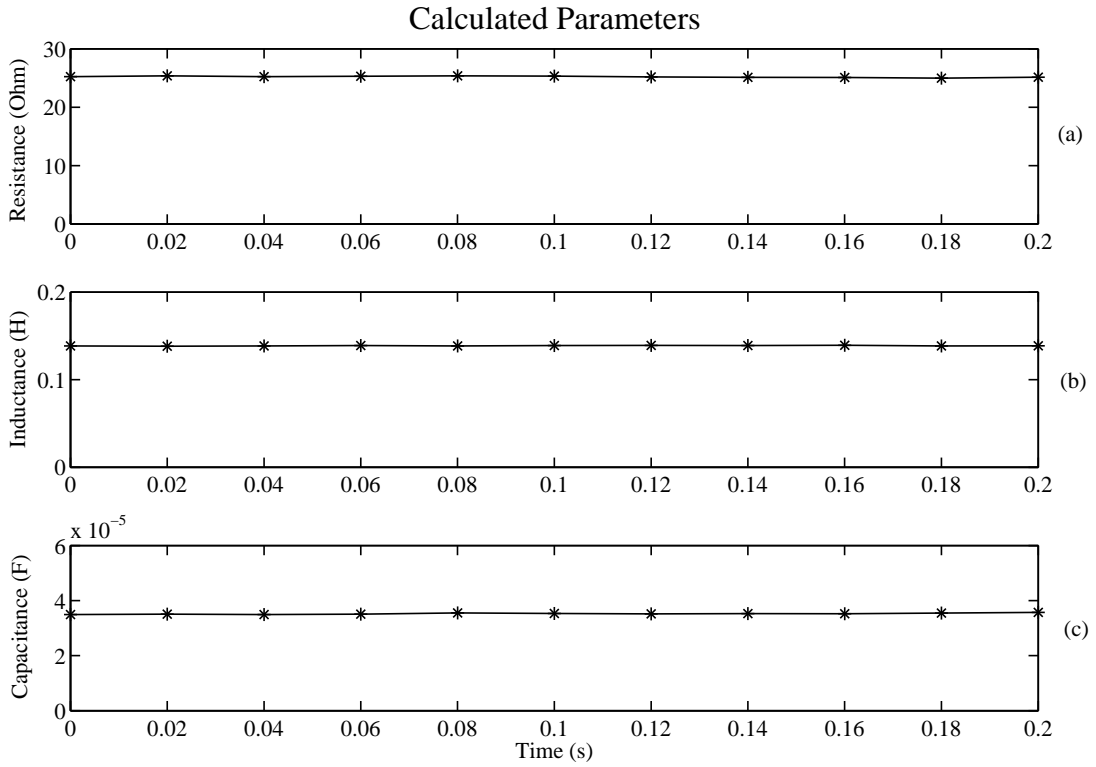


Figure 7.12: The line parameters calculated using Method 3 for case one.

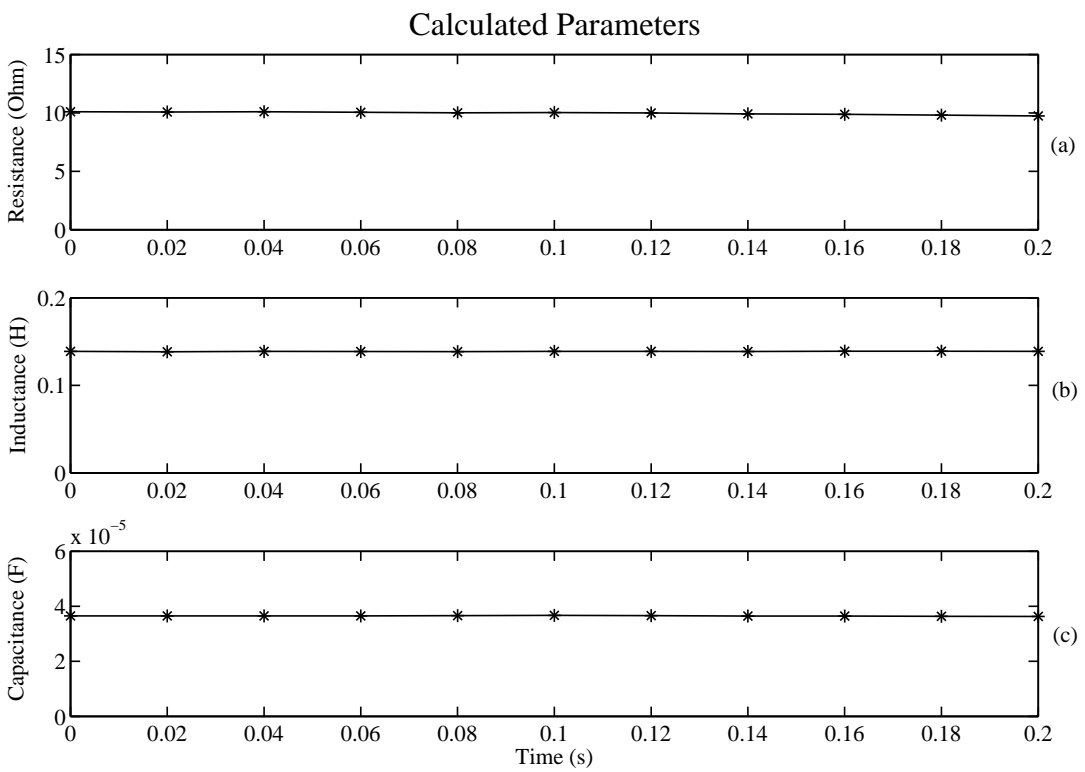


Figure 7.13: The line parameters calculated using Method 3 for case two.

	Case 1	Case 2
R max (Ω)	25.32	10.1
R min (Ω)	24.98	9.74
L max (mH)	139.3	139.0
L min (mH)	137.8	138.4
C max (μF)	35.72	36.71
C min (μF)	34.92	36.3
Actual R (Ω)	24.6	9.6
Actual L (mH)	120.43	120.43
Actual C (μF)	39.71	39.71
R max error (Ω)	0.72	0.50
L max error (mH)	18.87	18.57
C max error (μF)	4.79	3.41
Max % R error	2.93%	5.21%
Max % L error	15.67%	15.42%
Max % C error	12.06%	8.59%

Table 7.6: Errors introduced in the lab due to the use of Method 3 on the medium model.

7.3.3 Long line

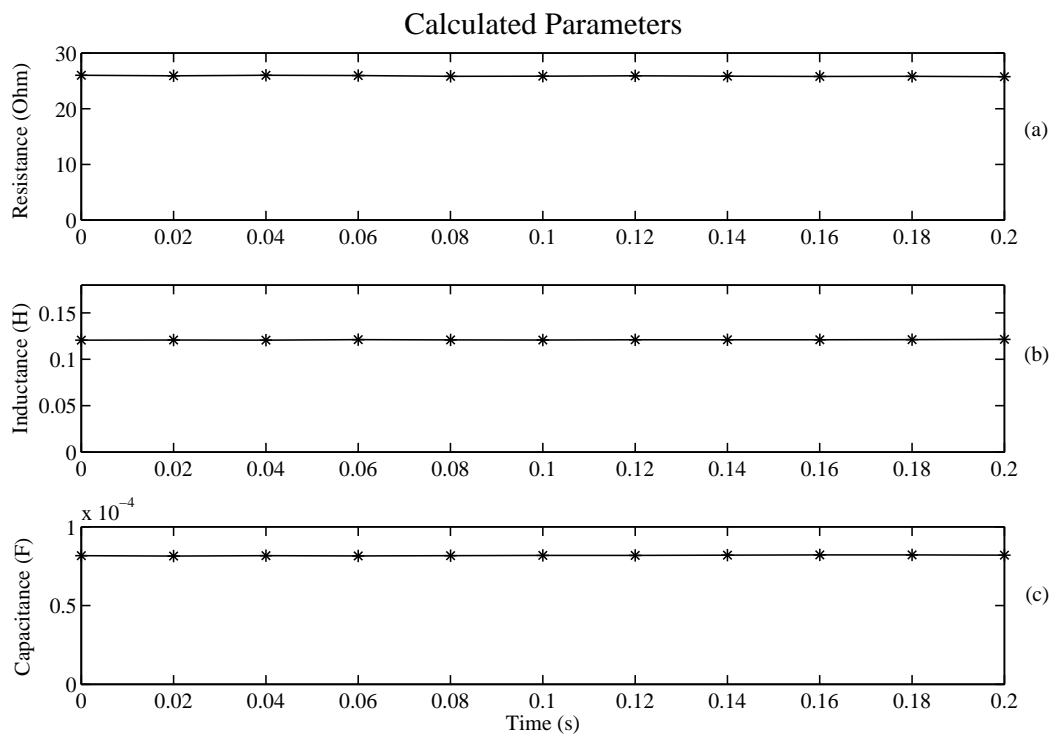


Figure 7.14: The line parameters calculated using Method 3 for case one.

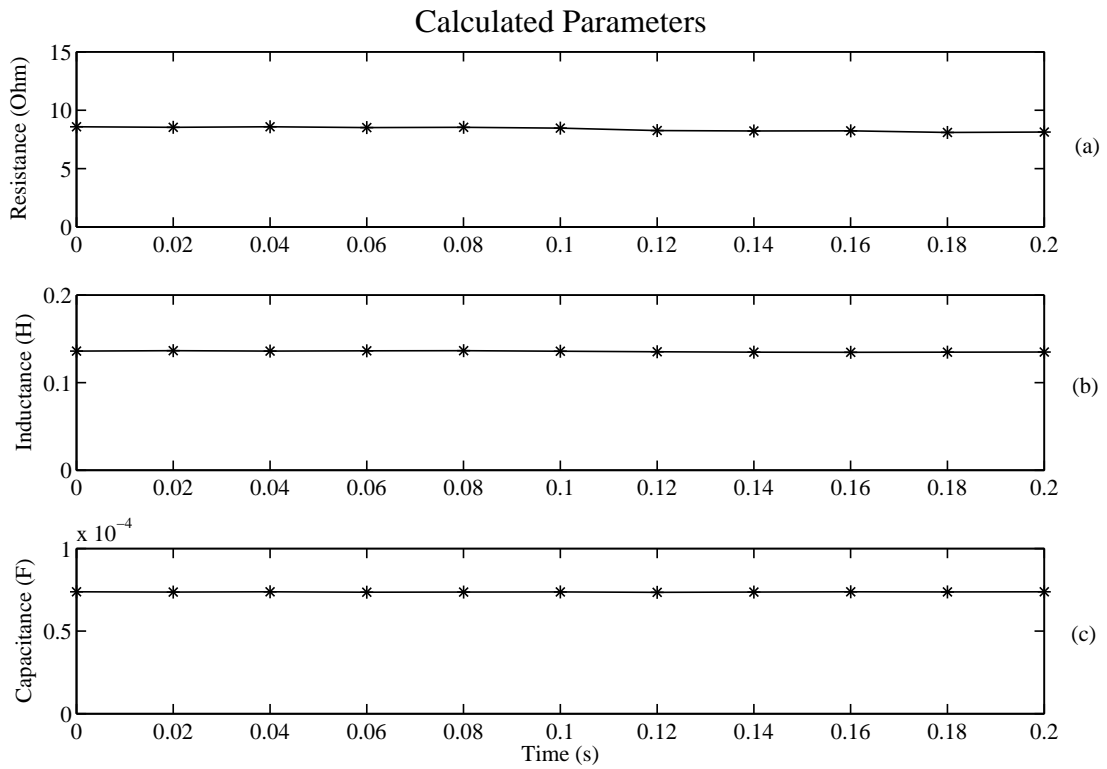


Figure 7.15: The line parameters calculated using Method 3 for case two.

	Case 1	Case 2
R max (Ω)	25.99	8.58
R min (Ω)	25.73	8.09
L max (mH)	121.5	136.5
L min (mH)	120.7	134.7
C max (μF)	82.17	73.81
C min (μF)	81.40	73.42
Actual R (Ω)	24.6	9.6
Actual L (mH)	120.43	120.43
Actual C (μF)	79.62	79.62
R max error (Ω)	1.39	1.51
L max error (mH)	1.07	16.07
C max error (μF)	2.55	6.20
Max % R error	5.65%	15.73%
Max % L error	0.89%	13.34%
Max % C error	3.2%	7.79%

Table 7.7: Errors introduced in the lab due to the use of Method 3 on the long model.

7.4 DISCUSSION OF RESULTS

The voltage and power across an actual power line is very high when compared to the setup used in the laboratory. For a transmission line a low capacitance or inductance value would have a measurable influence on the voltage and current values calculated. In order to have measurable influences in the laboratory, the inductance and capacitive values had to be much bigger than those of a traditional transmission line. The problem with this is that when the capacitance is included with the inductance in the lab circuit there is a small amount of resonance that tends to distort the current waveform. This effect is most prominently seen on the medium line circuit. This introduces measurement errors into the results from the laboratory.

7.4.1 Method 1

In Method 1 only one constant load was present during the 10 cycles used for the measurement. The results of Table 7.1 compare very close to the actual measurements for the short line. The maximum error introduced in the measurement was 5.83% under the conditions described in Chapter 5. Note that the maximum recorded errors occurred when the system was lightly loaded. Under heavy loading the error dropped as low as 1.79%. The large current that flows under heavy loaded conditions dominates the measurement errors which is not the case when the line is lightly loaded.

Both Method 1 and Method 2 rely on heavy loading conditions. This is to ensure that there is a clear distinction between the line and load parameters. The errors introduced with Method 1 can be partly ascribed to errors in measuring equipment. Another reason for the errors is the phase difference in sampling frequency between the sending and receiving end measurements. Since the clock frequency is not exactly matched, one side may start recording before the other. This impact is kept to a minimum by using a high sampling frequency.

For the medium line the results that were recorded under light loading is between 21.98% and 25.99%. This is unacceptable. The reason for the large error is the capacitance. The capacitive influence is determined by the size of the capacitance and voltage on the line. Under light loading the capacitive influence of the line dominates the measured current. Under heavy loading, the load influences the current more than the capacitance. This is

the current that flows through the resistance and inductance of the line. Under heavy loading the results are thus more accurate. This was seen from Table 7.2 where the maximum error under heavy loading is 5.05%. For the long line the results are given in Table 7.3. The results are very erratic and unreliable with errors that are as high as 40.33%.

The results obtained using Method 1 was quite accurate for the short line model as well as the medium transmission line. For use in simulation packages, an error of close to 10% is considered acceptable³. Method 1 cannot be applied to long transmission lines as the error introduced is too large.

7.4.2 Method 2

The results for the short line is given in Table 7.4. These results were obtained using the same model as in Method 1. Under heavy loading the results for the resistance showed an accuracy within 9.69%. As in the previous section, the maximum error (15.21%) occurred under light loading. Method 2 relies on active and reactive power calculations. The phase shift results in the inaccurate calculation of the active and reactive powers. This in combination with inaccurate magnitude measurements result in the errors experienced. From Figure 7.7 through to Figure 7.8 it can also be seen that the result under light loading is less stable than for heavy loading. So the maximum error is deceiving. The average error would be under 10%.

The inductance measurement had a maximum error of 8.15%. The inductive reactance is bigger than the resistance value on the line. For this reason the inductance measurement was more accurate than that of the resistance. This was also seen in the resistance results for case two. The resistance in case one is more than twice the size of the resistance in case two. Hence the accuracy of the resistance measurement under case one was higher than for case two.

The capacitance used in the laboratory was high, even for the medium transmission line. The reactive power calculated for the transmission line is thus largely influenced by this capacitance. It is not possible to get the correct inductance and resistance values when the reactive power has a large capacitive influence. The result can be seen in Figure 7.9.

³This conclusion was made after a discussion with utility representatives

It is thus clear that Method 2 cannot be applied to the long transmission line.

7.4.3 Method 3

For the short transmission line the resistance and inductance values were calculated with Method 3. From Table 7.5 it can be seen that the maximum error introduced by Method 3 for the short line was 4.59%.

For the medium transmission the resistance measurement was accurate to within 6% (Table 7.6). The inductance and capacitive values measured were not as accurate. The maximum errors were under 16%. Errors are introduced in the results by means of phase and magnitude inaccuracies. The distorted current could also account for some of the error. From the simulations it was seen that if these errors can be eliminated the measurements are very accurate.

Method 3 was the only method that could provide results for the long transmission line. Case one provided very good results with a resistance error of 5.65% (Table 7.7). The capacitance had a maximum error of 3.2% and the inductance an error of 0.89%. A maximum initial phase error of 1 data point can be introduced between the measurements of the two DSP's. This phase error could account for the difference in accuracies between case one and two. The errors for case two are under 16% as was the result for the medium line.

Method 1 and 2 proved to be accurate for calculating the parameters for a short or a medium transmission line. However when the capacitive influence becomes large these methods cannot be used. Method 1 and 2 would be well suited for calculating the parameters of the distribution lines as they are not as long as transmission lines. For transmission lines the best method would be Method 3. As shown by the results, if the measurement errors can be kept to a minimum Method 3 is very accurate.

The main concern is the accuracy of the VT's and CT's in the substations. Probes used in the laboratory are highly accurate, while the substation VT's and CT's could easily introduce an error of as much as 5%. Hence, percentage errors which will be incurred in the field implementation could be much larger than the errors shown here.

7.5 ALTERNATIVES CONSIDERED

7.5.1 *Method*

In the simulation, the problem of different clock frequencies, does not have an impact. In practice this problem is of concern. By using only the first 10 cycles of data for the computation of the impedance in Method 1, the results proved that the proposed solution to the problem is valid.

7.5.2 *Timing considerations*

From the literature study, two ways of synchronizing the time for the measurements were investigated. Fast Switched Ethernet provides timing that is accurate enough for the application of time-stamping. However in order to guarantee the accuracy of the time data, the amount of switches on the network is limited to only one [15]. Also taking into consideration that measurements are made hundreds of kilometers apart, the cost involved in setting up the network is not feasible.

It was decided to use GPS modules from UBlox that would not only make installation easier, but also provides the correct timing with minimal communication and computation. Further taking into consideration that GPS technology is becoming increasingly affordable, it was a logical choice.

8 FIELD RESULTS

Field results were obtained from actual transmission lines operating on the South African network. In order to test the viability of the proposed project, various lengths of power lines that are loaded at different levels had to be considered. Since these lines are knitted across the whole of South Africa, it presented a problem for the measurement of the operating values on all of these transmission lines. This is especially true if the test system was to be installed in every substation. In order to overcome this problem, fault recorders currently installed by the utility company was used.

8.1 ACQUIRING LINE DATA

8.1.1 *Line recorders*

By default the utility has Siemens fault recorders installed on the sending and receiving side of every transmission line. These recorders operate at a maximum sampling frequency of 2.5kHz, which results in 50 discreet points of data per cycle of the fundamental. However the use of these fault recorders introduced problems that had to be dealt with.

The first problem is that these recorders are not connected to the same timing source. This means that the time recorded with the data could differ by several seconds between the sending and receiving sides. This in itself makes the application of Method 1 very difficult, as this method needs synchronized data. The second problem is that these recorders only record data once an event has occurred. This event is typically a fault that occurs on the network. A way around this is to trigger the recorders remotely. The recorders have to be triggered individually, which means that the difference in time becomes problematic.

8.1.2 *Acquiring usable data*

Once an event has been identified one second of pre-fault data is recorded in conjunction with the actual fault and a few seconds post-fault data. The length of the actual recordings might vary from substation to substation due to the settings on the recorder itself. Once the data has been recorded it is stored in an electronic database. The methods proposed in this project depend on steady state conditions. This makes post-fault data unusable for this application.

When there is a fault on the line there is an instantaneous increase in neutral current from zero to some sizable and measurable value⁴. This neutral current can be measured at both the sending and the receiving sides. By using the neutral current as the reference point, the data can be aligned to an accuracy of one data point which is the same as the accuracy obtained by a GPS unit. Once the data has been aligned, the different methods can be applied to the test data to determine the line parameters.

The one second of pre-fault data is thus gathered from the sending and receiving sides of the transmission line, that was stored by both the recorders, for a specific event. By default this data is in OSCOP format, which is a compacted file developed by Siemens. The OSCOP files is exported to ASCII format and then imported into a program such as Microsoft Excel or MATLAB, where the discreet data can be analysed.

This method is only used to determine whether the actual proposed system will work in the calculation of the line parameters. The reason for this is that the records have to be considered individually. One must first determine whether the sending side data can be used. Only if the sending side data is of use can one consider the receiving side data. The receiving side data then has to be evaluated to determine whether the record is of use. Once this is done the two different sets of data have to be manually aligned in phase in order for the calculations to be done. This method is very tedious, and for permanent implementation, a separate unit would be installed that would be triggered by the synchronizing pulse of a GPS module.

8.2 RESULTS FROM FIELD DATA

8.2.1 *Impedance calculations*

A total of six transmission lines on the transmission network were used to get the field measurements. Table 8.1 provides details of the lines including their lengths, voltage levels and parameters, all of which were obtained from the utility. In this section the calculated values are graphed and compared to what the utility accepts to be the actual values.

Only calculations for Method 1 and Method 3 are shown since Method 2 did not provide

⁴This applies in most cases except three phase balanced faults

Feeder	Voltage	Length	R	X	Z
A-B	400kV	112km	1.79Ω	30.24Ω	30.29Ω
C-D	400kV	39km	1.02Ω	12.19Ω	12.23Ω
E-F	400kV	100km	2.06Ω	26.96Ω	27.04Ω
G-H	400kV	30km	0.84Ω	9.60Ω	9.64Ω
I-J	765kV	435km	5.43Ω	117.16Ω	117.29Ω
K-L	400kV	219.6km	5.23Ω	71.94Ω	72.13Ω

Table 8.1: Summary of the different lines that were used for the field results.

acceptable results⁵.

Method 1

For the first line, A-B, the pre-fault data for three separate incidents were used to determine the impedance values.

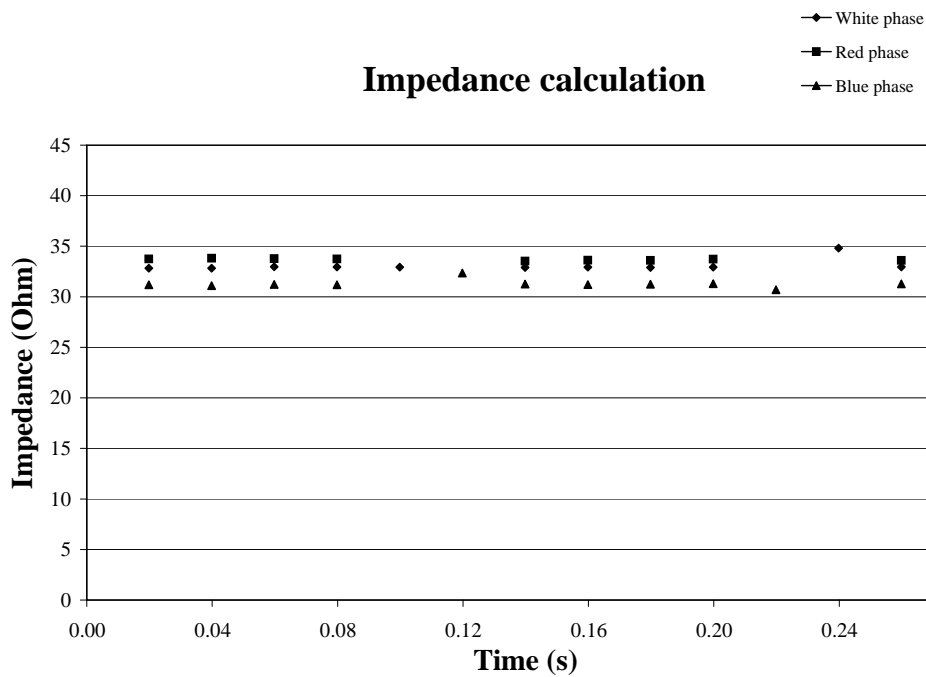


Figure 8.1: Impedance values determined for A-B using test data from 16-02-2003.

Figure 8.1 shows three separate values that were calculated. These results are for each of the three phases. The legend on the graph further explains which set of data points belong to the corresponding phase. It must be noted that not all the phases have recorded values

⁵The next section will provide a more in depth discussion as to why Method 2 failed to provide proper results

for every data point. These values have been filtered out as they are either too large or small to fit with the common norm. This is the result of fluctuations in the measurement of the voltage and/or current, that is most likely due to noise experienced by the recorders. Figure 8.2 shows the reason for the erroneously calculated impedance values. From the figure it can be clearly seen that the values are due to errors in measurement. This is not an isolated event as some measurements from the substations had to be discarded.

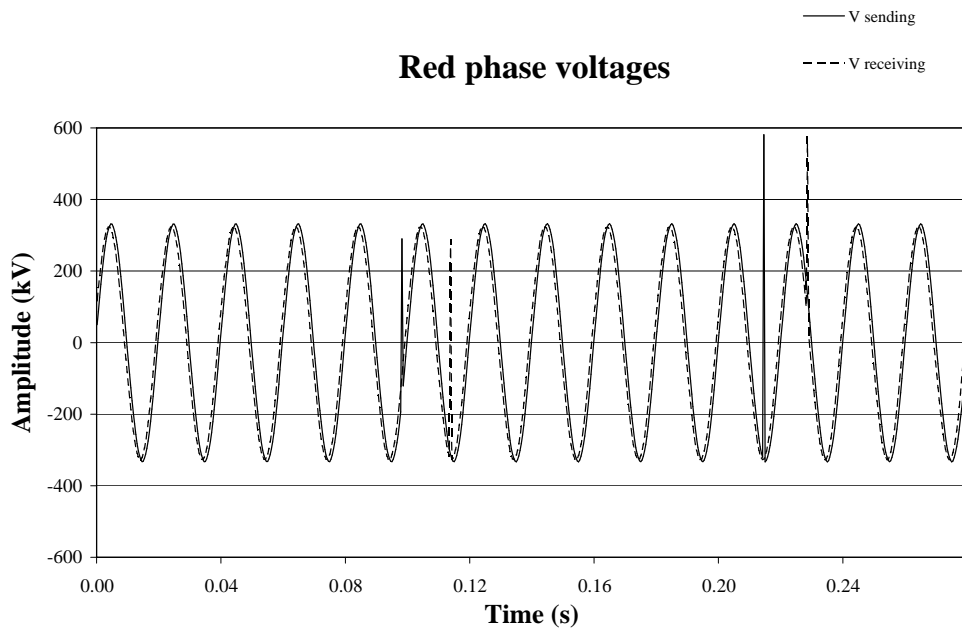


Figure 8.2: Red phase voltage measured by the sending and receiving side recorders.

The other results that were obtained for the A-B line on 6 June 2005 and 12 August 2005 are shown in Figure 8.3 and Figure 8.4.

Table 8.2 shows a summary of the results obtained for the three cases of the A-B line. The minimum, maximum as well as the largest percentage error is shown for all three phases as compared to the utility values. The maximum percentage error is calculated with (7.1).

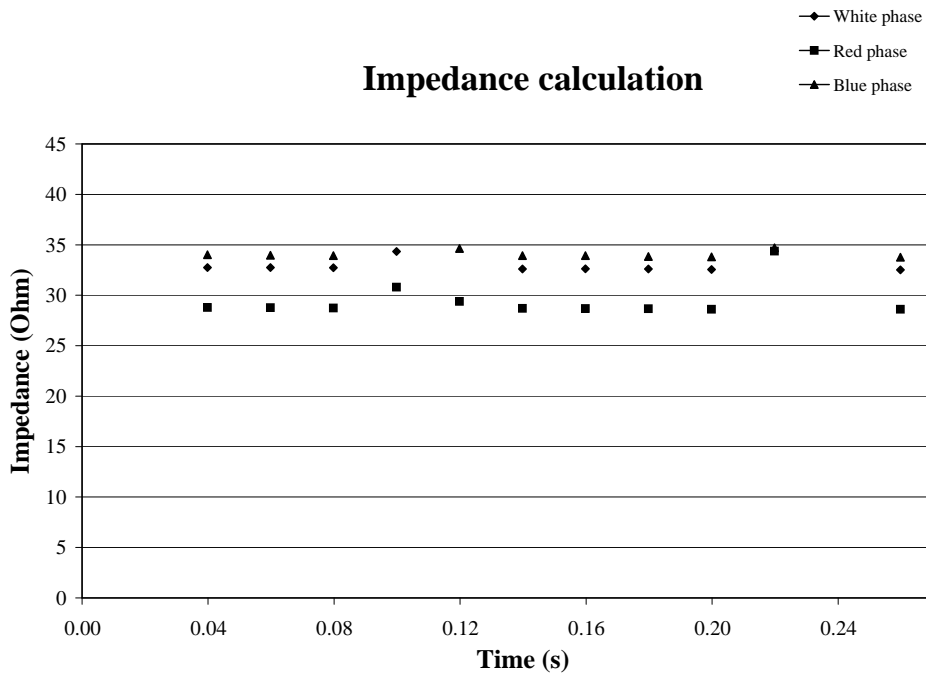


Figure 8.3: Impedance values determined for A-B using test data from 06-06-2005.

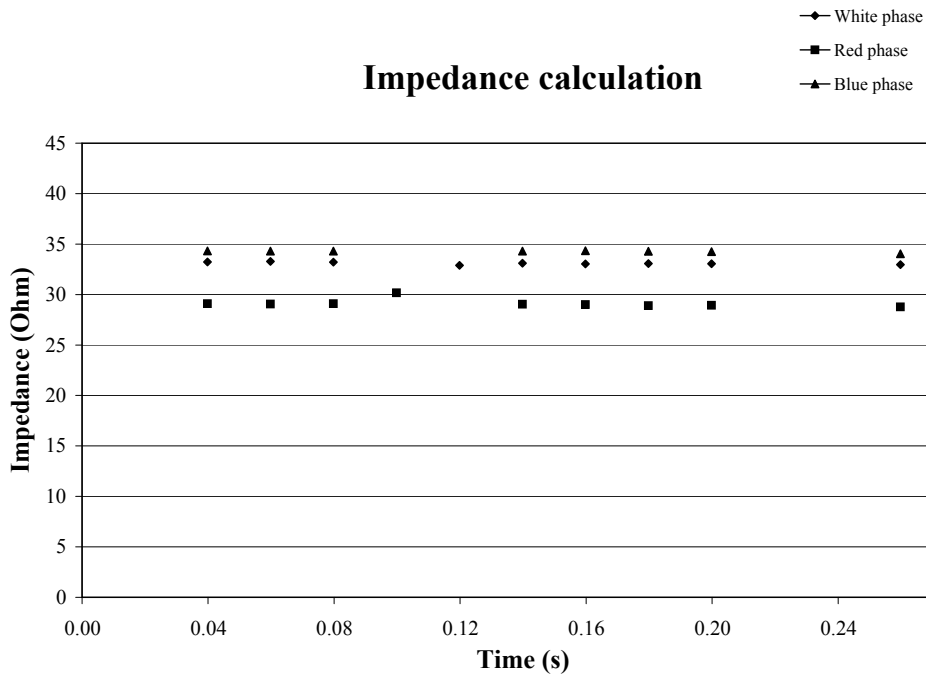


Figure 8.4: Impedance values determined for A-B using test data from 12-08-2005.

	Phase	Z max	Z min	Z error
16-02-2003	Red	34.49Ω	33.61Ω	13.90%
16-02-2003	White	34.82Ω	32.81Ω	15.00%
16-02-2003	Blue	32.35Ω	30.70Ω	6.80%
06-06-2005	Red	30.79Ω	28.68Ω	5.32%
06-06-2005	White	34.33Ω	32.51Ω	13.34%
06-06-2005	Blue	34.71Ω	33.78Ω	14.59%
15-07-2005	Red	30.17Ω	28.9Ω	4.59%
15-07-2005	White	33.28Ω	32.23Ω	9.87%
15-07-2005	Blue	35.34Ω	34.05Ω	16.67%

Table 8.2: A-B results from measured values.

C-D is the next line considered. From the database of fault data, only one data set was found to be of use. Figure 8.5 shows the impedance values that were calculated.

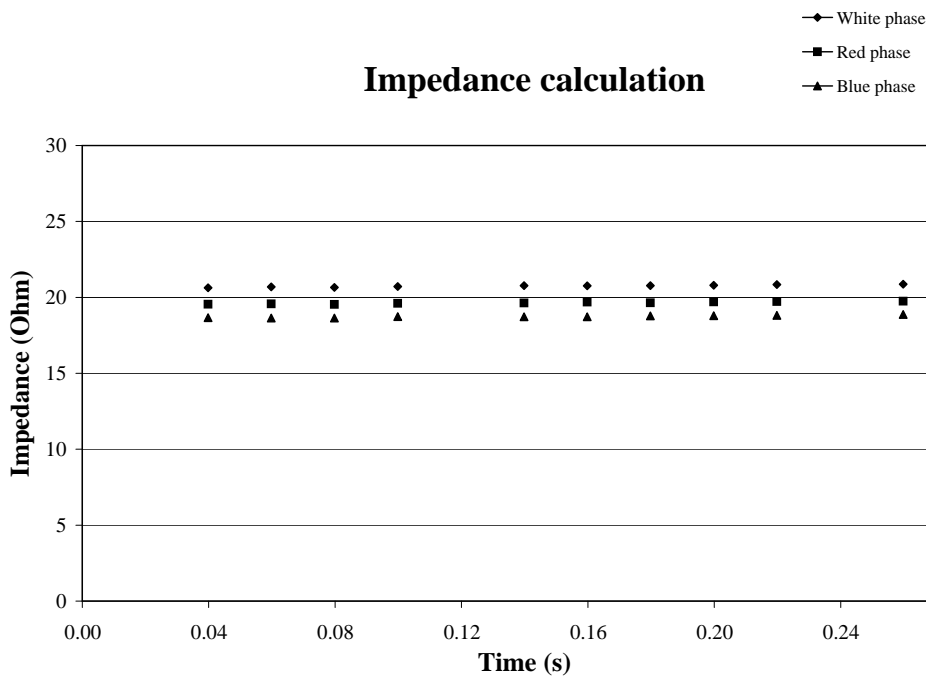


Figure 8.5: Impedance values determined for C-D using test data from 24-03-2006.

As with the A-B line, there were some data points that were of no use due to measurement errors. The results that were found is included in Table 8.3. This is the norm for the rest of the transmission lines. The figures of the computed impedance is followed by a table that summarizes the findings for that particular line.

	Phase	Z max	Z min	Z error
24-03-2006	Red	19.75Ω	19.53Ω	61.49%
24-03-2006	White	20.87Ω	20.63Ω	70.65%
24-03-2006	Blue	18.88Ω	18.64Ω	54.37%

Table 8.3: C-D results from measured values.

The following set of graphs, Figure 8.6 to Figure 8.7, represent the results for the E-F line. Figure 8.8 was drawn for the G-H line. Figure 8.9 and Figure 8.10 is for the I-J power line and the last three, Figure 8.11 to Figure 8.13, are results obtained from the K-L transmission line.

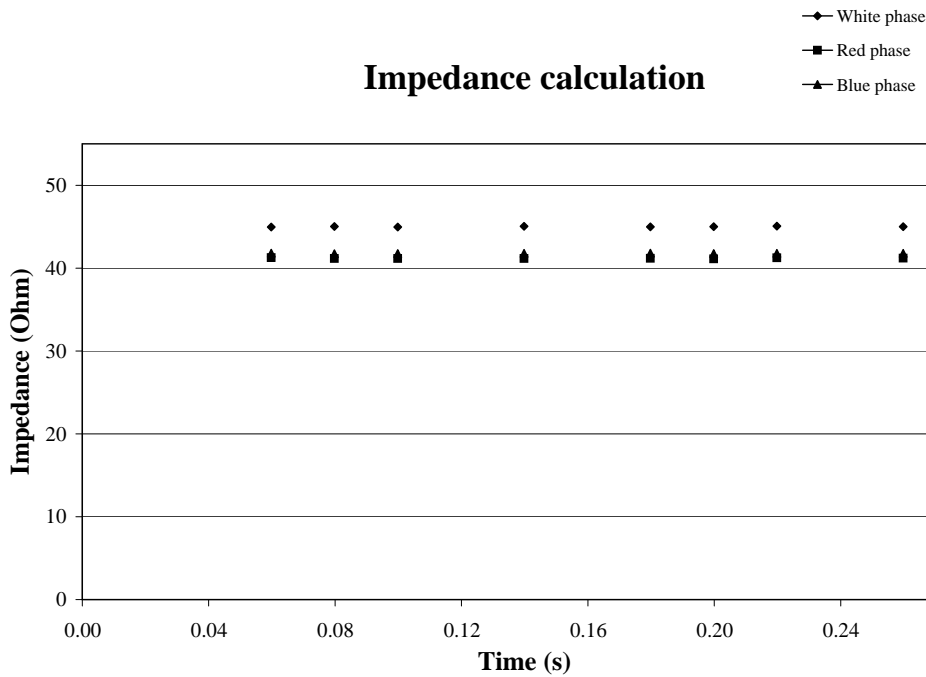


Figure 8.6: Impedance values determined for E-F using test data from 11-05-2000.

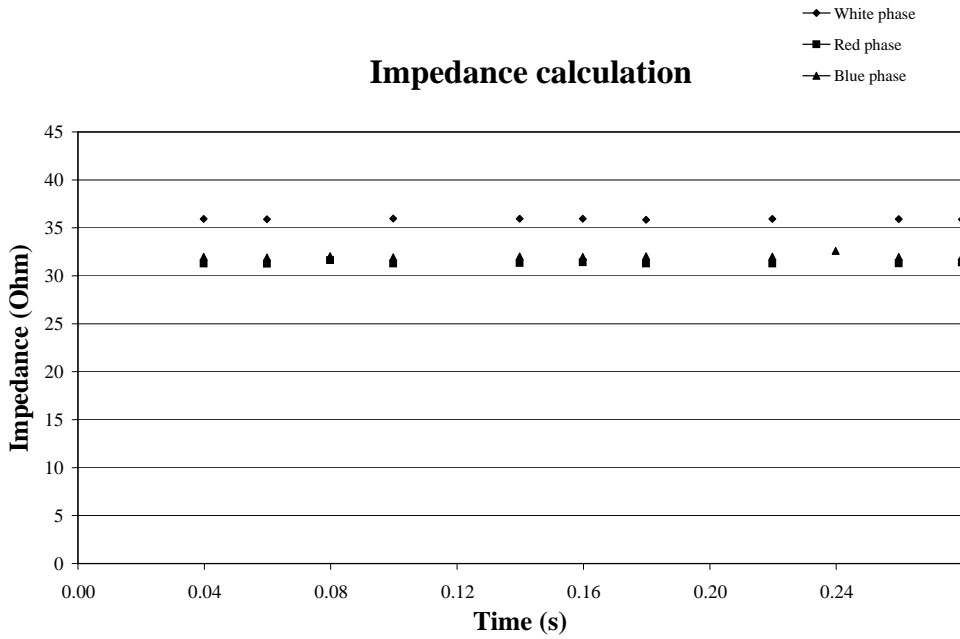


Figure 8.7: Impedance values determined for E-F using test data from 16-07-2000.

	Phase	Z max	Z min	Z error
11-05-2000	Red	41.18Ω	41.12Ω	52.29%
11-05-2000	White	44.85Ω	44.77Ω	65.87%
11-05-2000	Blue	41.68Ω	41.58Ω	54.14%
16-07-2000	Red	31.64Ω	31.26Ω	17.01%
16-07-2000	White	35.58Ω	35.52Ω	31.58%
16-07-2000	Blue	32.06Ω	31.62Ω	18.57%

Table 8.4: E-F results from measured values.

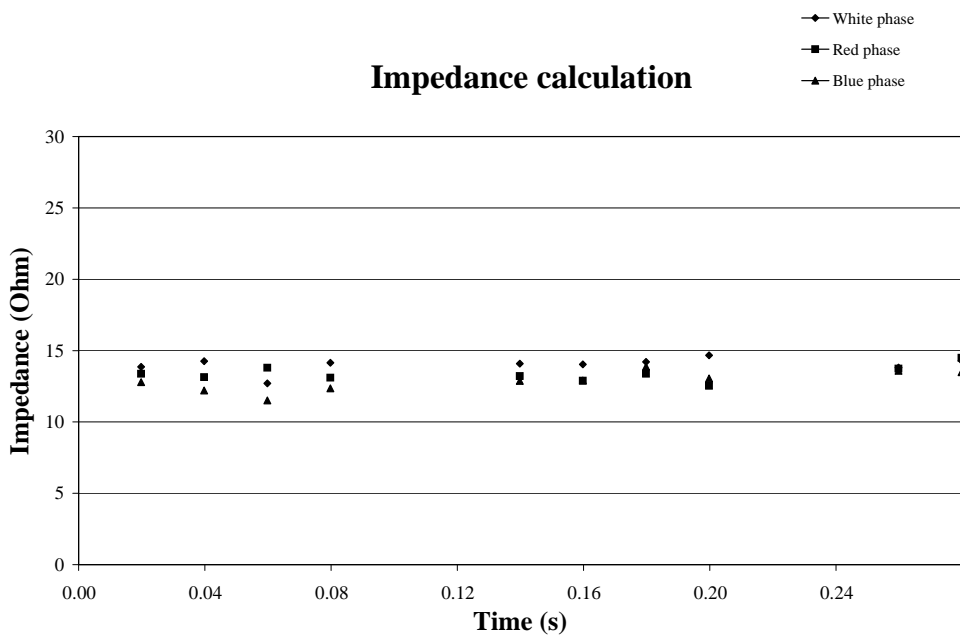


Figure 8.8: Impedance values determined for G-H using test data from 13-12-2004.

	Phase	Z max	Z min	Z error
13-12-2004	Red	14.49Ω	12.52Ω	50.31%
13-12-2004	White	14.68Ω	12.7Ω	52.28%
13-12-2004	Blue	13.87Ω	11.51Ω	43.88%

Table 8.5: G-H results from measured values.

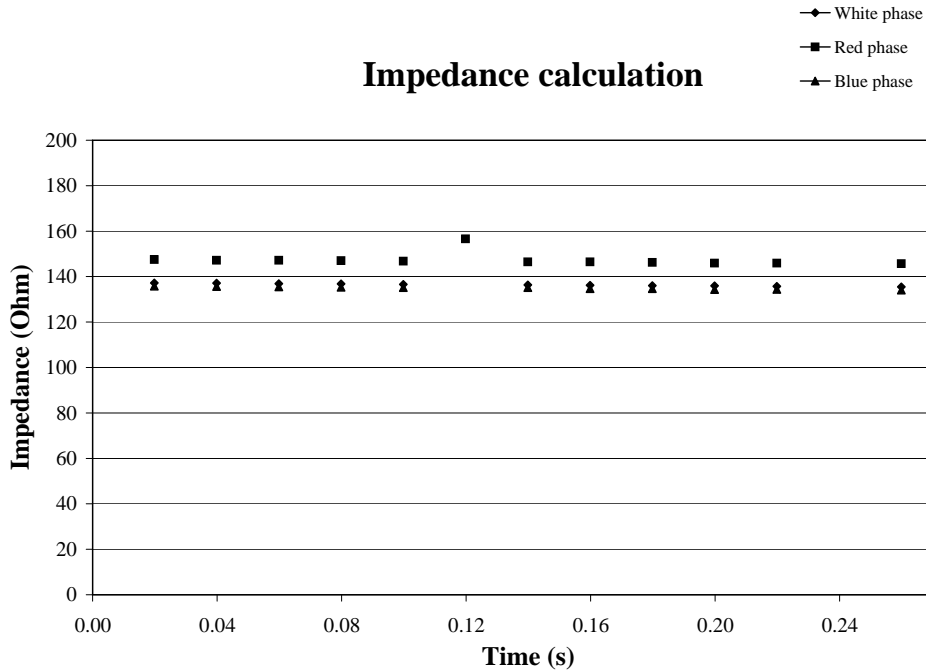


Figure 8.9: Impedance values determined for I-J using test data from 13-11-2005.

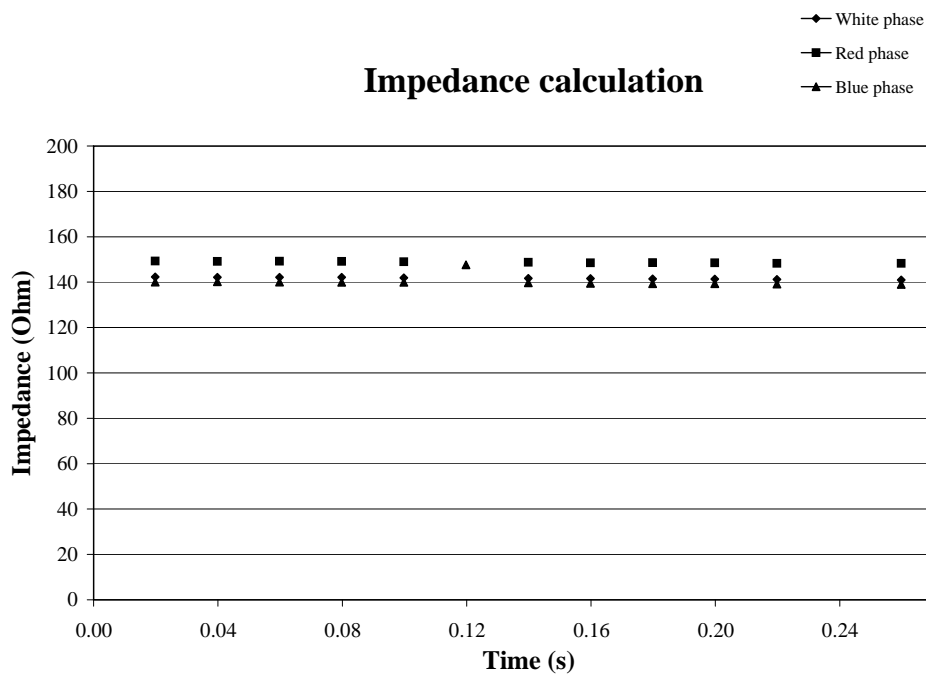


Figure 8.10: Impedance values determined for I-J using test data from 20-03-2006.

	Phase	Z max	Z min	Z error
13-11-2005	Red	135.62Ω	129Ω	15.63%
13-11-2005	White	120.68Ω	119.30Ω	2.89%
13-11-2005	Blue	120.48Ω	119.06Ω	2.72%
20-03-2006	Red	148.55Ω	145.96Ω	26.65%
20-03-2006	White	140.17Ω	131.34Ω	19.51%
20-03-2006	Blue	147.67Ω	138.59Ω	25.90%

Table 8.6: I-J results from measured values.

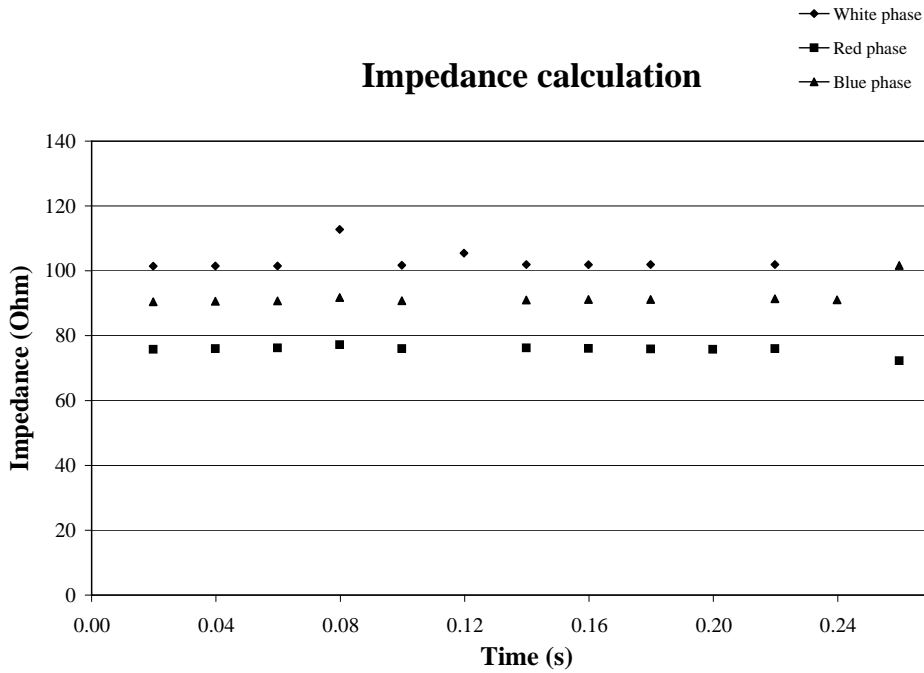


Figure 8.11: Impedance values determined for K-L using test data from 04-09-2004.

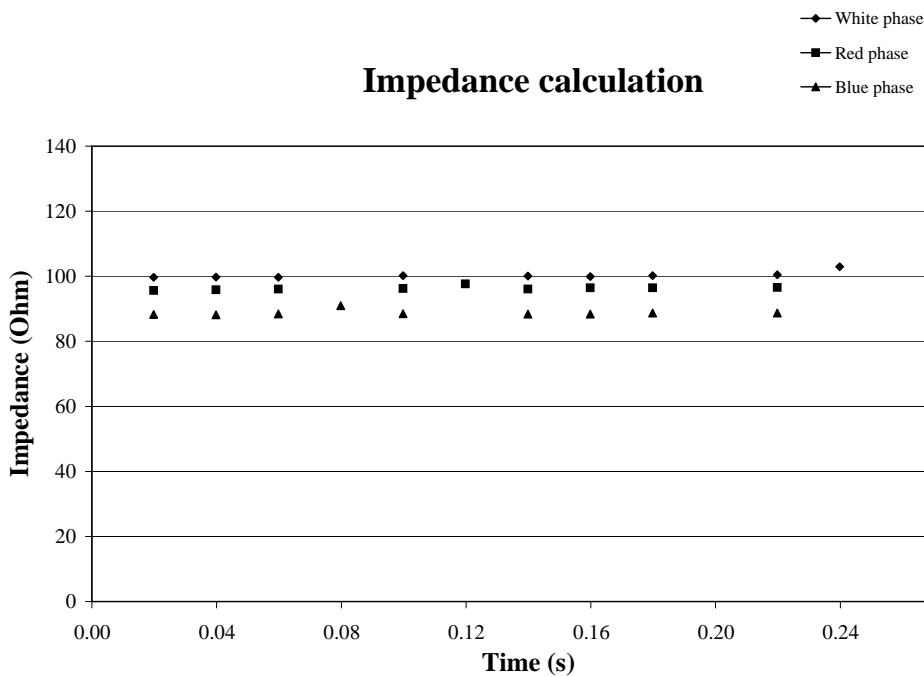


Figure 8.12: Impedance values determined for K-L using test data from 10-02-2006.

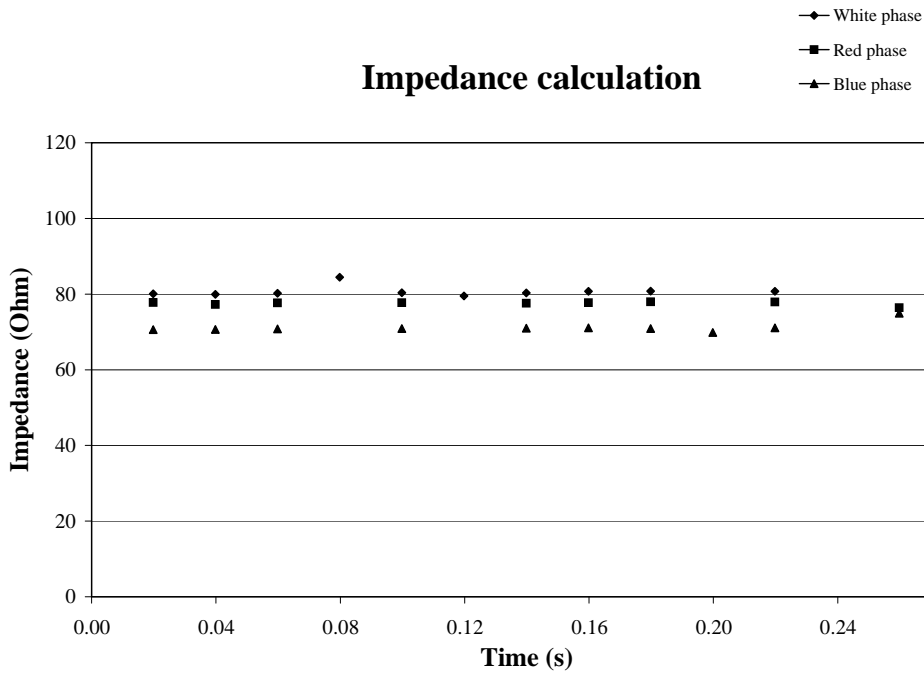


Figure 8.13: Impedance values determined for K-L using test data from 25-03-2006.

	Phase	Z max	Z min	Z max error
04-09-2004	Red	73.25Ω	67.99Ω	5.74%
04-09-2004	White	110.93Ω	98.27Ω	53.79%
04-09-2004	Blue	97.68Ω	87.03Ω	35.42%
10-02-2006	Red	97.68Ω	95.61Ω	35.42%
10-02-2006	White	102.95Ω	86.03Ω	42.73%
10-02-2006	Blue	90.95Ω	88.15Ω	26.09%
25-03-2006	Red	77.97Ω	75.9Ω	8.10%
25-03-2006	White	84.46Ω	79.53Ω	17.09%
25-03-2006	Blue	80.69Ω	69.86Ω	11.87%

Table 8.7: K-L results from measured values.

Method 3

Chapter 5 showed that Method 3 is based on the data of two independent cases that are loaded differently. Most of the lines did not have two independent results from the recorded data. Thus lines G-H and C-D could not provide results. This shows the importance of having separate measuring devices for parameter calculation. In this way measurements can be made when the transmission line is lightly loaded and when it is heavily loaded. This would provide data that can be used by Method 3. Another benefit of such measurements is that it can be used to estimate line losses during peak demand periods.

One line that did provide results that are in the expected range is K-L. The results for line K-L is given in Figure 8.14 - Figure 8.16 and Table 8.8. The percentage errors were calculated with (7.1).

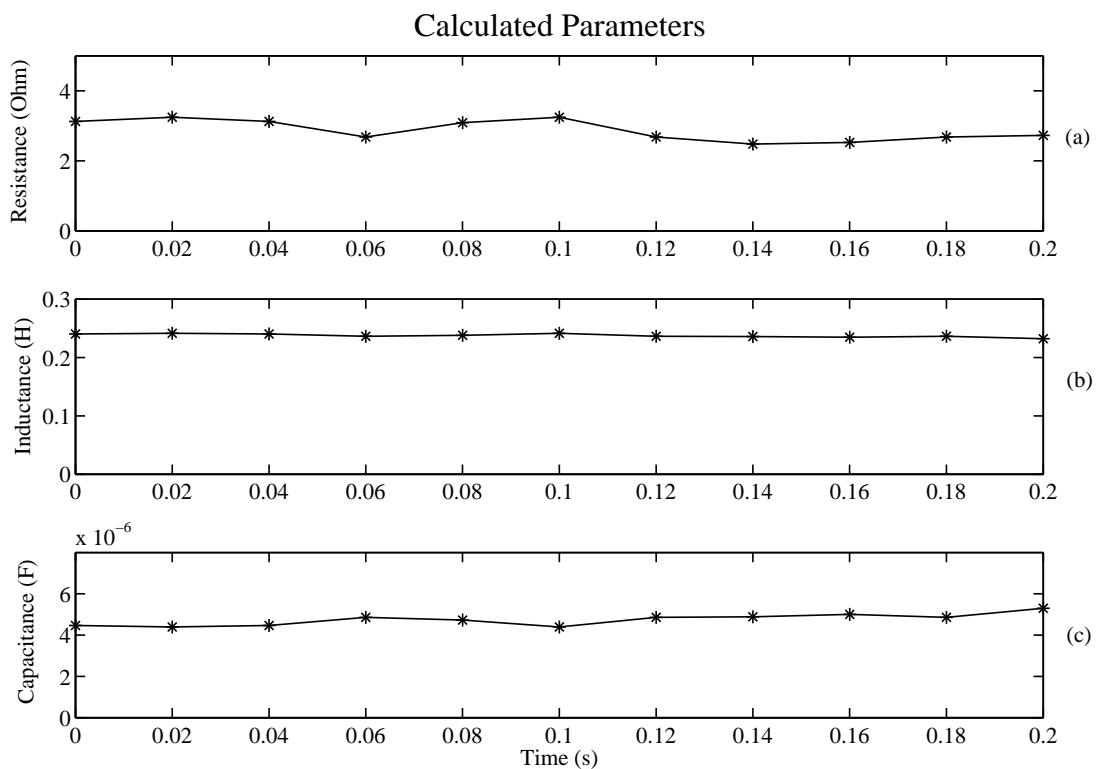


Figure 8.14: Parameter values determined for K-L using test data (Red phase).

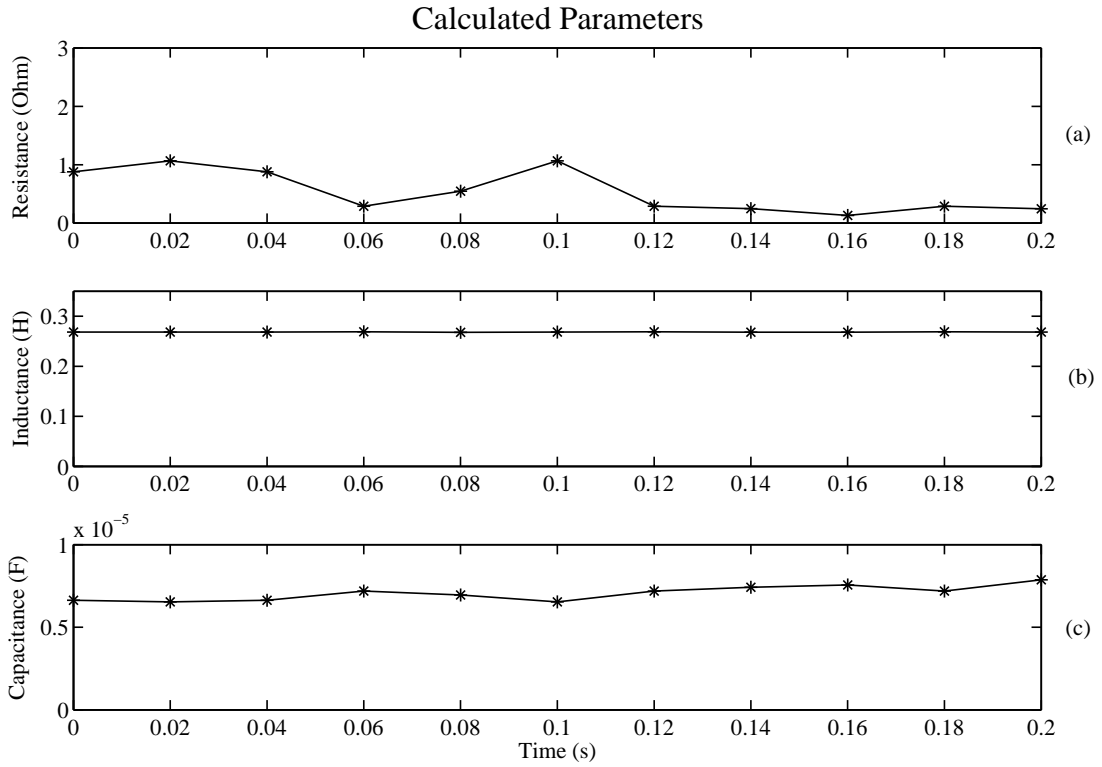


Figure 8.15: Parameter values determined for K-L using test data (White phase).

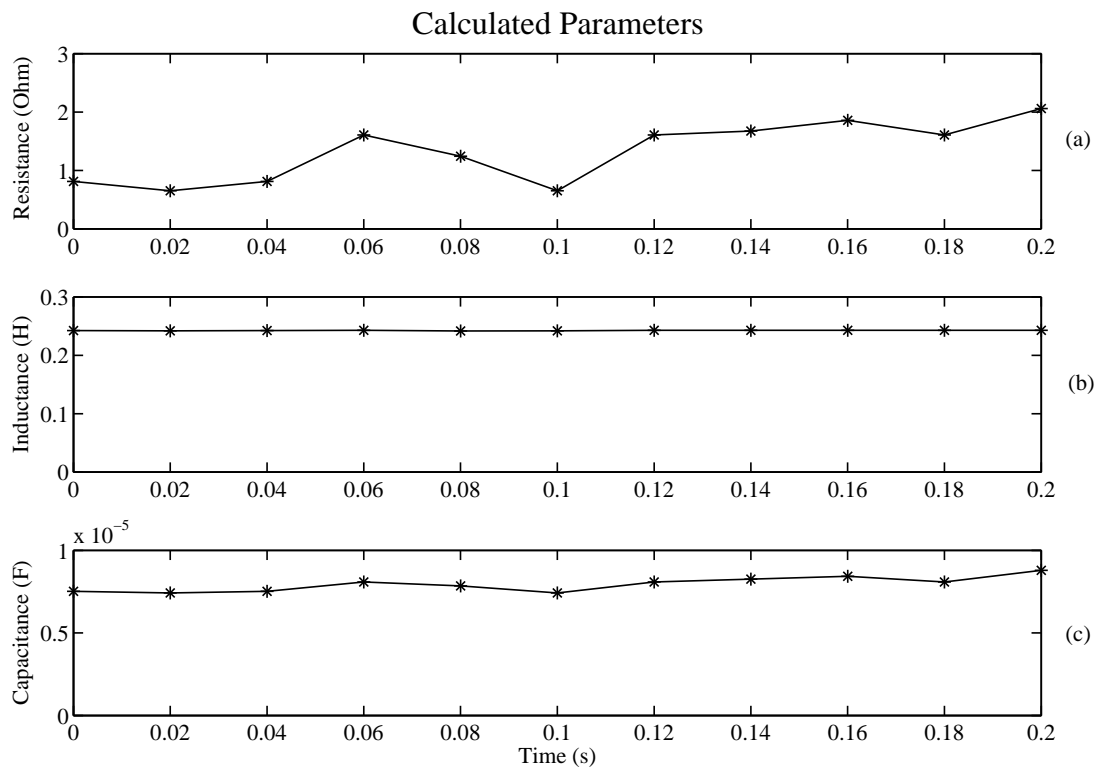


Figure 8.16: Parameter values determined for K-L using test data (Blue phase).

	Red phase	White phase	Blue phase
Rmax (Ω)	3.248	1.067	2.059
Rmin (Ω)	2.480	0.131	0.651
Lmax (mH)	241.5	269.0	242.8
Lmin (mH)	232.1	267.9	241.8
Cmax (μ F)	5.302	7.874	8.794
Cmin (μ F)	4.393	6.535	7.417
Rmax % error	52.58%	97.50%	87.55%
Lmax % error	5.46%	17.47%	6.03%
Cmax % error	-	-	-

Table 8.8: K-L results from measured values.

8.2.2 SIL curve

Data taken directly from recorders on either side of the K-L line, was used in the construction of the SIL curve. Only this line had enough fault data on record to draw an actual SIL curve. In the simulation results it was mentioned that the power factor of a line is of importance when drawing a practical SIL curve. The power factor was calculated for all the cases on record of line K-L. All the measurements in Figure 8.17 had a power factor larger than 0.9.

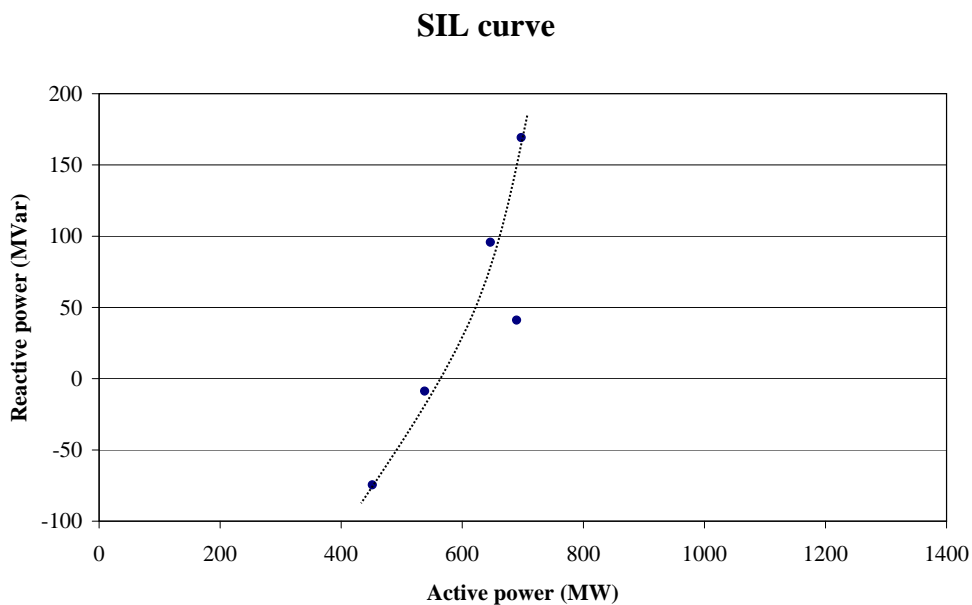


Figure 8.17: Practical SIL curve drawn from utility field data.

The SIL curve has the shape that would be expected from a typical SIL curve.

8.3 DISCUSSION OF RESULTS

8.3.1 *Parameter calculations*

To calculate the impedance the first proposed method *i.e.* the instantaneous subtraction of the sending and receiving end voltages was used. Method 3 was also applied to calculate the inductance, resistance and capacitance individually. Method 2 was excluded from the results because of inaccuracies. The CT's and VT's at substations introduced errors. This is because the active and reactive power used by the transmission line was very small when compared to the active power delivered to the load. A small error in the voltage and current can thus have a dramatic effect on the resultant parameters calculated. The power delivered to the load is mostly active. Therefore, the reactive power to the load is not mentioned. Reactive power is generally provided by reactive sources at the load. This is the most economical method. For shorter transmission lines the error gets large as line parameters become smaller, thus the ratio between the load and line powers becomes larger.

For the short transmission line the capacitive effect is neglected. The line capacitance increases with increasing length of the line. The surge impedance loading effect was explained earlier in the document. It showed that reactive power can be absorbed or provided by the line depending on the active power transferred. Thus the line capacitance makes it difficult to separate the resistance and the impedance of a line when Method 1 and 2 are used. This is because the active and reactive power ratio (power factor) varies largely with the load. It was not possible to use Method 2, as this method depends heavily on the active and reactive power ratio across the line.

In the simulation results the influence of CT's and VT's are not modelled. Also, because lab results were done at much lower voltages than the transmission lines, test equipment could be used that were much more accurate than traditional CT's and VT's. Finally, the ratio between line and load power was much smaller than what is experienced on an actual power line. The afore mentioned factors ensure that the laboratory and simulation results could provide accurate parameters using Method 2. However the practical transmission lines are more of a challenge. Nevertheless most of the distribution lines in industry are short to medium lines which negates most of the capacitive effect on the lines. So Method

2 could still prove to be useful.

Method 1

The results obtained in this section are unacceptable, with large errors recorded for the line parameters. As with Method 2, Method 1 is also largely influenced by the accuracy of the CT's and the VT's. The importance of highly accurate measuring equipment was discussed in Chapter 5. The accuracy of CT's and VT's provides a major challenge. A large percentage of the total error is ascribed to this. Compensation is difficult since the error that is introduced is unknown in magnitude and phase.

Method 1 is still relatively accurate since it relies on both magnitude measurement and phase difference between sending and receiving voltages. There is a sizable phase shift between the sending and receiving side voltages since line parameters largely comprise of reactance.

A second contributing factor to the inaccuracy of the results from Method 1 is the sampling frequency. The data storage devices used by the utility uses a maximum sampling frequency of 2.5kHz. The sampling frequency used in the laboratory is twice this value. This resulted in more data points per cycle of waveform. The field data from the utility was aligned by means of the neutral fault current that triggered the initial recording. However the clock frequency of the recorders on the sending and receiving side of the transmission line are not synchronized. This means that a maximum error of one discreet data point can be introduced between the initialization of the recordings at the two separate recorders. Figure 8.18 quantifies the impact that the data point has on the measured impedance.

The first set of data points shows the results obtained for the A-B transmission line (16-02-2003) for the red phase. The second set of values shows the same data where the receiving side values have just been sifted down by one data point. The figure shows an increase in impedance error from 13.90% to 46.05%. The percentage error is calculated by comparing the utility values with the maximum deviation in Figure 8.18. A higher sampling frequency would ensure that this error is smaller. Another solution to this problem is to align the system clocks of the measuring units by means of GPS generated synchronizing pulses.

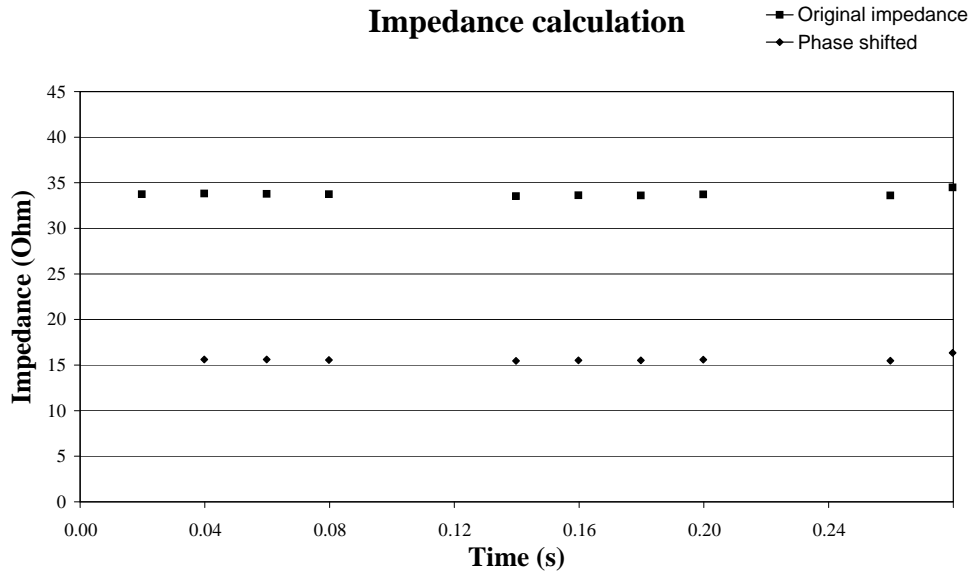


Figure 8.18: The effects on measured impedance with the introduction of one data point phase shift.

Since the reasons for the errors are known, each of the individual lines is considered. The first results were computed for the A-B line. The results obtained were very accurate, even if the CT and VT errors were ignored. A maximum error of 15% and a minimum of under 5% is recorded. This suggests that Method 1 works on medium transmission lines in a network.

Figure 8.5 shows the three graphs representing the impedance for each of the three phases of line C-D. Although the error is large in terms of percentage it must be noted that this is a very short line with an impedance that is quite small relative to other lines. The calculations are thus very sensitive to errors introduced by VT's and CT's. Even with the errors, results are stable. This tends to attest to a system with constant errors. If errors are constant and the magnitudes known, it is possible to compensate for them by means of gains. This will only work if the sampling error can be minimized.

Line E-F shows two graphs that are nearly identical in shape except for the change in measured impedance. These two graphs show the problem that is introduced with an error in clock frequency. Since the sampling is not synchronized, Figure 8.7 and Figure 8.6 have different errors. This result in conjunction with Figure 8.18 highlights the problem introduced by the sampling mismatch between two recorders.

The G-H line has similar characteristics to that of C-D. The only difference is that C-D is more heavily loaded. This confirms that the method works for both heavy and lightly loaded lines

The last two lines that were analyzed were the I-J line and the K-L line. Both these lines can be classified as long transmission lines. I-J is above the length of 240 kilometers while K-L is quite close to 240 kilometers. Long lines have a large capacitive influence. The I-J line provided good results when compared to the utility parameters, especially for the first graph (Figure 8.9). Long lines have larger impedance values. This improves the results as the resultant voltage drop across the line is larger as compared to shorter lines.

The first graph of the K-L line, Figure 8.11, shows values that differ. This results in errors that vary between 5% and 53%. Because the results between opposing phases differ significantly, the assumption is that the errors are due to measurement. This could have been due to a faulty CT and/or VT or a calibration error on the recorder. This assumption is further supported since the white and blue phases keep their relation to each other for all three the figures, while the red phase does not. During the final two figures the red phase's position changes to a value that more closely correlates to that of the white and blue phases. The error was thus rectified.

The impedance values that were calculated for the lines were compared to values used by the utility. The accuracy of these values are unknown. Thus, errors on the measured values can be either larger or smaller than what has been stated.

Method 3

Section 8.2.1 explains why parameters of lines C-D and G-H could not be calculated. The parameters of lines A-B, E-F and I-J could not be calculated either. Method 3 has to have two sets of data for the calculation of line parameters. These two sets of data has to be for different loading conditions. The larger the difference in loading between the two sets of data, the better the parameters can be calculated. The loading from the three lines did not vary enough to provide acceptable results. Line K-L though had data for a wide variety of loads. Line K-L was therefore used to construct the SIL curve.

For the red phase of line K-L, Method 3 introduced a maximum error of 52.58% and 5.46% for the resistance and inductance, respectively. The resistance makes up a very small part of the series line impedance. For this reason the resistance values calculated are much more sensitive to measurement errors than the inductance. Capacitance errors are not given in Table 8.8. The utility did not supply values for the line capacitance from their system.

Results from the white phase is much worse than those for the red phase. The maximum error for the resistance is calculated to be 97.5%. For the reason mentioned above the inductance had a much smaller error of 17.47%. The influence of CT and VT errors can be seen in the error differences calculated between red and white phases. The blue phase had errors of 87.55% and 6.03% for the resistance and inductance.

These results clearly show that Method 3 can be a very useful method for the calculation of the line parameters. When this method is employed though, more accurate measurements would be needed. These errors mentioned should just serve as a guideline as there is some doubt about the accuracy of the utility parameters.

8.3.2 *SIL curve*

Figure 8.17 is a SIL curve that was constructed from the data acquired from the K-L line. A SIL curve cannot be drawn for short transmission lines. This is because the SIL characteristic of a line depend on the capacitance of that line. The K-L line has a length of 219.6 kilometers which means it is very close to the length of a long transmission line. Thus the capacitive effect is present on the line.

When one compares Figure 8.17 to Figure 6.10 and Figure 6.11, the shape of the graph is clearly that of a SIL curve. There is one point that is out. This can be ascribed to the data being collected from fault recorders. The recorder will sense an event like the tripping of a breaker from a fault condition. This does not mean that the pre-event data is in steady state. The actual fault could have started gradually while increasing in severity until the protection reacted. This is quite likely what happened. The reactive and active power readings were taken as an average value over the pre-fault data and not just over

one cycle of the fundamental. Therefore this cannot be due to faulty measurement.

The SIL curve shows a surge impedance loading value of approximately 575MW. In order to draw a useful and complete SIL curve one would typically need data over a wide range of operating conditions. Since faults cannot be induced, it makes sense to implement test equipment that would sample power values at predetermined times. A good choice for these sampling times would be 7:00, 12:00 and 20:00 when power consumption is high, and then later at night when loading is low. This makes sense as there is no control as to whether the data recorded for a fault would be during low or high loading conditions. A second reason that this should be a separate unit is the fact that all the available data ever recorded for the K-L line had to be employed to draw the SIL curve. It would not be of practical use to have to wait ten years for a SIL curve to be drawn.

8.4 ALTERNATIVES CONSIDERED

It was initially planned to install measuring units at substations for the collection of data. Figure 8.19 shows the planned implementation.

Using the setup of Figure 8.19, the sampling frequency would be increased from 2.5kHz to 5.0kHz. This would reduce the phase shift introduced by the Siemens recorders. The GPS unit would initialize the recording. This will remove any phase shift that might be introduced by using the neutral current for data synchronization. However, it would be a daunting task to install twelve measuring units in different substations that are located hundreds of kilometers apart. This approach would also have been very expensive.

The connection of test equipment directly on line would be the best alternative. This way the VT's and CT's would be excluded from the measurements. This is also unpractical, as high end equipment that are very accurate is needed. This type of measuring equipment is very expensive and not readily available in South Africa.

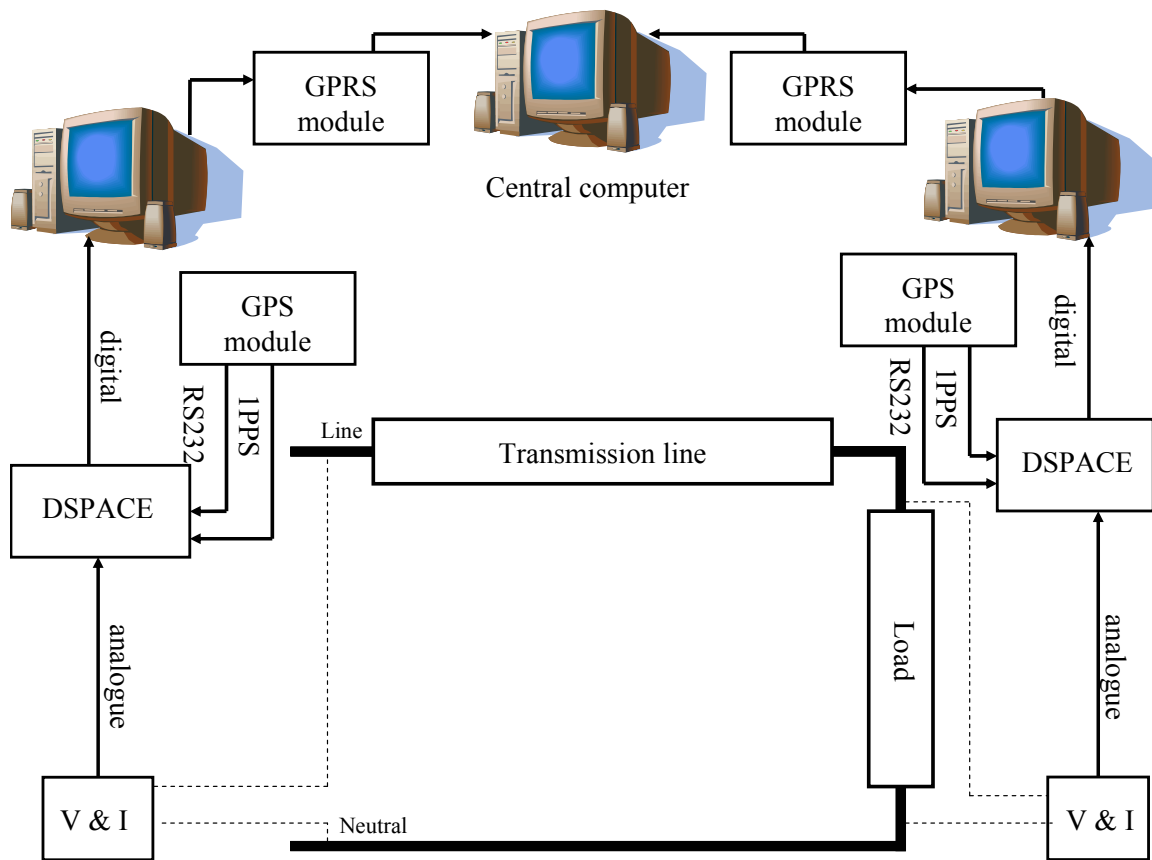


Figure 8.19: The connection diagram for the proposed setup in the field implementation.

9 SUMMARY OF FINDINGS

This section is included to provide a summary of the errors introduced into the measurements as well as proposed solutions. Figure 9.1 provides a visual representation of the errors.

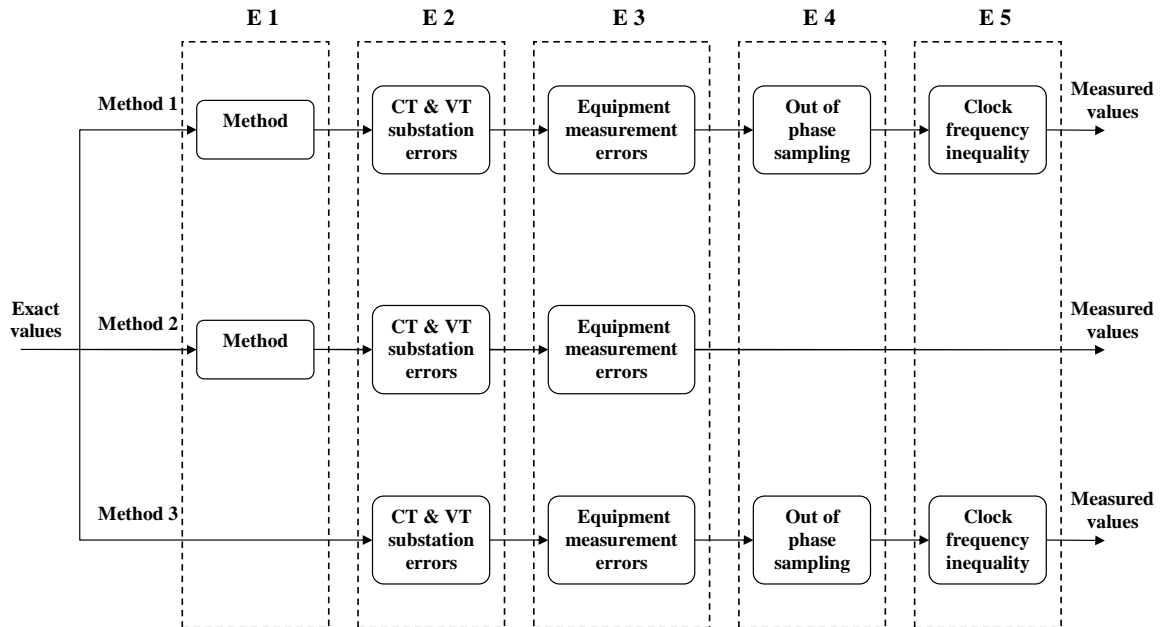


Figure 9.1: Summary of all the errors introduced into the measurements.

Three methods were proposed for determining the line parameters. These methods use voltage and current measurements to determine the line parameters. Method 1 also calculates the direction of capacitor current. Aside from this, neither Method 1 nor Method 2 consider the capacitive effect of the line. Since both Methods 1 and 2 are based on approximate line models, an error is introduced. This error is shown in Figure 9.1 as *E1*. From simulation and laboratory results it was proven that these methods are accurate for short and medium lines as long as the magnitude of the other errors are limited. Method 3 is not influenced by *E1* as it calculates the capacitance of the line.

E2 is the second error that is presented in the figure. CT and VT errors were discussed at length in Chapter 4. This error presents a problem since the accuracy of the substation VT's and CT's is unknown. Further research will have to be conducted in order to quantify these errors. The results obtained from the field data was stable which points to a constant error. If the size of a constant error is known, it can be compensated for by

adding gains to the measurements.

Measuring equipment that is very accurate needs to be used for the sampling of the data. Section 4.2 graphically showed the influence that unmatched probes had on the resultant calculation. By using more expensive measuring equipment that is more accurate the influence of $E3$ can be minimized.

Sampling that is out of phase ($E4$) refers to a constant error in the phase angle between the two measuring units. This error is introduced when two measuring units are initialized without being connected to a common reference point. Although the measuring units may be operating at the exact same clock frequency. They can sample at different times. The maximum phase error that is introduced in this way is one data point. The error can be reduced by increasing the sampling frequency. In this way there will be more data points for a fixed time period which means the maximum error is reduced. This is the solution that was used for the lab tests. Another solution would be to connect both measuring units to an external clock that makes use of a common reference. This common reference is the 1PPS output from a GPS module.

$E5$ is introduced into the system when data from two recorders, that operate at different clock frequencies, are compared with each other. Figures that are provided in section 4.1 show the influence $E5$ has on the calculated impedance values. The clock differences are directly related to the quality of the oscillators used by the recorders. One way to reduce this difference is by using a high quality external oscillator. By combining the external oscillators with a GPS unit's 1PPS output, any possible drift between the frequencies of two oscillator units will be removed. When the oscillators used by the recorders are of a high quality the frequency drift will be small. Taking measurements directly after the recorders are initialized, will also remove the introduced error as the frequency drift will still be small.

Method 2 was not based on the subtraction of instantaneous voltage values. It used the rms values calculated over a cycle of data. Therefore $E4$ and $E5$ does not apply to Method 2. On the other hand Method 1 and Method 3 rely on the phase angle between measured values.

10 CONCLUSION

10.1 WORK PRESENTED

This document investigated methods to determine transmission line parameters. Method 1 showed that by using synchronized data it is possible to obtain the impedance of lines with variable lengths. This method was tested over a range of lines, from very short to long. The loading of the line was varied. Accuracy posed a challenge due to phase errors introduced by unmatched sampling frequencies and system clocks. Although the accuracy can be improved using different methods, the concept was proven and leaves room for further investigation.

Method 2 can be used to determine the impedance and the phase angle. This enables one to determine the resistance and inductance of the line. The method yielded good simulation and laboratory results as long as the line length was kept short. The field implementation produced less than favorable results. Errors are attributed to erroneous measurements and ignoring the shunt capacitance of the line. The short transmission line can be modelled without capacitance. This means that Method 2 will work if the measurements are taken accurately. It is however not recommended for application on long lines.

Method 3 improves on Method 2 in that it calculates not only the inductance and resistance, but also the capacitance. Good results were obtained for short, medium and long line models. This was the only method that provides reliable results for the long transmission line. The only negative aspect is that this method takes greater computational effort than the others. From the work done Method 2 and/or Method 1 can be used for distribution lines as they are short in length. For transmission lines, Method 3 would be best as it uses the measurements to calculate the capacitance as well.

The shape and values of the SIL curve can be determined as shown in section 8.2.2. The SIL value is close to what is predicted in text books. In [31], a transmission line with a line voltage of 345kV will have a surge impedance loading value of 415MW. The SIL value increases with an increase in operating voltage. This means that for a 400kV line the measured SIL value of 575MW would be expected. The time span for data acquisition

is unacceptable. For this reason it is recommended to implement stand-alone measuring units.

Further research will have to be done to make it a viable concept that can be used in practice. This research was aimed at determining whether it would be possible to determine the parameters of a line from measured data. The results proved that it is feasible, subject to the accuracy of measurement equipment.

10.2 FUTURE RESEARCH

The influence of errors introduced by the CT's and the VT's in the substations is highlighted. These errors are responsible for most of the computational inaccuracies. For future testing of the proposed methods, gains and phase shifters can be used to compensate the errors introduced by the CT's and the VT's. In order to compensate for an error, its magnitude has to be known first. To quantify the errors at each substation, all the VT's and CT's installed on the network will have to be tested. This would entail comparing measurements made by a specific CT or VT and comparing the values with that of a highly accurate measuring device. For the CT's and VT's already installed on the network this will have to be done during planned downtime. This is worth the effort as more accurate measurements can be achieved. A new VT or CT that is to be installed on the network can be tested first for accuracy. This way a database containing the needed adjustment for every measurement made on the entire network can be constructed. This database can be used to calibrate measuring equipment to provide more reliable data.

Results obtained from using the methods proposed in this document can be improved by using external oscillators. These external oscillators can be employed to provide the clock frequencies of the devices that does the actual data sampling (typically a DSP). By using an external oscillator in conjunction with a GPS unit to generate the clock frequency [24], the two units will not only run at exactly the same frequency, but will also sample at exactly the same instant in time. This will effectively remove any phase errors that are introduced from the measurements.

An alternative to the external clock is to increase the sampling frequency of the measur-

ing devices. This method is limited by the clock frequency of the unit. If the sampling frequency is very high then the phase error between two sampling points is reduced. The added benefit of having a large sampling frequency in combination with highly accurate measurements is that higher order harmonics can be accurately measured.

If this proposed method is made practically implementable, the goal would be to link the parameters to the SCADA system used by Eskom. By doing this, up to date parameters will be available to national control. This would also be of use to the engineer that needs to simulate a part of the system.

REFERENCES

- [1] J. J. Grainger and W. D. Stevenson, *Power System Analysis*. Singapore: McGraw-Hill, 1994, pp. 141–233.
- [2] B. M. Weedy and B. J. Cory, *Electric Power Systems*, 4th ed. New Jersey: John Wiley and Sons, Ltd, 1998.
- [3] B. R. Gungor, *Power systems*. Orlando, Florida: Harcourt Brace Jovanovich, Inc, 1988.
- [4] C. R. Paul, K. W. Whites, and S. A. Nasar, *Introduction to Electromagnetic Fields*, 3rd ed. USA: McGraw-Hill, 1998.
- [5] T. Gonen, *Modern Power System Analysis*. USA: John Wiley and Sons, Inc, 1988.
- [6] J. L. Blackburn, *Symmetrical Components for Power Systems Engineering*. New York: Marcel Dekker, Inc, 1993.
- [7] J. Glover and M. Sarma, *Power System Analysis and Design*. CA: Brooks/Cole, 2002, p. 224.
- [8] R. N. Nayak, Y. K. Sehgal, and S. Subir, “Ehv transmission line capacity enhancement through increase in surge impedance loading level,” in *Proceedings of the Power India Conference*. IEEE, April 2006, p. 4.
- [9] G. N. Alexandrov and G. V. Podporkyn, “Improvement of the efficiency of 35 to 220 kv lines,” in *Proceedings of the International Conference on AC and DC Power Transmission*. IEEE, September 1991, pp. 226 – 231.
- [10] W. Lewandowski, J. Azoubib, and W. J. Klepczynski, “Gps: primary tool for time transfer,” in *Proceedings of the IEEE*, vol. 87, Issue 1. IEEE, January 1999, pp. 163 – 172.
- [11] P. Moore and P. Crossley, “Gps applications in power systems. i. introduction to gps,” *Power Engineering Journal*, vol. 13, Issue 1, pp. 33 – 39, February 1999.
- [12] D. Itagaki, K. Ohashi, I. Shuto, and H. Ito, “Field experience and assessment of gps signal receiving and distribution system for synchronizing power system protection,

- control and monitoring,” in *Proceedings of the Power India Conference*. IEEE, April 2006, p. 8.
- [13] “Hewlett-packard application note 1285: Traveling wave fault location in power transmission,” pdf, 2000, [http://www.fi.uba.ar/materias/6644/info/reflectometria /a](http://www.fi.uba.ar/materias/6644/info/reflectometria/a) last accessed May 2006.
- [14] G. J. Geier, T. M. King, H. L. Kennedy, R. D. Thomas, and B. R. McNamara, “Prediction of the time accuracy and integrity of gps timing,” in *Proceedings of the 49th International Frequency Control Symposium*. IEEE, 31 May-2 June 1995, pp. 266 – 274.
- [15] T. Skeie, S. Johannessen, and O. Holmeide, “Highly accurate time synchronization over switched ethernet,” in *Proceedings of the 8th conference on Emerging Technologies and Factory Automation*. IEEE, 2001, pp. 195–204.
- [16] H. Lee and A. Mousa, “Gps travelling wave fault locator systems: investigation into the anomalous measurements related to lightning strikes,” *IEEE Trans. Power Delivery*, vol. 11, no. 3, pp. 1214–1223, Jul 1996.
- [17] E. M. Anderson, *Electric Transmission Line Fundamentals*. Virginia: Prentice-Hall, 1985.
- [18] S. M. Wentworth, *Fundamentals of Electromagnetics with Engineering Applications*, 1st ed. New Jersey: John Wiley and Sons, Inc, 2005.
- [19] X. Zeng, K. K. Li, Z. Liu, and X. Yin, “Fault location using traveling wave for power networks,” in *Proceedings of the 39th Industry Applications Conference Annual Meeting*, vol. 4. IEEE, October 2004, pp. 2426 – 2429.
- [20] X. Zeng, Y. Zhou, Z. Liu, and G. Lin, “The sensor of traveling-wave for fault location in power systems,” in *Proceedings of the Power System Technology Conference*, vol. 2. IEEE, November 2004, pp. 1518 – 1521.
- [21] A. Elhaffar and M. Lehtonen, “An improved gps current traveling-wave fault locator in ehv transmission networks using few recordings,” in *Proceedings of the International Conference on Future Power Systems*. IEEE, November 2005, p. 5.

- [22] J. Kappenman, M. Gordon, and T. Guttormson, “High-precision location of lightning-caused distribution,” in *Transmission and Distribution*. IEEE/PES, 2001, pp. 1036–1040.
- [23] M. Kezunovic, “Monitoring of power system topology in real-time,” in *Proceedings of the 39th annual Hawaii International Conference on System Sciences*, vol. 10. IEEE, Jan 2006, pp. 244b–244b.
- [24] H. Gao, J. He, and S. Jiang, “Gps synchronized digital current differential protection for transmission lines,” *Elsevier Electric Power Systems Research*, vol. 62, pp. 29–36, 2002.
- [25] T. Longland, T. W. Hunt, and W. A. Brecknell, *Power Capacitor Handbook*. Thetford, Norfolk: The Thetford Press, Ltd, 1984.
- [26] R. C. Dugan, M. F. McGranaghan, S. Santoso, and H. W. Beaty, *Electrical Power Systems Quality*, 2nd ed. USA: McGraw-Hill, 2003.
- [27] M. Grobler and R. Naidoo, “Determining transmission line parameters from gps time-stamped data,” in *Proceedings of the 32nd Industrial Electronics conference ,Paris*. IEEE, November 2006.
- [28] R. J. Smith and R. C. Dorf, *Circuits, Devices and Systems*, 5th ed. New Jersey: John Wiley and Sons, Inc, 1992.
- [29] G. Rizzoni, *Principles and applications of Electrical Engineering*, 2nd ed. USA: Irwin, 1991.
- [30] R. E. Wilson, G. A. Zevenbergen, D. L. Mah, and A. J. Murphy, “Calculation of transmission line parameters from synchronized measurements,” *Electric Machines and Power Systems*, Taylor and Francis, vol. 27, pp. 1269–1278, 1999.
- [31] A. R. Bergen and V. Vittal, *Power systems analysis*, 2nd ed. Upper saddle river, New Jersey 07458: Prentice Hall, 2000, p. 85.